A Memory-Kernel-Free Approach to Time-Dependent Lattice Fermion Models

Dissertation

with the aim of achieving a doctoral degree at the Faculty of Mathematics, Informatics and Natural Sciences
Department of Physics at the University of Hamburg

submitted by
CHRISTIAN GRAMSCH

Hamburg, November 2017

This work was typeset with LaTeX.

Acknowledgements

Kurzfassung

Wir zeigen rigoros, dass jedes zeitabhängige wechselwirkende Gitterfermionenmodell auf ein anderweitig entsprechendes nicht-wechselwirkendes Modell abgebildet werden kann. Dieses effektive Modell ist so konstruiert, dass es exakten Zugriff auf die Einteilchen-Green-Funktion erlaubt — zum Preis einer exponentiell großen Anzahl zusätzlicher *virtueller* Freiheitsgrade. Da die Physik des Systems invariant unter zeitabhängigen unitären Transformationen bleibt, welche ausschließlich diese virtuellen Freiheitsgrade involvieren, betrachten wir zwei mögliche Realisationen des effektiven Modells: Zuerst wählen wir das virtuelle Subsystem in diagonaler Form, wodurch sich bei Ausintegration der virtuellen Plätze die Nichtgleichgewichts-Selbstenergie als Überlagerung nichtwechselwirkender isolierter Moden erweist — die Lehmann Darstellung. Dieses Resultat is sehr nützlich, wenn eine numerische Lösung der Dyson-Gleichung im Kontext von Approximationen benötigt wird, welche eine genährte Selbstenergie aus einem kleinen Referenzsystem bestimmen. Indem man anstatt der Selbstenergie das effektive Modell bestimmt, wird ein Markovscher Zeitpropagationsalgorithmus möglich, d.h. ohne Verwendung einer Erinnerungsfunktion. Wir demonstrieren dies explizit am einfachen Beispiel der zeitabhängigen Cluster-Störungstheorie (CPT), indem wir die Langzeitdynamik eines inhomogenen Anfangszustands nach einem Quanten-Quench, beschrieben durch das Hubbard Modell auf einem 10×10 Quadratgitter, simulieren. Wir zeigen, dass die Verletzung von Erhaltungssätzen im Regime kleiner Hubbard-Wechselwirkungen moderat bleibt, und, dass Prethermalisierungsphysik im Clusteransatz enthalten ist. Daraufhin leiten wir eine *erhaltende* CPT ab, welche die fundamentalen Erhaltungssätze respektiert. In Form lokaler Zwangsbedingungen für die spinabhängige Teilchen- und Doublonendichte verwenden wir dabei die Erhaltungssätze, um die zeitabhängige Hüpfmatrix im Referenzcluster zu bestimmen. In einer ersten Rechnung betrachten wir die Dynamik eines zweidimensionalen Hubbard-Modells nach einem Quench auf schwache Wechselwirkung. In der Tat ergibt sich in eine starke Veränderung der Dynamik in der erhaltenden CPT. Die Doublonendichte zeigt eine monotone Relaxation, während sich in einer gewöhnliche CPT-Rechnung stark oszillierendes Verhalten findet. Im Folgenden verlassen wir das Thema clusterbasierter Theorien und leiten eine alternative, block-tridiagonale Darstellung des effektiven Modells ab. Die Konstruktion ist analog zum Mori-Zwanzig-Formalismus, welchen wir auf Keldysh-Matsubara-Green-Funktionen verallgemeinern. Basierend auf diesem Resultat leiten wir einen selbstkonsistenten Zweipol-Ansatz ab und zeigen, wie Erhaltungssätze in diesem erzwungen werden können. Zuletzt diskutieren wir mögliche zukünftige Anwendungen.

Abstract

We rigorously prove that any time-dependent, interacting lattice fermion model can be mapped to a corresponding noninteracting model. By construction, this effective model gives exact access to the one-particle Keldysh-Matsubara Green's function of the system – at the cost of introducing an exponentially large number of *virtual* one-particle degrees of freedom. As the physics of the system are invariant under time-dependent unitary transformations involving these virtual degrees of freedom only, we explore two distinct realizations of the effective model: First, we choose the virtual subsystem to be diagonal which, upon tracing out the virtual sites, yields the nonequilibrium self-energy as a superposition of noninteracting isolated modes—the Lehmann representation. This result is highly useful to efficiently solve Dyson's equation numerically in contexts where an approximate self-energy is obtained from a small reference system. Calculating the effective noninteracting model instead of the self-energy, a memory-kernel-free time-propagation algorithm becomes possible. This is demonstrated explicitly by choosing the nonequilibrium cluster perturbation theory (CPT) as a simple approach to study the long-time dynamics of an inhomogeneous initial state after a quantum quench in the Hubbard model on a 10×10 square lattice. We demonstrate that the violation of conservation laws is moderate for weak Hubbard interaction and that prethermalization physics are contained in the cluster approach. Improving upon plain CPT, we construct a *conserving* generalization. In form of local constraints on the local spin-dependent particle and the doublon density, we use the macroscopic conservation laws to self-consistently fix the time-dependent hopping in the reference cluster. Using a simple two-site cluster in a proof-of-concept calculation, we consider the dynamics of the two-dimensional, particle-hole-symmetric Hubbard model following a weak interaction quench. Indeed we find the dynamics profoundly altered in the conserving CPT. The doublon density shows a monotonous relaxation while strongly oscillating behavior is found within the plain CPT. Leaving the topic of cluster-based theories, we also derive a second form of the effective model which is block-tridiagonal. The construction is analog to the Mori-Zwanzig projection technique which we generalize to Keldysh-Matsubara Green's functions. Based on our results we derive a selfconsistent nonequilibrium two-pole approach and explain how to enforce conservation laws. Finally, possible future applications are discussed.

Contents

Contents

1. Introduction

In flood tides of life, in tempests of doing,
Up and down running,
The here with there joining,
Birth with the grave,
An eternal ocean,
A weaving, reweaving,
A life aglow, burning,
So seated before time's humming loom,
I weave the Godhead's living costume.

— Spirit of Earth in Goethe's Faust[1]

In his colorful self-description, Goethe's Spirit of Earth pinpoints one of the key aspects of our everyday experience: Our world is dynamic. Nevertheless, in solid state physics, research has long been focused mainly on the time-independent properties of condensed matter systems. And for good reason. The defining notions of electronic transport, for example, *conductor* and *insulator*, are to be understood in the limit of small electrical fields. Here, linear response theory applies and one can show that the dissipative response of an equilibrated system to a small perturbation is determined by the system's equilibrium properties alone. This key insight is known as the fluctuation-dissipation theorem [3] and its roots reach back as early as the beginning of the 20th century with works of Einstein [4], Nyquist [5], and Onsager [6]. Considering the effect of a small electrical field on the electronic subsystem of a solid, the theorem allows to relate the conductivity in Ohm's law to an equilibrium current-current correlation function [3]. Of course, this conductivity will be highly dependent upon the phase, e.g., zero for an insulator at zero temperature or finite for a metal. A bit more exotic, the system could also be superconducting such that the conductivity is divergent. Standard parameters available to an experimentalist to tune a system into a specific phase are chemical doping, temperature changes or the application of pressure [7]. With the impressive advancements in experiment, i.e., the continuing refinement of pump-probe experiments [8–12] and the ever increasing control over ultracold atoms in optical lattices [13–19], a desire to explore new possibilities of phase manipulation has emerged. The idea is to excite the system far away from equilibrium into a transient state. Then, it is *time* that may drive the system through multiple transient phases before equilibrium, the Spirit's eternal ocean, is reached.

---

[1] English translation by Martin Greenberg [1]. The German original [2] reads: *In Lebensfluten, im Taten-sturm / Wall ich auf und ab, / Wehe hin und her! / Geburt und Grab, / Ein ewiges Meer, / Ein wechselnd Weben, / Ein glühend Leben, / So schaff ich am sausenden Webstuhl der Zeit / Und wirke der Gottheit lebendiges Kleid.*

1. Introduction

From an experimental perspective, pump-probe spectroscopy provides a state of the art option for the study of such non-adiabatic dynamics in solids. Especially suited for the investigation of the electronic structure is the time- and angle-resolved photoemission spectroscopy (trARPES). Based on the photoelectric effect, the electronic degrees of freedom are excited by an initial femtosecond laser pulse. The wavelength is commonly chosen in the infrared range such that the photon energy is to low to dislodge electrons. At a later time, the excited electronic many-body state is probed with a second, ultraviolet laser pulse. Through multiple measurements, the transient dynamics of the momentum-resolved electronic spectral function can be captured. In comparison to standard ARPES [20], the extra time-dependent layer offers a possibility to disentangle purely electronic from lattice effects. For example, charge density waves could be ruled out as the underlying cause of a transient metallic phase in a photo-excited Mott insulator [9]. From a technical viewpoint, the ultrashort lifetime of such photo-induced transient phases is a highly desirable feature in the context of ultrafast electronic devices [21]. It is thus to no surprise, that their systematic investigation proceeds to draw a considerable amount of attention [8–12].

A theorist starting out for a systematic investigation of out-of-equilibrium phenomena in condensed matter systems, on the other hand, soon stands face-to-face with a highly complicating aspect. It stands for incredible rich physics combined with a dramatic increase in complexity as no other: Strong correlations due to the Coulomb interaction. Already in equilibrium, this poses a tremendous challenge. A prime example is given by the Mott-transition [22, 23]: While from a single-particle viewpoint, i.e., band theory [24], any crystalline solid with a half-filled valence band is predicted to be a metal, this prediction must be reconsidered if electronic interactions are taken into account. A simple delocalization of the electrons into their kinetic ground state is now hindered as it comes accompanied by a large potential energy due to the electron-electron repulsion. In case the potential energy dominates, the electronic charges become localized by the system's attempt to maximize the distance between them—the correct prediction is a (Mott-)insulator. A much more involved example is provided by high-temperature superconductivity in copper oxides. In these highly-correlated systems, a large variety of phenomena is found. Depending on temperature and doping, one observes, for example, "strange" but also normal, i.e., Fermi-liquid, metallic behavior as well as antiferromagnetic ordering, and, of course, superconductivity with unusual high transition temperatures (up to 135K at normal pressure) [25].

After having identified electronic correlations as a key aspect for many condensed matter systems, the natural pathway to proceed is the formulation of a minimal model that allows for an isolated study. Such a model is given by the Fermi-Hubbard model (in the following simply *Hubbard model*). It is not only the paradigmatic model for the Mott transition [23] but also considered as highly relevant in the context of high-T_c superconductivity [26]. Introduced independently by Hubbard [27], Kanamori [28] and Gutzwiller [29] in 1963, it is defined by a rather innocent-looking improvement over a standard tight-binding Hamiltonian: A single extra term is added which accounts for an energy penalty if two electrons of opposite spin occupy the same Wannier orbital. However, one should not be deceived from the apparently simple structure. From a mathematical point of view, the complexity of the problem is increased dramatically. The tight-binding model

is integrable, i.e., it can completely be described by a single-particle Hamiltonian whose dimension scales linear with system size. Nevertheless, many-particle expectation values, like, e.g., the current-current correlation function required to evaluate the resistivity in Ohm's law, are easily accessible by means of Wick's Theorem. The Hubbard model, on the contrary, can be seen as the prototype of a nonintegrable model (in two and higher dimensions): It must be described by a many-body Hamiltonian with a dimension scaling exponentially in system size due to the interaction term. In particular, this implies a breakdown of Wick's Theorem. So even if one is able to obtain an (approximate) one-particle solution, one can, in general, not infer higher-order correlation functions from this information alone.

If considering out of equilibrium dynamics in the Hubbard model, the situation is even worse. The standard protocol, preparation of an equilibrium initial state which is subsequently evolved using a time-dependent Hamiltonian, already accentuates a major difficulty. If the initial state problem is not simply integrable, we are faced with *two* many-body problems: Initial state preparation and time evolution. A beautiful example how this may reflect in the mathematics is given by nonequilibrium dynamical mean-field theory (DMFT) [30]. In the DMFT, the lattice problem is selfconsistently expressed in terms of an Anderson impurity embedded in a noninteracting bath. Interestingly, if using a Hamiltonian-based formulation, two baths are needed to account for the dynamical case in contrast to one for a standard equilibrium calculation. The first describes the initial state correlations and their decay, while the second is initially uncoupled but builds up such that it describes the long-time dynamics [31].[2] A closely related problem is the loss of time-translational invariance which highly complicates the Green's function formalism— the standard toolkit of many-body theory [32]. Instead of a diagonal spectral representation, one must work with time-non-local quantities which renders analytical as well as numerical investigations far more challenging. Lastly, one should mention a difficulty intrinsic to our very goal, the description of dynamical phase transitions which emerge during the time-propagation of the many-body interacting state [33–36]. If subject to such a transition, the time-evolution features non-analytic points which are difficult to capture correctly using approximate methods. In the simplest case, one finds such non-analyticities being smeared out [37]. However, one may also imagine situations where the breakdown of the Taylor series in the vicinity of such a point renders standard tools such as, e.g., the Magnus expansion [38] unusable.

Due to its simple structure, the time-dependent Hubbard model suggests itself as the perfect toy model for the development of new methods for the study of nonequilibrium dynamics in correlated systems. Indeed, in response to the high demand, a number of well-known equilibrium methods have seen generalizations to time-dependent setups and have successfully been applied to the Hubbard model. Amongst the most powerful is certainly the previously mentioned DMFT whose origins date back over 25 years [39–41]. Assuming its impurity problem can be solved without further approximations, it provides the exact solution in the limit of infinite lattice dimension. The first appearance

---

[2] In contrast to intuition, it is the atomic limit and not a simple tight-binding initial state that allows for a description of the dynamics using only one bath. This is due to the fact that the dynamic mean-field represents the contribution of the surrounding lattice which is zero only in the atomic limit. See Ref. 31 for the details.

concerning nonequilibrium physics is due to Schmidt and Monien [42] who generalized its selfconsistency condition using the Keldysh formalism [43]. A first successful application was carried out in 2006 by Freericks, Turkowski and Zlatić [44]. Since then, a considerable amount of progress has been made [30]. Nevertheless, important methodological challenges are still investigated, e.g., overcoming the dynamical sign problem of Monte-Carlo-based impurity solvers [45, 46] or dealing with the rapid increase of necessary bath sites in Hamiltonian-based approaches [31, 47–49]. Both limit the accessible timescale. In this context, also the self-consistency condition itself should be mentioned which requires solving Dyson's equation on the Keldysh-Matsubara contour—a difficulty most severe for inhomogeneous setups [50]. Taylor-made for the opposite limit, one dimension, we have the density-matrix renormalization group (DMRG) [51]. First proposed by White in 1992 [52], it has seen a generalization to nonequilibrium in 2004 [53–55]. Concerning the 1D Hubbard model, the DMRG is highly successful on short and intermediate timescales where it provides the exact solution, e.g., Refs. 56–58. Access to large times, however, is inhibited due to an exceeding growth of the entanglement entropy. In the context of exactly solving the 1D Hubbard model, also the famous Bethe-ansatz solution, found by Lieb and Wu in 1968 [59, 60], comes to mind. Yet, while there are attempts to also study out-of-equilibrium phenomena [61], a systematic generalization of Bethe-ansatz techniques to nonequilibrium seems still to be lacking [62]. Lastly, one should also mention Monte-Carlo simulations. In equilibrium, these offer indeed numerically exact solutions in certain parameter regimes, e.g., Refs. 63, 64. However, simulations of nonequilibrium dynamics (out of the context of other methods such as the DMFT) still seem to be rather rare [65].

If one is interested in exactly studying out-of-equilibrium dynamics in the Hubbard model, the available methods restrict oneself to one (DMRG) and infinite dimensions (DMFT) and not too large timescales. Especially two-dimensional systems, where the DMRG is inapplicable and the central approximation of the DMFT, locality of spatial correlations, becomes highly inaccurate, are difficult to access. Interestingly, help may come from a rather unexpected direction: Experiment. Namely, in the form of ultracold atoms in optical lattices [13]. In spirit of Feynman's idea of a quantum simulator [66], these systems are well isolated and offer such a precise control over the kinetic as well as the interaction parameters of the trapped atoms that they seem well-suited for a systematic investigation of the Bose- as well as the Fermi Hubbard model [14]. Indeed, concerning the latter, metallic as well as Mott-insulating phases have been realized [15, 16]. After the preparation of an equilibrated phase, also nonequilibrium dynamics can be initiated, for example, by suddenly changing a parameter [17]. A promising recent development, which presumably will also stimulate future out-of-equilibrium studies, concerns the implementation of spatially-resolved microscopy which allows to study spin and charge correlations with local, per site resolution [18, 19]. Despite these successes, a remaining stumbling block should be mentioned which concerns the cooling of the atoms into regimes of even higher quantum degeneracy [14]. While the atomic gases are ultracold in an absolute sense, the relevant temperature scale is set by the Fermi temperature, T_F, which is of the order of hundreds of nano-Kelvin. The lowest relative temperatures reached so far, $0.03 - 0.05\,T/T_F$ [67], are thus quite high in comparison to a real material. For copper, for example, where $T_{F\text{-Cu}} \approx 8.6 \times 10^4\,\text{K}$ [24], this would equal $T = 0.05\,T_{F\text{-Cu}} \approx 4.3 \times 10^3\,\text{K}$.

To understand the current limit, let us consider the standard technique for the last cooling stage, evaporative cooling [68]: In the equilibrated, trapped gas, the energy of each single atom varies considerably about its mean due to particle-particle collisions. This is exploited, by removing the atoms with the highest energies and waiting for the subsequent rethermalization at lower temperature. While quite effective for bosons, the Pauli principle poses a fundamental limit in the fermionic case. Taking a mean-field viewpoint, one expects a Fermi sea to develop at low temperatures such that the number of unoccupied low-energy states becomes small. Therefore, the scattering into such states becomes a rare event, while scattering into an occupied low-energy state is forbidden. As a result, evaporative cooling becomes ineffective. Overcoming this, but also other challenges [14], is of fundamental interest in the search for better cooling techniques and the *"progress on the theory of dynamics and thermalization in strongly correlated systems will have a strong impact on guiding experiments to cool into new regimes"* [14].

Of course, there are attempts to overcome the limitations of the mentioned techniques. Considering for example the DMFT, there are cluster extensions [69] or the nonequilibrium dual-fermion approach [70]. Considering the DMRG, the so called projected entangled pair states (PEPS) [71] should be mentioned, which presumably will see a generalization to nonequilibrium in the future. However, these approaches are computationally very demanding. While one can expect them to become of growing importance in the long term due to the ever increasing computer power, simpler, more flexible approaches are needed in the short term. Indeed, such approaches have been suggested, for example, the generalization of the Gutzwiller variational technique [29] to nonequilibrium [72, 73]. While its efficient evaluation makes use of the limit of infinite lattice dimension (the so called Gutzwiller approximation [74]), so that its application implies assuming the locality of spatial correlations, it is computationally much less demanding. For simple setups, one can even aim for an analytical solution as has been shown for interaction quenches in the homogeneous Hubbard model [73]. A different, promising method is given by the nonequilibrium self-energy functional theory (SFT) [75, 76]. Similar to the Gutzwiller method, it is a variationally controlled approximation. The variational principle, however, is not wave-function-based (in equilibrium, the Ritz variational principle; in nonequilibrium the Dirac-Frenkel variational principle [77]) but Green's-function-based and intimately linked to the Luttinger-Ward functional [75, 76]. By means of finding optimal values for the one-particle part of a small, and as such easy to solve, cluster system, it selfconsistently includes the effect of short-range correlations into the calculation. A remaining limitation, however, concerns the computationally expensive inversion of Dyson's equation on the Keldysh-Matsubara contour [76]. Going beyond intermediate times is therefore prohibited. Underlining the potential of such light-weight, approximate methods, both, the nonequilibrium Gutzwiller as well as the nonequilibrium SFT, correctly capture important features of the dynamical Mott transition [73, 78] in qualitative agreement with the nonequilibrium DMFT [79]. Furthermore, due to being computationally much less demanding, longer timescales compared to the DMFT are accessible. Therefore, as an important aspect, also the influence of the ramp duration on the dynamical Mott transition could be studied [78, 80].

In this thesis, we develop new methodological tools to enable the study of nonequilibrium dynamics in the presence of short-range spatial correlations. Special emphasis is

put on avoiding an intrinsic bottleneck of Green's-function-based approaches in nonequilibrium, namely, the solution of Dyson's equation on the Keldysh-Matsubara contour in which the nonequilibrium self-energy serves as a memory kernel. To this end, we develop an exact mapping of time-dependent interacting to noninteracting fermionic lattice models. The idea is linked to a rather fundamental property of the nonequilibrium self-energy, namely, that it can be decomposed into a superposition of noninteracting isolated modes, better known as its Lehmann representation. This property was first conjectured and numerically verified in the context of nonequilibrium DMFT [50], where it could indeed be exploited to make a fully inhomogeneous setup numerically tractable. After recalling some important notions of nonequilibrium many-body theory in Chapter 2 – in particular the generalization of the well-known Lehmann representation of equilibrium Green's functions to nonequilibrium – we give an in-depth introduction into the general idea in Chapter 3. We proceed with a *rigorous* proof of the existence of the Lehmann representation of the nonequilibrium self-energy. We detail how our proof enables to reach long timescales in the context of cluster-based methods and present a numerical algorithm for an efficient computational implementation. With these tools at hand, we consider cluster perturbation theory (CPT) as a simple numerical test case in Chapter 4. Indeed, we find that our time-local (i.e., memory-kernel-free) algorithm allows to access much longer times in comparison to previous studies. Yet, we also rediscover the main drawbacks of the simple, non-selfconsistent embedding approach of the CPT. In general, it violates important conservation laws such as energy and particle number conservation. We address these issues in Chapter 5 where we develop a *conserving* cluster perturbation theory by enforcing local constraints which correspond to the macroscopic conservation laws. To this end, we make fully use of the time-local algorithm developed for the nonequilibrium CPT. As a proof of principle, we numerically solve weak quenches in the homogeneous Hubbard model. By design, we find conservation laws fulfilled. In comparison to a plain CPT calculation, this has a profound impact on the dynamics.

Motivated by the successful application of the mapping idea in the context of cluster-based methods, we also investigate a somewhat different route in Chapter 6. In the context of equilibrium studies of the Hubbard model, so called n-pole approximations have gained some popularity [27, 81–85]. We show that the time-dependent noninteracting Hamiltonian resulting from the mapping procedure can be constructed such that it corresponds to a nonequilibrium n-pole approximation thus generalizing this idea. The concept is closely related to the continued fraction expansion in the Mori-Zwanzig projection technique [86–88] which we formulate for the first time using Keldysh-Matsubara Green's functions. Applying the idea to the time-dependent Hubbard model, we derive a fully self-consistent nonequilibrium two-pole approximation, much in the spirit of Roth [81, 82]. Finally, we show how to implement conservation laws in the nonequilibrium two-pole approximation.

Lastly, in Chapter 7, we summarize the main results and give an outlook to possible future developments.

2. Nonequilibrium formalism

Equilibrium many-body theory [89] is largely based on Green's functions and has its historical roots in quantum field theory and its diagrammatic perturbative methods [90, 91]. Targeted at zero temperature problems, we have the Feynman-Dyson perturbation theory which is formulated on the real-time axis and based on the idea of adiabatic switching of the interaction and the Gell-Mann-Low theorem [92]. At finite temperature, the appropriate ansatz is given by the imaginary-time Matsubara technique [93] which exploits the structural similarity between the statistical and the time-evolution operator. Results for the real time axis are then obtained from analytical continuation. Despite their intrinsic differences, if perturbatively expanding the corresponding Green's function with the help Wick's theorem [94] one finds that the same set of diagrams emerges for both approaches. Key insights gained from diagrammatic manipulations, like the linked-cluster theorem or the existence of a self-energy and Dyson's equation, thus apply to both cases [32]. This on first sight astounding finding can be traced back to the fact that both can be derived as the limiting cases of a more general unifying theory which describes time-dependent phenomena as well: The nonequilibrium Keldysh-Matsubara formalism.

Its main idea is the introduction of an L-shaped time contour (cf. Fig. 2.1), in this thesis referred to as the Keldysh-Matsubara contour. Due to a corresponding contour-ordering operator, the correct placement of the time-evolution and the statistical operator is beautifully taken care of. Leading up to the formalism in its modern form, the nowadays most famous publication was written by Keldysh and published in 1964 [43]. He showed that the so called "vacuum stability condition" in the zero-temperature formalism can be dropped if one introduces a contour that makes a round trip along the real time axis. As a remaining restriction, his approach relies on an adiabatic switching of the interaction as the only possibility to take into account initial state correlations. A proper generalization was given by Danielewicz in 1984 [95], who in this context also derived an appropriately generalized version of Wick's theorem, by showing that an extension of Keldysh's contour into the imaginary-time domain allows for a description of arbitrary thermal initial states. A fully comprehensive view, which also includes the possibility of non-thermal, correlated initial states was finally given by Wagner in 1991 [96]. While the mentioned publications clearly advanced the contour idea, let us note that the development of nonequilibrium many-body theory is by far not limited to these authors. Other influential works include, for example, Martin and Schwinger [97] as well as Kadanoff and Baym [98].[1] Finally, we refer to Ref. 32 for a pedagogical introduction into nonequilibrium many-body theory.

In the following, we briefly motivate the Keldysh-Matsubara contour as an elegant tool for the investigation of nonequilibrium phenomena (Section 2.1). We proceed by defining

---

[1] Some personal historical viewpoints of researchers who were involved in the field's early developments can be found in Refs. 99, 100 and 101.
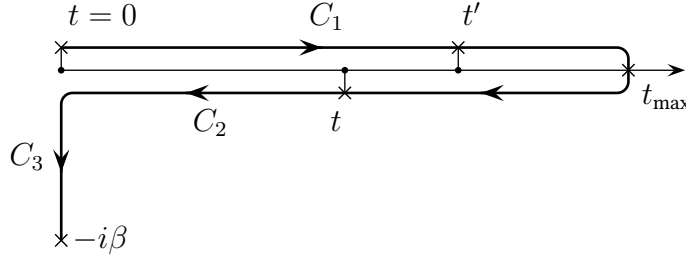
Figure 2.1.: Keldysh-Matsubara contour C. C_1 denotes the upper branch, C_2 the lower branch and C_3 the imaginary Matsubara branch. Together, the upper and lower branch define the Keldysh part $\mathcal{K} = C_1 \cup C_2$ of the contour. As an illustration of the concept of contour ordering, consider the shown example: Here, t is later than t' in sense of the contour, denoted as $t >_C t'$ in the text. A contour-ordered expression involving the Hamiltonian at these times, for example, would therefore yield: $\mathcal{T}_C \{H(t')H(t)\} = H(t)H(t')$. We further note that for two variables on the upper branch, i.e., $t_1, t_2 \in C_1$, the contour-ordering operator $\mathcal{T}_C$ reduces to conventional time-ordering operator $\mathcal{T}$: $\mathcal{T}_C \{H(t_1)H(t_2)\} = \mathcal{T} \{H(t_1)H(t_2)\}$.

contour-ordered Green's functions and derive its equations of motion in Section 2.2. As an important cornerstone of this thesis, we end this chapter with the introduction of the Lehmann representation of contour-ordered Green's functions (Section 2.3).

2.1. The Keldysh-Matsubara contour

We consider a time-dependent Hamiltonian $H(t) = H_0(t) + H_{\text{int}}(t)$ where $H_0(t)$ is assumed to be its noninteracting quadratic part while $H_{\text{int}}(t)$ contains the quartic terms. We further assume a scenario where the system is initially in equilibrium with Hamiltonian $H_{\text{ini}} = H(0)$ due to being in contact with a surrounding environment. At time $t = 0$, the system is decoupled from its environment and a unitary time-evolution is initiated. From Schrödinger's equation we obtain the time-ordered propagator $\mathcal{U}(t,0) = \mathcal{T}\exp\left(-i\int_0^t H(t')\mathrm{d}t'\right)$, with Planck's constant $\hbar$ set to one. Furthermore, we introduce the convention that operators with a hat carry a time dependence according to the Heisenberg picture, i.e., $\hat{A}(t) \equiv \mathcal{U}^\dagger(t,0)A\mathcal{U}(t,0)$, for an arbitrary, time-independent observable A. The expectation value $\langle \hat{A}(t) \rangle_H$ at time t is defined as

$$\langle \hat{A}(t) \rangle_H \equiv \mathrm{tr}\left(\rho\mathcal{U}^\dagger(t,0)A\mathcal{U}(t,0)\right), \quad \rho = \frac{1}{Z}\exp\left(-\beta H_{\text{ini}}\right). \tag{2.1}$$

Here, β denotes the inverse temperature, with Boltzmann's constant k_B set to one. For a convenient notation, we assume a term $-\mu N$ to be absorbed into the noninteracting part of the Hamiltonian, i.e., $H_0(t)$, where μ denotes the chemical potential and N the particle number operator. ρ then refers to the grand-canonical density matrix and consequently $Z = \mathrm{tr}\left(\exp\left(-\beta H_{\text{ini}}\right)\right)$ to the grand-canonical partition function. The trace $\mathrm{tr}\left(\cdot\right)$ runs over the full Fock space.

By employing the contour-ordering operator $\mathcal{T}_C$, cf. Fig. 2.1, we can express Eq. (2.1) as

$$\langle \hat{A}(t) \rangle_H = \frac{1}{Z} \mathrm{tr} \left(\mathcal{T}_C \left\{ \exp(S) A(t) \right\} \right), \quad S \equiv -i \int_C H(t') \mathrm{d}t'. \tag{2.2}$$

We emphasize that the introduction of a dummy contour-time dependence $A(t)$ on the right hand side of this expression is necessary to ensure a correct placement of A when evaluating the contour ordering. We further emphasize that the action S is defined only within the context of a contour-ordered expression.

So far, Eq. (2.2), does not seem to be much more than an elegant way of rewriting the initial expression. However, the true power of this formulation is revealed if we consider a perturbative expansion. To this end, it is convenient to define $S = S_0 + S_{\mathrm{int}}$, where $S_0 \equiv -i \int_C H_0(t') \mathrm{d}t'$ and $S_{\mathrm{int}} \equiv -i \int_C H_{\mathrm{int}}(t') \mathrm{d}t'$. Since the contour-ordering operator takes care of correctly positioning all involved operators, we are allowed to split up the matrix exponential such that $\exp(S) = \exp(S_0) \exp(S_{\mathrm{int}})$. Furthermore, the grand-canonical partition function can be rewritten as $Z = \mathrm{tr}(\mathcal{T}_C \exp(S))$ since the integrations along the upper and lower branch of the contour cancel each other. By expanding in powers of S_{int}, we therefore obtain a perturbation theory in the interaction which can be evaluated by means of Wick's theorem. Using the standard set of rules, a diagrammatic perturbation theory can be set up, cf. for example Ref. 32. It is worthwhile to note that this derivation was carried out completely in the Schrödinger picture. The simplicity is a direct consequence of the powerful contour-ordering idea.

Let us finally comment on how to obtain the zero- and finite-temperature formalism from the more general Keldysh-Matsubara formalism. The latter is obtained rather trivially by setting $t_{\mathrm{max}} = 0$ which reduces the contour to its Matsubara branch. To obtain the former, we assume the noninteracting part of the Hamiltonian $H_0(t)$ to be time-independent and the interacting part to be switched adiabatically, i.e., $H_{\mathrm{int}}(t) = e^{-\epsilon|t|}V$, with $\epsilon > 0$ and $\epsilon \to 0$ at the end of the calculation. In the limit $t \to -\infty$ the system is thus uncorrelated and Wick's theorem applies. Additionally, we perform the zero-temperature limit $\beta \to \infty$ so that the density matrix, assuming no degeneracies, reduces to a pure state $\rho(-\infty) = |\psi(-\infty)\rangle\langle\psi(-\infty)|$ and consequently we have $Z = 1$. Exploiting that adiabatic switching leaves $|\psi(-\infty)\rangle$ intact up to a phase factor, we are allowed to replace $\langle\psi(-\infty)|U^\dagger(t, -\infty) = \frac{\langle\psi(-\infty)|U(\infty,t)}{\langle\psi(-\infty)|U(-\infty,\infty)|\psi(-\infty)\rangle}$. Finally, we interpret the time-ordering as a contour-ordering on the branch C_1 (going from $t = -\infty$ to $t_{\mathrm{max}} = \infty$) of the Keldysh-Matsubara contour such that we arrive at

$$\langle \hat{A}(t) \rangle_H = \frac{\langle\psi(-\infty)|\mathcal{T}_C \left\{ e^{-i\int_{C_1} H(t')\mathrm{d}t'} A(t) \right\} |\psi(-\infty)\rangle}{\langle\psi(-\infty)|\mathcal{T}_C \, e^{-i\int_{C_1} H(t')\mathrm{d}t'}|\psi(-\infty)\rangle}, \tag{2.3}$$

which is the well-known starting point of zero-temperature perturbation theory. Let us emphasize that the interpretation of the imaginary-time ordering in the Matsubara approach as a contour-ordering on the branch C_3 and similarly the interpretation of the time ordering in the zero-temperature formalism as a contour-ordering on the branch C_1 implies structural identity to the Keldysh-Matsubara formalism up to the explicit form of the involved contour. It is therefore to no surprise that the same set of diagrams emerges in all three cases (see Ref. [32] for a more in-depth discussion).

2.2. Nonequilibrium Green's functions for fermionic lattice models

While our considerations so far have been completely general, we will from now on restrict the discussion to time-dependent, fermionic lattice models. The Hamiltonian reads

$$H(t) = \sum_{ij}(T_{ij}(t) - \delta_{ij}\mu)c_i^\dagger c_j + \frac{1}{2}\sum_{kk'll'}U_{kk'll'}(t)c_k^\dagger c_{k'}^\dagger c_{l'} c_l, \tag{2.4}$$

where the indices i, j run over the possible one-particle orbitals (lattice sites, local orbitals, spin projection, ...). Fermions in such states are created (annihilated) by the operators $c_i^\dagger$ (c_i). Without loss of generality, we assume the symmetry relation $U_{kk'll'}(t) = -U_{k'kll'}(t) = -U_{kk'l'l}(t) = U_{k'kl'l}(t)$ to hold for the interaction term which leads to a leaner notation.

A quantity central to this thesis is the contour-ordered one-particle Green's function. It is defined as

$$G_{ij}(t, t') = -i\langle \mathcal{T}_C\, \hat{c}_i(t)\hat{c}_j^\dagger(t')\rangle_H = \frac{-i}{Z}\mathrm{tr}\left(\exp\left(-\beta H_\mathrm{ini}\right)\left[\mathcal{T}_C\, \hat{c}_i(t)\hat{c}_j^\dagger(t')\right]\right). \tag{2.5}$$

Its equations of motion read

$$i\partial_t G_{ij}(t, t') = \delta_{ij}\delta_C(t, t') + \sum_k \left[T_{ik}(t) - \mu\delta_{ik}\right]G_{kj}(t, t') \tag{2.6}$$

$$- i\sum_{k'll'}U_{ik'll'}(t)\langle \mathcal{T}_C\hat{c}_{k'}^\dagger(t)\hat{c}_{l'}(t)\hat{c}_l(t)\hat{c}_j^\dagger(t')\rangle,$$

$$-i\partial_{t'} G_{ij}(t, t') = \delta_{ij}\delta_C(t, t') + \sum_k G_{ik}(t, t')\left[T_{kj}(t') - \mu\delta_{kj}\right]$$

$$- i\sum_{kk'l'}U_{kk'jl'}(t')\langle \mathcal{T}_C\hat{c}_i(t)\hat{c}_k^\dagger(t')\hat{c}_{k'}^\dagger(t')\hat{c}_{l'}(t')\rangle.$$

It is worthwhile to note that the equations of motion reflect the main complication of many-body theory: The set of equations is non-closed due to the interaction term which couples the one-particle Green's function to correlation functions of second order. The same pattern repeats itself if one calculates the equations of motion of higher-order correlation functions. A systematic analysis leads to the Martin-Schwinger hierarchy [97], a solution of which, however, is not possible without making approximations.

The standard way to relate the two-particle terms back to the one-particle Green's function is based on defining the so called *self-energy* Σ:

$$[\Sigma \circ G]_{ij}(t, t') = -i\sum_{k'll'}U_{ik'll'}(t)\langle \mathcal{T}_C\hat{c}_{k'}^\dagger(t)\hat{c}_{l'}(t)\hat{c}_l(t)\hat{c}_j^\dagger(t')\rangle, \tag{2.7}$$

$$[G \circ \Sigma]_{ij}(t, t') = -i\sum_{kk'l'}U_{kk'jl'}(t')\langle \mathcal{T}_C\hat{c}_i(t)\hat{c}_k^\dagger(t')\hat{c}_{k'}^\dagger(t')\hat{c}_{l'}(t')\rangle.$$

Here, we have made use of a shorthand notation for the convolution of contour matrices. For example:

$$[G \circ \Sigma]_{ij}(t, t') = \int_C \mathrm{d}t_1 \sum_l G_{il\sigma}(t, t_1)\Sigma_{lj\sigma}(t_1, t'). \tag{2.8}$$

We will employ the same notation for matrix products involving time-local quantities by assuming an implicit contour Dirac delta function $\delta_C(t, t')$ to be present. For example, $T(t)$ should be replaced by $T(t)\delta_C(t, t')$ in a contour convolution, so that

$$[T \circ G]_{ij\sigma}(t, t') = \int_C dt_1 \sum_l T_{il\sigma}(t)\delta_C(t, t_1)G_{lj\sigma}(t_1, t') \tag{2.9}$$
$$= \sum_l T_{il\sigma}(t)G_{lj\sigma}(t, t').$$

A common way to establish that the self-energy is a well-defined object relies on an explicit construction by means of diagrammatic perturbation theory [32]. As part of this thesis, we follow a different route and construct the self-energy in a rather special form which highlights its mathematical structure: The so called *Lehmann representation*, cf. Chapter 3.

Making use of Eq. (2.7), the equation of motion of the one-particle Green's function can be expressed in terms of the one-particle Green's function and the self-energy. The result is known as *Dyson's equation*:

$$G = G_0 + G_0 \circ \Sigma \circ G. \tag{2.10}$$

G_0 denotes the noninteracting propagator. Its (contour) inverse can be stated analytically

$$[G_0^{-1}]_{ij}(t, t') = [\delta_{ij}(i\partial_t + \mu) - T_{ij}(t)]\,\delta_C(t, t'). \tag{2.11}$$

While the dynamics of Eq. (2.10) is purely Markovian for $\Sigma = 0$, the self-energy can be interpreted as a memory kernel introducing retardation effects in case of non-vanishing interaction. We will investigate this further in Chapter 3.

It is worthwhile to note that, while a formal solution for the one-particle Green's to Eq. (2.10) is easily found, this solution involves the self-energy as an unknown object. A closed set of equations can be obtained by expressing the self-energy as the sum of all dressed skeleton diagrams [32]. This gives an independent equation, $\Sigma = \Sigma_U[G]$, where $\Sigma_U[\cdot]$ is a functional on the space of one-particle Green's functions. This functional is universal in the sense that it only depends on the interaction term U but not on the hopping T. Summing the diagrammatic series to a closed form expression, however, has so far not been possible even for the most simple interaction terms like the completely local Hubbard interaction. In practice, one therefore has to truncate the series if aiming at a numerical solution (e.g., Ref. 102).

2.3. Lehmann representation of the nonequilibrium Green's function

In many-particle theory, the term *Lehmann representation* refers to the decomposition of the interacting Green's function into a superposition of noninteracting, isolated modes. For equilibrium Green's functions, this is a standard textbook result, e.g. Ref. 89. It uncovers their analytical properties and can be used to show that the related spectral function is positive definite. The Lehmann representation is further essential for the evaluation of

2. Nonequilibrium formalism

diagrams through contour integrations in the complex frequency plane, for the derivation of sum rules, etc. It refers to the expression

$$G_{ij}(\omega) = \sum_{mn} \frac{e^{-\beta E_m} + e^{-\beta E_n}}{Z} \frac{\langle m|c_i|n\rangle\langle n|c_j^\dagger|m\rangle}{\omega - (E_n - E_m)}, \tag{2.12}$$

where $|m\rangle$ refers to the m-th eigenstate with eigenenergy E_m of the initial Hamiltonian (i.e., $H_{\text{ini}}|m\rangle = E_m|m\rangle$) and Z to the grand-canonical partition function. We identify the Green's function of an isolated mode ($h_{\text{mode}} = \epsilon c^\dagger c$) in frequency space

$$g(\epsilon; \omega) = \frac{1}{\omega - \epsilon} \tag{2.13}$$

and define the "Q-matrix" [103, 104]: $Q_{i(m,n)} = z_{(m,n)}\langle m|c_i|n\rangle$, where we introduced the quantity $z_{(m,n)} = \sqrt{(e^{-\beta E_m} + e^{-\beta E_n})/Z}$. As a useful property, the rows of the Q-matrix fulfill the orthonormality condition

$$\sum_{mn} Q_{i(m,n)}Q_{j(m,n)}^* = \langle\{c_i, c_j^\dagger\}\rangle_H = \delta_{ij}. \tag{2.14}$$

Here, $\{A, B\} = AB + BA$ denotes the anticommutator. We emphasize that the Q-matrix is not quadratic. This implies in particular $\sum_i Q_{i(m,n)}Q_{i(m',n')}^* \neq \delta_{mm'}\delta_{nn'}$. Using the Q-matrix and $g(\epsilon; \omega)$, the Green's function is expressed as

$$G_{ij}(\omega) = \sum_{mn} Q_{i(m,n)}g(\epsilon_{(m,n)}; \omega)Q_{j(m,n)}^*, \quad \epsilon_{(m,n)} \equiv E_n - E_m. \tag{2.15}$$

A natural generalization of the Lehmann representation to nonequilibrium Green's functions based on Eq. (2.15) was discussed recently in the context of nonequilibrium dynamical mean-field theory, cf. Ref. 31. First of all, consider the following replacement for the Q-matrix

$$Q_{i(m,n)} \rightarrow Q_{i(m,n)}(t) = z_{(m,n)}\langle m|\hat{c}_i(t)|n\rangle e^{i\epsilon_{(m,n)}t}. \tag{2.16}$$

The orthonormality condition, Eq. (2.14), generalizes to $\sum_{mn} Q_{i(m,n)}(t)Q_{j(m,n)}^*(t) = \delta_{ij}$. Furthermore, $Q(t)$ is equal on the upper and lower branch of the Keldysh-Matsubara contour while being constant constant on the Matsubara branch with $Q(-i\tau) = Q(0)$ and $\tau \in [0, \beta]$. This restricts the dependence on imaginary-time, which corresponds to a frequency dependence in equilibrium, cf. Eq. (2.15), to the Green's function of the isolated mode. The correct replacement for $g(\epsilon; \omega)$ is obtained by using the Keldysh-Matsubara formalism to solve $h_{\text{mode}} = \epsilon c^\dagger c$ for the one-particle Green's function:[2]

$$g(\epsilon; \omega) \rightarrow g(\epsilon; t, t') = i[f(\epsilon) - \Theta_C(t, t')]e^{-i\epsilon(t-t')}. \tag{2.17}$$

---

[2] A curious reader might wonder, why the mathematical structure is so much more complex in nonequilibrium. In particular: Why does the Fermi distribution only appear here? The reason lies in the complexity of the backtransformation from spectral representation to imaginary time within the Matsubara formalism. With ω_n being the fermionic Matsubara frequencies and $\tau - \tau' \in (0, \beta)$, we have $g(\epsilon; -i\tau, -i\tau') = \frac{-i}{\beta}\sum_n g(\epsilon; i\omega_n)e^{-i\omega_n(\tau-\tau')} = \int_{-\infty}^{\infty}\frac{d\omega}{2\pi}(g(\epsilon; \omega+i0) - g(\epsilon; \omega-i0))f(\omega)e^{-\omega(\tau-\tau')}$. The equality is based on the residue theorem and exploits that, on the imaginary axis, the Fermi distribution has simple poles at the Matsubara frequencies. The Fermi distribution therefore arises naturally as port of the backtransformation.

$f(\epsilon) = (e^{\beta\epsilon}+1)^{-1}$ denotes the Fermi-function while $\Theta_C(t,t')$ refers to the contour variant of the Heaviside step function ($\Theta_C(t,t') = 1$ for $t \geq_C t'$, $\Theta_C(t,t') = 0$ otherwise). Finally, the Lehmann representation of the nonequilibrium Green's function is given by

$$G_{ij}(t,t') = \sum_{mn} Q_{i(m,n)}(t)g(\epsilon_{(m,n)};t,t')Q^*_{j(m,n)}(t'). \qquad (2.18)$$

Of course, this result can also be obtained rigorously. To this end, it is sufficient to expand the definition of the nonequilibrium Green's function, Eq. (2.5), using the eigenstates $|m\rangle$ of the initial Hamiltonian H_{ini} and then to identify the Q-matrix and the solution of the isolated mode, $g(\epsilon; t, t')$.

The special form of the nonequilibrium Green's function, Eq. (2.18), highlights its mathematical structure. It features $g(\epsilon; t, t')$, which is analytically known as the nonequilibrium solution of an isolated mode, as the only quantity that depends on both contour times. The complicated Q-matrix, on the other hand, is time local. To explicitly mention a possible application, let us note that in Ref. 31 it was used to prove that the nonequilibrium DMFT action, a quantity dependent on two-contour times, can be mapped onto a single-impurity Anderson Hamiltonian, a quantity dependent on a single time variable. Such a mapping allows for powerful Hamiltonian-based methods being used as impurity solvers, e.g., the multi-configuration time-dependent Hartree method [48] or, most promising, the time-dependent DMRG [47].

3. Lehmann representation of the nonequilibrium self-energy

In the last chapter we have introduced some basic notions of out-of-equilibrium many-body theory for fermionic lattice models. Most importantly for this thesis: The Lehmann representation of the nonequilibrium Green's function, which uncovers the mathematical structure of its dependence on the two contour times. The explicit construction of a Lehmann representation for the *self-energy*, on the other hand, turns out to be more tedious yet useful nevertheless. This is already true for the equilibrium case. In a recent work, for example, a highly non-trivial diagrammatic construction has been worked out [106] which was subsequently used to cure the problem of possibly negative spectral functions arising from a summation of a subclass of diagrams.

In nonequilibrium, additional complexity arises from the arbitrary time dependence of the model parameters so that even the existence of a Lehmann representation of the self-energy is unclear a priori. However, *if existent* it allows to map Dyson's equation onto a Markovian (i.e., memory-kernel-free) propagation scheme as was pointed out recently [50]. This can lead to a tremendous speedup within numerical applications as solving Dyson's equation scales cubically in the maximum propagation time compared to a linear scaling in the mapped Markovian case. We recapitulate the idea in Sec. 3.1. In Section 3.2, one of the main results of this thesis is presented: We explicitly construct the Lehmann representation of the nonequilibrium self-energy in case of an arbitrary time-dependent interacting lattice fermion model. In the course of this we show that any such model can exactly be mapped to a *noninteracting* lattice fermion model. Section 3.3 details the numerical foundations allowing for a practical implementation. Finally, a summary is given in Section 3.4.

3.1. Motivation

In several Green's-function-based methods, an approximate self-energy Σ' is obtained from a small reference system by using exact diagonalization. The desired one-particle Green's function G of a much larger system is then obtained through Dyson's equation

$$G_{ij}(t, t') = [G_0]_{ij}(t, t') + \int_C \int_C \mathrm{d}t_1 \mathrm{d}t_2 \sum_{k_1 k_2} [G_0]_{ik_1}(t, t_1) \Sigma'_{k_1 k_2}(t_1, t_2) G_{k_2 j}(t_1, t'), \quad (3.1)$$

15

where G_0 denotes the noninteracting Green's function (i.e., $U = 0$) of the model given by Eq. (2.4). Typical examples include dynamical mean-field theory (DMFT) [39, 40, 42, 44], where Σ' is obtained from a single-impurity Anderson model [31], or cluster perturbation [107–112] and self-energy functional theory [75, 76, 113], where Σ' stems from a small reference system. To solve Eq. (3.1) numerically, a discretization of the continuous time-contour C is necessary (cf. Fig. 2.1). The number of time steps required to reach a given maximal time is dependent on the lowest relevant timescale that is set by a given Hamiltonian. Based on this discretization, the effort required to solve Eq. (3.1) for G scales cubically in the number of time steps and also the system size. Despite this challenge also the memory consumption, which scales quadratically in these quantities, poses a problem. Progress was made recently [50] by introducing a mapping of Eq. (3.1) onto a Markovian propagation-scheme.

The idea proposed by the authors of Ref. 50 relies on the *assumption* that the self-energy can be written in the following form:

$$\Sigma'_{ij}(t, t') = \delta_C(t, t')\Sigma'^{\mathrm{HF}}_{ij}(t) + \sum_s h_{is}(t)g(h_{ss}; t, t')h^*_{js}(t). \tag{3.2}$$

Here, $\Sigma'^{\mathrm{HF}}_{ij}(t)$ denotes the time-local Hartree-Fock term. This decomposition is very similar to the expression Eq. (2.18) for the Green's function. We will refer to this as the Lehmann representation of the self-energy. The immediate and important advantage of the Lehmann representation is that the self-energy can be interpreted as a hybridization function [31, 50]. This property allows to write down an effective noninteracting model with Hamiltonian

$$H_{\mathrm{eff}}(t) = \sum_{ij}(T_{ij}(t) + \Sigma'^{\mathrm{HF}}_{ij}(t))c_i^\dagger c_j + \sum_{is}(h_{is}(t)c_i^\dagger f_s + \mathrm{H.c.}) + \sum_s h_{ss}f_s^\dagger f_s. \tag{3.3}$$

The s-degrees of freedom represent "virtual" orbitals in addition to the physical degrees of freedom labeled by i. They form an "effective medium" with time-independent on-site energies h_{ss} and hybridization strengths $h_{is}(t)$ such that the *interacting* Green's function of the original model is the same as the Green's function of the effective noninteracting model on the physical orbitals:

$$G_{ij}(t, t') = -i\langle \mathcal{T}_C\, \hat{c}_i(t)\hat{c}_j^\dagger(t')\rangle_{H_{\mathrm{eff}}}. \tag{3.4}$$

With this simple construction, the inversion of the Dyson equation can be avoided in favor of a Markovian (i.e., memory-kernel-free) time propagation within a noninteracting model.

As a successful benchmark, an interaction quench in an inhomogeneous Hubbard model was treated with nonequilibrium DMFT in Ref. 50 using self-consistent second-order perturbation theory as impurity solver. On the theoretical side, however, it remained an open question if the existence of a Lehmann representation must be postulated or if this is a general property of the nonequilibrium self-energy.

In the following we explicitly derive Eq. (3.2) for the exact self-energy corresponding to the general, interacting Hamiltonian defined in Eq. (2.4), i.e., we show that the exact

self-energy can always be written in the form of a Lehmann representation. The proposed construction scheme is not only useful as an analytical tool but also well suited for numerical applications where an approximate self-energy is obtained from a small reference system using exact diagonalization. In this case, the number of virtual orbitals is constant and the effort for solving Eq. (3.1) scales linearly in $t_{\max}$. This is a great advantage if one is interested in long-time dynamics.

3.2. Analytical construction

We start our construction from the Lehmann representation of G as stated in Eq. (2.18) and define $\alpha \equiv (m, n)$ as a shorthand notation for the remainder of this chapter (cf. Fig. 3.1). For our model Hamiltonian (2.4) the associated one-particle excitation energies ϵ_α and the Q-matrix are given by Eq. (2.16). The self-energy is related to this representation through Dyson's equation $\Sigma = G_0^{-1} - G^{-1}$. However, the inverse G^{-1} cannot directly be calculated with Eq. (2.18) since $Q(t)$ is not quadratic. As a first step we block up the matrix $Q(t)$ to a quadratic form. This is achieved by interpreting its orthonormal rows (cf. the remark beneath Eq. (2.16)) as an incomplete set of basis vectors. $Q(t)$ itself is an incomplete unitary transform from this viewpoint. We now pick an arbitrary, pairwise orthonormal completion of this basis to find an unitary transform $O(t)$ that contains $Q(t)$ in its upper block (cf. Fig. 3.1). The next steps of our discussion will be independent of the particular completion that is chosen. The only mathematical requirement is that it is as smooth (and thus differentiable) in the time variable t as $Q(t)$; see Section 4.4 for numerical details on the construction of $O(t)$.

The completed unitary transform $O(t)$ describes additional virtual orbitals (labeled by the index s, see Fig. 3.1 and Eq. (3.3)). For convenience, we also absorb in the definition of $O(t)$ the extra factor $\mathcal{E}_{\alpha\alpha'}(t) = \delta_{\alpha\alpha'}\exp\left(-i\epsilon_\alpha t\right)$ that stems from the noninteracting Green's function $g(\epsilon_\alpha; t, t')$ (cf. Eqs. (2.18) and (2.17)). For clarity in the notations we use the following index convention throughout this work

$$\text{physical orbitals: } i, j, \quad \text{virtual orbitals: } r, s, \tag{3.5}$$
$$\text{physical } or \text{ virtual orbitals: } x, y, \quad \text{excitations: } \alpha, \alpha'.$$

Like every time-dependent unitary transform, $O(t)$ is generated by an associated Hermitian matrix. We define

$$h_{xy}(t) = \sum_\alpha [i\partial_t O_{x\alpha}(t)] O_{\alpha y}^\dagger(t). \tag{3.6}$$

Indeed, by integration we have

$$O(t) = \mathcal{T}\exp\left(-i\int_0^t h(t')\mathrm{d}t'\right) O(0) \tag{3.7}$$

and furthermore $h(t)$ is Hermitian:

$$h(t) = [i\partial_t O(t)]O^\dagger(t) = i\partial_t[O(t)O^\dagger(t)] - O(t)i\partial_t O^\dagger(t)$$
$$= \left([i\partial_t O(t)]O^\dagger(t)\right)^\dagger = h^\dagger(t). \tag{3.8}$$

3. Lehmann representation of the nonequilibrium self-energy
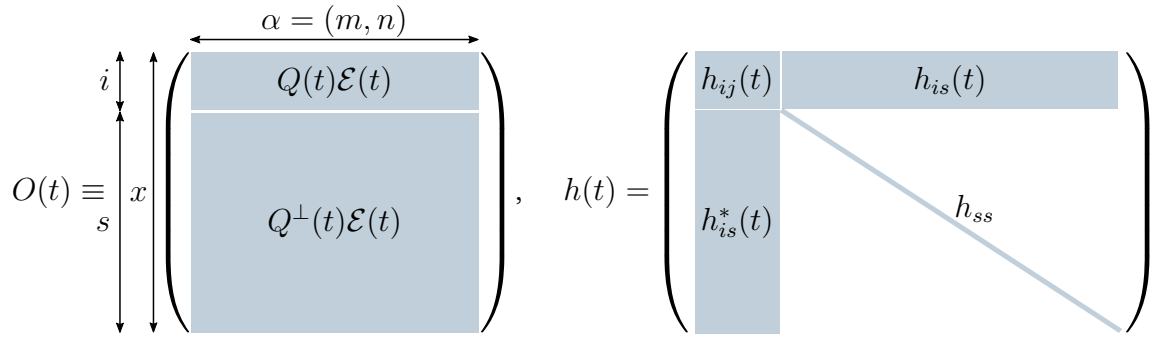
Figure 3.1.: Unitary completion of the time-dependent matrix $Q(t)$. The matrix $Q^\perp(t)$ contains a completing set of orthonormal basis vectors in its rows. For convenience, the phase factor $\mathcal{E}_{\alpha\alpha'}(t) = \delta_{\alpha\alpha'}\exp(-i\epsilon_\alpha t)$ is also absorbed into $O(t)$. The generating, Hermitian matrix $h(t)$ (cf. Eq. (3.6)) can be assumed as diagonal and time-independent in the virtual sector.

We now require the virtual part $h_{ss'}(t)$ to be diagonal and time-independent such that $h_{ss'}(t) = h_{ss}(0)\delta_{ss'}$. To this end we use our freedom in choosing the completing basis vectors $Q^\perp(t)$ which allows us to perform the associated unitary transform in the virtual sector (see Fig. 3.1). With the resulting $h_{xy}(t)$ we define the single-particle Hamiltonian $H_{\text{eff}}(t)$

$$H_{\text{eff}}(t) = \sum_{xy} h_{xy}(t)a_x^\dagger a_y, \qquad (3.9)$$

which has precisely the form of the effective Hamiltonian stated in Eq. (3.3). The requirement of a diagonal virtual sector defines the effective Hamiltonian uniquely up to rotations in invariant subspaces.

At time $t = 0$, the effective medium can be stated in a diagonal form which is useful for the evaluation of the corresponding one-particle Green's function. We recall that we required $O(t)$ to be as smooth as $Q(t)$ and take a look at

$$[i\partial_t O(t)]_{t=0} = h(0)O(0) = O(0)M, \qquad (3.10)$$

where $M = O^\dagger(0)h(0)O(0)$. In particular, Eq. (3.10) implies $[i\partial_t Q(t)\mathcal{E}(t)]_{t=0} = Q(0)M$ (cf. Fig. 3.1), while Eq. (2.16) easily evaluates to $[[i\partial_t Q(t)\mathcal{E}(t)]_{i\alpha}]_{t=0} = Q(0)_{i\alpha}\epsilon_\alpha$. We can thus identify $M_{\alpha\alpha'} = \delta_{\alpha\alpha'}\epsilon_\alpha$. Putting everything together we find

$$h_{xy}(0) = \sum_\alpha O_{x\alpha}(0)\epsilon_\alpha O_{y\alpha}^*(0). \qquad (3.11)$$

We require that the effective medium is initially in thermal equilibrium with the same inverse temperature β and the same chemical potential μ as the physical system. The associated one-particle Green's function of the medium is defined as

$$F_{xy}(t,t') = -i\langle \mathcal{T}_C \hat{a}_x(t)\hat{a}_y^\dagger(t')\rangle_{H_{\text{eff}}}. \qquad (3.12)$$

Recalling the diagonal form of the effective medium at $t = 0$ (cf. Eq. 3.11) and using that the effective Hamiltonian (3.9) is noninteracting, we can easily rewrite this expression

into

$$F_{xy}(t, t') = i \sum_{\alpha} O_{x\alpha}(t)[f(\epsilon_\alpha) - \Theta_C(t, t')]O_{y\alpha}^*(t'). \tag{3.13}$$

The physical sector of F is by construction identical with the Lehmann representation of G:

$$F_{ij}(t, t') = \sum_{\alpha} Q_{i\alpha}(t)g(\epsilon_\alpha; t, t')Q_{j\alpha}^*(t') = G_{ij}(t, t'). \tag{3.14}$$

F encodes the full information on the one-particle excitations of the system defined by the Hamiltonian (2.4). Eq. (3.14) further stresses the fact that in principle any (sufficiently smooth) completion of $Q(t)$ to a unitary transform $O(t)$ leads to a valid effective Hamiltonian. The physical sectors of $O(t)$ and $h(t)$ remain independent of its choice. The virtual sectors, on the other hand, are affected and only the special choice of $O(t)$ (cf. the discussion above and below Eq. (3.9)) guarantees a diagonal form of the effective medium.

Having found an effective, noninteracting model that reproduces the correct Green's function, it remains to link this back to the self-energy. The time-non-local (correlated) part $\Sigma_{ij}^C(t, t')$ follows by tracing out the virtual orbitals. This procedure is straightforward as they are all noninteracting and we can use, e.g., a cavity-like ansatz [31] or an equation of motion based approach [50]. This results in a hybridization-like function

$$\Sigma_{ij}^C(t, t') \equiv \sum_{s} h_{is}(t)g(h_{ss}; t, t')h_{js}^*(t') \tag{3.15}$$

that encodes the influence of the virtual sites on the physical sector. The Green's function at the physical orbitals is then obtained from a Dyson-like equation

$$F_{ij}(t, t') = \left[\frac{1}{F_0^{-1} - \Sigma^C}\right]_{ij}(t, t'), \tag{3.16}$$

where

$$[F_0^{-1}]_{ij}(t, t') = [i\partial_t - h_{ij}(t)]\delta_C(t, t'), \tag{3.17}$$

with $\delta_C(t, t') = \partial_t \Theta_C(t, t')$ as the contour delta function.

To make the final connection to the self-energy we evaluate the physical sector of h. With

$$i\partial_t Q_{i(m,n)}(t)e^{-i\epsilon_{(m,n)}t} = z_{(m,n)}\langle m|[\hat{c}_i(t), \hat{H}(t)]|n\rangle \tag{3.18}$$
$$= \sum_{j}(T_{ij}(t) - \mu\delta_{ij})Q_{j(m,n)}(t) + \sum_{ji'j'}U_{ii'jj'}(t)z_{(m,n)}\langle m|\hat{c}_{i'}^\dagger(t)\hat{c}_{j'}(t)\hat{c}_j(t)|n\rangle$$

we obtain

$$h_{ij}(t) = T_{ij}(t) - \delta_{ij}\mu + \Sigma_{ij}^{HF}(t), \tag{3.19}$$
$$\Sigma_{ij}^{HF}(t) \equiv 2\sum_{i'j'}U_{ii'jj'}(t)\langle \mathcal{T}_C\hat{c}_{i'}^\dagger(t)\hat{c}_{j'}(t)\rangle_H = 2\sum_{i'j'}U_{ii'jj'}(t)\langle \mathcal{T}_C\hat{a}_{i'}^\dagger(t)\hat{a}_{j'}(t)\rangle_{H_{\text{eff}}}.$$

At the physical orbitals the effective Hamiltonian is thus determined by the Hartree-Fock Hamiltonian. By comparison of Eq. (3.16) with Dyson's equation, Eq. (2.10), we finally identify

$$\Sigma_{ij}(t, t') = \delta_C(t, t')\Sigma_{ij}^{\mathrm{HF}}(t) + \Sigma_{ij}^{\mathrm{C}}(t, t'), \tag{3.20}$$

concluding our construction of the self-energy. Let us stress that with Eqs. (3.9), (3.15) and (3.19) we now have an *explicit* recipe to construct the Lehmann representation of the self-energy. This representation is further unique as follows from the uniqueness of the corresponding effective Hamiltonian (cf. the discussion above and below Eq. (3.9)).

3.2.1. Useful properties

With the Hamiltonian of the effective medium, Eq. (3.9), at hand, a number of useful properties follow immediately:

Positive spectral weight

By taking a look at the Matsubara branch only, one can link the Lehmann representation of the self-energy to the positive definiteness of its equilibrium spectral function. With $\Sigma^{\mathrm{M}}(\tau - \tau') \equiv -i\,\Sigma(-i\tau, -i\tau')$ we can perform the usual Fourier transform from imaginary time to Matsubara frequencies and then find the analytical continuation $\Sigma^{\mathrm{M}}(\omega)$ to the complex-frequency plane (see for example Ref. 31). The spectral function is defined as

$$C_{ij}^{\Sigma}(\omega) = \frac{i}{2\pi}[\Sigma_{ij}^{\mathrm{M}}(\omega + i0) - \Sigma_{ij}^{\mathrm{M}}(\omega - i0)] \tag{3.21}$$

for real ω. It can be calculated explicitly from the matrix elements of the effective Hamiltonian. One finds:

$$C_{ij}^{\Sigma}(\omega) = \sum_{s} h_{is}(0)h_{js}^{*}(0)\delta(\omega - h_{ss}), \tag{3.22}$$

where $\delta(\omega)$ is the Dirac delta function. The positive definiteness for every ω is immediately evident.

Higher-order correlation functions

The self-energy and its time derivatives can be used to calculate certain expectation values of higher order. Most prominent example is the interaction energy E_{int} which can be stated as

$$E_{\mathrm{int}}(t) = \frac{-i}{2}\int_{C} \mathrm{d}\tilde{t} \sum_{ij} \Sigma_{ij}(t, \tilde{t})G_{ji}(\tilde{t}, t^{+}), \tag{3.23}$$

as follows from Eq. (2.7). By comparing the equations of motion of $G_{ij}(t, t')$ and $F_{xy}(t, t')$ this contour convolution can be simplified using the effective Hamiltonian. One finds

$$\int_C d\tilde{t} \sum_j \Sigma_{ij}(t, \tilde{t}) G_{ji'}(\tilde{t}, t') = \sum_j [h_{ij}(t) - T_{ij}(t)] F_{ji'}(t, t')$$
$$+ \sum_s h_{is}(t) F_{si'}(t, t'). \quad (3.24)$$

This is a remarkable relation as the contour integration can be avoided in favor of a simple matrix multiplication.

In fact, arbitrary many-particle correlation functions can be expressed using relations analogous to Eq. (3.24). Consider, for example, the definition

$$\eta_{(ijk)x}(t) \equiv \sum_{mn} z_{(m,n)} \langle m | \hat{c}_i^\dagger(t) \hat{c}_j(t) \hat{c}_k(t) | n \rangle O^\dagger_{(m,n)x}(t) \quad (3.25)$$

Then

$$-i \sum_x \eta_{(ijk)x}(t) F_{xl}(t, t^+) = \sum_{mn} [z_{(m,n)}]^2 \langle m | \hat{c}_i^\dagger(t) \hat{c}_j(t) \hat{c}_k(t) | n \rangle f(\epsilon_{(m,n)}) \langle n | \hat{c}_l^\dagger(t) | m \rangle$$
$$= \langle \hat{c}_l^\dagger(t) \hat{c}_i^\dagger(t) \hat{c}_j(t) \hat{c}_k(t) \rangle_H. \quad (3.26)$$

Of course, while $\eta_{(ijk)x}(t)$ is easily stated through Eq. (3.25) if the system can be diagonalized exactly, an explicit expression might not be available in the context of approximate methods. This is similar to, for example, self-consistent perturbation theory where G and Σ are the only available quantities. In this case, only a small subset of multi-particle correlation functions is directly accessible.

Quantum quenches

A convenient tool to drive quantum systems out of equilibrium is given by the so-called quantum quenches. Here, one (or more) parameters of the system are changed suddenly. This sudden change reflects itself as a discontinuous time dependence of the effective Hamiltonian: Assume that the system is subjected to a quench at time $t = 0$, so that $H_{\text{ini}} \to H_{\text{final}} = \text{const}$. Initially the system is in thermal equilibrium and the effective Hamiltonian is given by Eq. (3.11), where ϵ_α are the excitations energies of H_{ini}. The O-matrix is continuous at $t = 0$ despite the quantum quench (it only depends on $\hat{c}_i(t)$, cf. Eq. (2.16)). Its time derivative, however, is not and thus $h(t)$ jumps from $h(0)$ to

$$h_{ij}(0^+) = \sum_\alpha [i \partial_t O_{i\alpha}(t)]_{t=0^+} O^*_{j\alpha}(0). \quad (3.27)$$

After this jump, the effective Hamiltonian will in general not be constant for times $t > 0$, i.e., $h(t) \neq h(0^+)$.

3.3. Numerical construction of the effective Hamiltonian

As discussed above Eq. (3.9) and shown in Fig. 3.1, it is possible to enforce a diagonal virtual sector of the effective Hamiltonian. Such a sparse form is of course advantageous within in a numerical context as it improves the scaling of matrix-matrix and matrix-vector multiplications. Assuming h is of dimension $N_h \times N_h$, a matrix-matrix multiplication scales quadratic, instead of cubic, and a matrix-vector multiplication linear in N_h due to the sparse form.

It remains to design an algorithm which allows to determine a unitary completion of the Q-matrix which is equally smooth as Q itself (regarding its time argument) and indeed gives a diagonal form for the virtual sector when inserted into Eq. (3.6). To this end, we assume that a small cluster is solved using exact diagonalization and that all time derivatives $H^{(n)}(t) = \partial_t^n H(t)$ of the Hamiltonian are given analytically. Since all eigenvectors of the initial Hamiltonian are known, the numerical evaluation of Eq. (2.16) becomes straightforward if we have an expression for $\hat{c}_i(t)$. Since we are also interested in n-th order derivatives, let us first consider the propagator $U(t,0) = \mathcal{T}\exp\left(-i\int_0^t H(t')\mathrm{d}t'\right)$:

$$U^{(n)}(t,0) = \partial_t^{n-1}(-iH(t)U(t,0)) \tag{3.28}$$

$$= -i\sum_{k=0}^{n-1}\binom{n-1}{k}H^{(k)}(t)U^{(n-1-k)}(t,0).$$

Eq. (3.28) allows to determine the n-th derivative $U^{(n)}(t,0)$ iteratively as it only depends on $U^{(k)}(t,0)$ with $k < n$. Using further that

$$\partial_t^n \hat{c}_i(t) = \sum_{k=0}^n \binom{n}{k}U^{(k)}(t,0)\, c_i\, [U^{(n-k)}(t,0)]^\dagger\,, \tag{3.29}$$

we find the n-th derivative $\hat{c}_i^{(n)}(t)$ of the annihilation operator and thus of $Q^{(n)}(t)$, see Eq. (2.16). In the following we will therefore assume that $Q^{(n)}(t)$ is available to arbitrary order.

3.3.1. The equilibrium Hamiltonian

At time $t = 0$, the effective medium is given by Eq. (3.11). $Q(0)$ and ϵ_α are directly accessible from exact diagonalization. It such remains to construct $Q^\perp(0)$, i.e., a basis for the virtual sector. We define

$$P_{\alpha\alpha'} = \sum_i Q_{i\alpha}^*(0)Q_{i\alpha'}(0)\,, \tag{3.30}$$

which can be easily verified to be a projector. Its eigenvalues are therefore restricted to 0 and 1. Eigenvectors corresponding to 1 are given by $Q(0)^\dagger$ itself, eigenvectors corresponding to 0, on the other hand, form the desired matrix $[Q^\perp(0)]^\dagger$. However, if we insert

this result into Eq. (3.11) we will have $h_{ss'} \neq 0$ for $s \neq s'$, i.e., generally h will not be diagonal in the virtual sector. This is due to the fact that we picked the completing part $Q^{\perp}(0)$ randomly. Explicit diagonalization of h in the virtual sector yields a unitary transform R

$$h_{ss'} = \sum_r R_{sr} d_r R^*_{rs'}. \tag{3.31}$$

Replacing $Q^{\perp}(0) \to RQ^{\perp}(0)$, we get $h_{ss'} \to \delta_{ss'}d_s$, i.e., we have found the desired completing basis which gives h with a diagonal virtual sector.

3.3.2. Propagation scheme

Assume now that $O(t)$ as well as $Q^{(n \geq 1)}(t)$ are known for an arbitrary time t. This is at least the case for $t = 0^+$, since we have $O(0) = O(0^+)$ even for a discontinuous time-dependence of $H(t)$ (cf. Sec. 3.2.1) while $Q^{(n \geq 1)}(t)$ is directly accessible at all times if we employ exact diagonalization. We recall that $h(t)$ is required to be constant and diagonal in the virtual sector (cf. discussion below Eq. (3.8))

$$h_{ss'}(t) = \delta_{ss'}h_{ss}(0) \quad \Rightarrow \quad h^{(n \geq 1)}_{ss'}(t) = 0, \tag{3.32}$$

i.e., all time derivatives vanish in the virtual sector. Only the hybridization elements and the physical sector yield non-trivial elements. They follow from Eq. (3.6) as

$$h^{(n)}_{iy}(t) = i \sum_{k=0}^{n} \binom{n}{k} \sum_{\alpha} [\partial_t^{k+1}(Q_{i\alpha}(t)e^{-i\epsilon_\alpha t})][O^{(n-k)}(t)]^\dagger]_{\alpha y}. \tag{3.33}$$

$O^{(n)}(t)$, on the other hand, only depends on $h^{(k)}(t)$ and $O^{(k)}(t)$, with $k < n$:

$$O^{(n)}(t) = -i\partial_t^{(n-1)}h(t)O(t) \tag{3.34}$$

$$= -i \sum_{k=0}^{n-1} \binom{n-1}{k} h^{(k)}(t)O^{(n-1-k)}(t).$$

It is thus possible to iteratively calculate $h^{(n)}(t)$ and $O^{(n)}(t)$.

With $O^{(n)}(t)$ at hand, $O(t + \Delta t)$ can be computed directly from its Taylor series. Alternatively, we can base the propagation on $h^{(n)}(t)$ and the analytical relation

$$O(t + \Delta t) = \mathcal{T}\left\{ \exp\left(-i \int_t^{t+\Delta t} h(t')dt'\right) \right\} O(t). \tag{3.35}$$

Using the Magnus expansion [114], the time-ordered exponential can be systematically expanded in Δt^n and $h^{(n)}(t)$. Assuming that Δt lies within the convergence radius of the Magnus expansion (this is generally expected to be the case for sufficiently small Δt), we can reduce the propagation error arbitrarily by increasing the order. In practice, an evaluation of the Magnus expansion using commutator-free exponential time propagators [115] (CFETs) allows for an efficient numerical propagation which takes advantage of the sparse form of the effective Hamiltonian.

The same procedure can be reiterated again and again to propagate $O(t)$ to arbitrary large times. We emphasize that the whole procedure is numerically exact, i.e., the error is below machine precision, if Δt is chosen sufficiently small.

3.3.3. Dimensionality of the O-matrix

For a one-band system with two spin degrees of freedom, the dimension of the Fock space scales as $\dim(\mathcal{F}_{T,U}) = 4^L$ where L is the number of lattice sites. The *full O-matrix*, as constructed in Section 3.2, strictly fulfills $\sum_x O_{x(m,n)}(t)O^*_{x(m',n')}(t) = \delta_{nn'}\delta_{mm'}$ for all possible combinations of (m,n). It is therefore of dimension

$$O(t) \in \mathbb{C}^{4^{2L} \times 4^{2L}}, \tag{3.36}$$

as both, $\langle m|$ and $|n\rangle$, run through all eigenstates of the Hamiltonian $H_{T,U}$, cf. Eq. (2.16). Already for a 4-site system, a naive implementation will therefore yield an O-Matrix of dimension $O(t) \in \mathbb{C}^{65536 \times 65536}$ which, assuming complex numbers at double precision (i.e., 128 bit per complex number), would require 64 GB of memory for storage. In practice, however, it is commonly possible to exploit certain symmetries of the Hamiltonian to drastically reduce this dimension. In the following we will assume that the Hamiltonian is particle-hole symmetric and that the total spin-density is conserved.

The minimal dimension of the O-matrix follows from the number of non-vanishing terms of the Q-matrix, cf. Eq. (2.16). Any combination (m,n), with $Q_{i(m,n)}(t) = 0$ for all times, can be neglected when completing the Q-matrix to the unitary O-matrix. We will refer to any O-matrix with a dimension less than $4^{2L} \times 4^{2L}$, cf. Eq. (3.36), as *reduced O-matrix*. First of all, let us consider finite temperatures, i.e., $z_{(m,n)} > 0$. Our task is to count the number of non-vanishing excitations $\langle m|\hat{c}_{i\sigma}(t)|n\rangle$. Exploiting conservation of the total spin, we can represent each eigenstate as a direct product, i.e., $|m\rangle = |m_\uparrow\rangle \otimes |m_\downarrow\rangle$, so that $\langle m|\hat{c}_{i\sigma}(t)|n\rangle = \langle m_{\bar{\sigma}}|n_{\bar{\sigma}}\rangle\langle m_\sigma|\hat{c}_{i\sigma}(t)|n_\sigma\rangle$. The number of contributing terms, N_{ct}, follows as

$$N_{ct} = \sum_{l=0}^{L} \binom{L}{l}^2 \times \sum_{k=0}^{L-1} \binom{L}{k}\binom{L}{k+1} = \frac{(2L)!^2}{L!^2(L-1)!(L+1)!} \equiv f(L). \tag{3.37}$$

This gives the explicit values:

$$\beta \in \mathbb{R}: \quad \begin{array}{c|ccccccc} L & 1 & 2 & 3 & 4 & 5 & 6 & \dots \\ \hline N_{ct} & 2 & 24 & 300 & 3920 & 52920 & 731\,808 & \dots \end{array}$$

The resulting reduced O-matrix, $O(t) \in \mathbb{C}^{N_{ct} \times N_{ct}}$, still looks quite large. However, the number reduces further if we restrict ourselves to systems which are initially at zero temperature, i.e., $\beta \to \infty$. This limit yields $z^{(m,n)} = 0$ if $E_m \neq 0 \wedge E_n \neq 0$. For a half-filled system with an even number of lattice sites and a non-degenerate ground state one obtains

$$N_{ct} = 2 \times \binom{L}{L/2}\binom{L}{(L/2+1)} = 2 \times f(L/2), \tag{3.38}$$

while for an odd number of lattice sites, the ground state is at least two-fold degenerate at half-filling due to particle-hole symmetry. One therefore finds

$$N_{ct} = 2 \times \left(\binom{L}{(L+3)/2}\binom{L}{(L-1)/2} + \binom{L}{(L+1)/2}\binom{L}{(L-1)/2}\right)$$
$$= f\left(\frac{L+1}{2}\right). \tag{3.39}$$

Combining these results, we obtain the following table

$$\beta \to \infty: \quad \begin{array}{c|cccccccc} L & 1 & 2 & 3 & 4 & 5 & 6 & 7 & 8 & ... \\ \hline N_{\text{ct}} & 2 & 4 & 24 & 48 & 300 & 600 & 3920 & 7840 & ... \end{array}$$

Within a practical application, the exact number of contributing terms may deviate from the table entries stated for $\beta \in \mathbb{R}$ and $\beta \to \infty$. At finite temperature, a further reduction of terms is often possible by introducing a cutoff value ϵ_{cutoff} and neglecting all terms with $z_{(m,n)} < \epsilon_{\text{cutoff}}$. On the other hand, even at zero temperature the minimal dimension can be substantially larger if one finds a degenerate ground state. An important example is the noninteracting 2×2 cluster with next-neighbor hopping which turns out to have a 16-fold degenerate ground state at half filling. Numerics yield $N_{\text{ct}} = 512 \gg 48$. Nevertheless, the takeaway message is that the algorithm performs best for initial states prepared at zero temperature.

3.4. Summary

Concluding, we have shown that the self-energy of an arbitrary interacting fermionic lattice model can be decomposed into a superposition of noninteracting isolated modes called the *Lehmann representation*. Our proof provides a direct scheme to construct this Lehmann representation of the self-energy, and thus allows for a deeper theoretical understanding of the self-energy complementary to its diagrammatic definition. Interestingly, our argumentation also shows that the original interacting system can exactly be mapped onto an exponentially large, noninteracting system described by an effective Hamiltonian.

To be used within a practical application, we have stated an algorithm that allows to construct this effective, noninteracting Hamiltonian which underlies the Lehmann representation of the self-energy. Most interestingly, the number of virtual sites, which is identical to the number of noninteracting modes within the Lehmann representation, is only dependent on the system size for a given problem and thus constant over time. This property is very useful in the context of methods where a small reference system is solved exactly to approximate the dynamics of a much larger system. A concrete numerical example is part of the next chapter (Section 4.4). There, the algorithm is used in the context of nonequilibrium cluster perturbation theory to access long timescales.

4. Cluster perturbation theory (CPT)

Based on the current state of theoretical computer science it is believed that, independent of the concrete method, the computational effort required to exactly simulate an arbitrary fermionic lattice system is only tractable if the system under consideration is small enough.[1] Indeed, this statement clearly holds true for the mapping procedure introduced in the laster chapter which involves an exponential scaling in system size of the dimension of the relevant matrices (the O-matrix and the effective medium, $h(t)$, cf. Sec. 3.3.3). Like every other exact-diagonalization-based approach, it is therefore limited to a rather small number of lattices sites (e.g., using the Lanczos technique, the half-filled Hubbard model on 24 sites was simulated in Ref. 119). One intuitive idea to tackle larger systems is to view them as being built up from many small clusters. These small clusters are easily solved. The remaining problem is then to couple the obtained solutions back together to finally reach the desired description of the original object of interest: the large system. The question is obvious: *What is the right way to embed the cluster solutions into the larger, original lattice?*

Of course, no matter how intuitive our argumentation, if considering an arbitrary fermionic lattice system any computationally tractable answer must bring us immediately into the realm of approximations. In the context of nonequilibrium Green's functions, a first rather basic approach is given by cluster perturbation theory (CPT) [107, 108]. Assume that we have solved the problem regarding the movement of a single electron within a system of disconnected clusters, i.e., we know the probability amplitude (Green's function) of an electron's movement between two sites i and j. The idea of the CPT to take into account the missing coupling between the clusters, commonly referred to as the *intercluster-hopping*, is most easily understood from a statistical point of view: The probability amplitude of an electron moving from one site i to another site j is the sum of the probability amplitudes of an electron doing so by (i) never crossing a cluster boundary (ii) exactly once crossing a cluster boundary (iii) exactly twice crossing a cluster boundary (iv - ∞) and so forth. For a noninteracting system, where electron movement is the only degree of freedom, this is exact.

Sections 4.1 – 4.3 have been published as part of C. Gramsch and M. Potthoff, "Enforcing conservation laws in nonequilibrium cluster perturbation theory", Phys. Rev. B **95**, 205130 (2017). Copyright (2017) by the American Physical Society. Reproduced with permission.

Sections 4.4 and 4.5 have been published as part of C. Gramsch and M. Potthoff, "Lehmann representation of the nonequilibrium self-energy", Phys. Rev. B **92**, 235135 (2015). Copyright (2015) by the American Physical Society. Reproduced with permission.

[1] To give a concrete example, the 2D fermionic Hubbard model with local magnetic fields is known to be a computationally hard problem, both on classical and quantum computers [117]. Considering only the former, the search for an polynomial generic algorithm for treating interacting quantum systems relates to the famous yet currently unproven hypothesis P $\neq$ NP, see Ref. 118 for a recent review.

However, the picture breaks down if we are dealing with interacting Green's functions. Regarding the starting point, i.e., the probability amplitude describing an electron's movement in the system of decoupled clusters, the interaction is already taken into account. What we are missing is again the intercluster-hopping. Yet, when performing the same summation as before, it turns out that a large class of possible processes is not taken into account. The CPT restricts the electron-electron interaction to the same cluster, i.e., an electron travelling from i to j may on its way only interact with other electrons who have *never* left their cluster. This is a dramatic simplification. In the most extreme example of a single-site cluster, the interaction electrons cannot move at all and as such nonlocal correlations are completely ignored. On the brighter side, the quality of the approximation can be controlled systematically. By using larger clusters, where the interaction electrons are more mobile, we improve the results.

Although the general scheme of the CPT is rather simple, one faces additional complexity if dealing with out-of-equilibrium setups. Here, translational invariance with respect to time is broken. A diagonal spectral representation of the CPT Green's function is therefore insufficient which must instead be stated as a non-diagonal quantity on the Keldysh-Matsubara contour. In particular, solving the CPT equation requires a matrix inversion which scales cubically in the maximal propagation time. To overcome this limitation, the existence of a Lehmann representation of the self-energy (cf. Chapter 3) can be exploited. This allows to define a time-local one-particle Hamiltonian that generates the CPT Green's function at the price of an exponentially large number of additional, virtual one-particle degrees of freedom in the cluster size. The time propagation, on the other hand, becomes Markovian so that the computational effort scales linear in the maximal propagation time.

Using the Hubbard model as a toy model (Sec. 4.1), we formulate the cluster perturbation theory in its self-energy-based and in the new time-local Hamiltonian-based form in Sections 4.2 and 4.3. To prove that the latter can be superior if considering out-of-equilibrium setups, we proceed by investigating a concrete example in Section 4.4: The dynamics of a single magnetic moment after an interaction quench within the 2D Hubbard model. Exploiting the Markovian character, simulation times up to $t_{\mathrm{max}} = 10^4$ become accessible for this inhomogeneous problem where the inverse nearest-neighbor hopping serves as the time unit. Yet the limitations of the CPT also surface, most prominently in the form of a violation of fundamental conservation laws. Finally, a conclusion is given in Section 4.5.

4.1. The Hubbard model

From the generic fermionic Hamiltonian defined in Eq. (2.4), the single-band Hubbard model on an arbitrary lattice is obtained by introducing two spin species $\sigma \in \{\uparrow, \downarrow\}$ and defining the interaction as purely local with interaction strength $U(t)$. The hopping matrix $T(t)$ is assumed as spin-diagonal for simplicity. The Hamiltonian reads

$$H_{T,U}(t) = \sum_{ij\sigma}(T_{ij\sigma}(t) - \delta_{ij}\mu)c_{i\sigma}^{\dagger}c_{j\sigma} + U(t)\sum_{i} n_{i\uparrow}n_{i\downarrow}, \qquad (4.1)$$

where $n_{i\sigma} = c_{i\sigma}^\dagger c_{i\sigma}$ denotes the spin-dependent local density operator. A formal derivation from Eq. (2.4) is possible by replacing $i \to (i\sigma)$ and defining $T_{i\sigma j\sigma'}(t) = \delta_{\sigma\sigma'}T_{ij\sigma}(t)$ as well as $U_{k\sigma_1 k'\sigma_2 l'\sigma_3 l\sigma_4}(t) = \frac{U(t)}{2}\left(\delta_{kl}\delta_{k'l'}\delta_{\sigma_1\sigma_4}\delta_{\sigma_2\sigma_3} - \delta_{kl'}\delta_{k'l}\delta_{\sigma_1\sigma_3}\delta_{\sigma_2\sigma_4}\right)\delta_{kk'}\delta_{\sigma_1\bar{\sigma}_2}$. Here, $\bar{\sigma}$ indicates a flip of the spin index σ, i.e., $\bar{\uparrow} = \downarrow$ and vice versa.

Simplifications to the nonequilibrium formalism

Within this chapter, the dependence of the Green's function and other quantities on $T(t)$ and $U(t)$ is made explicit in the notation using subscripts where convenient (e.g., $G_{T,U}$, $\Sigma_{T,U}$, etc.). Due to the locality of the interaction term a number of simplifications arise in comparison with the completely general expressions stated in Chapter 2. The contour convolution of self-energy and one-particle Green's function simplifies to

$$[\Sigma_{T,U} \circ G_{T,U}]_{ij\sigma}(t,t') = -iU(t)[G_{T,U}^{(2l)}]_{ij\sigma}(t,t'), \tag{4.2}$$

where we defined the two-particle Green's function $G^{(2l)}$

$$[G_{T,U}^{(2l)}]_{ij\sigma}(t,t') = \langle \mathcal{T}_C \, \hat{n}_{i\bar{\sigma}}(t)\hat{c}_{i\sigma}(t)\hat{c}_{j\sigma}^\dagger(t')\rangle. \tag{4.3}$$

Analogously, we have

$$-i[G_{T,U}^{(2r)}]_{ij\sigma}(t,t')U(t') = [G_{T,U} \circ \Sigma_{T,U}]_{ij\sigma}(t,t'), \tag{4.4}$$

where $G^{(2r)}$ is defined as

$$[G_{T,U}^{(2r)}]_{ij\sigma}(t,t') = \langle \mathcal{T}_C \, \hat{c}_{i\sigma}(t)\hat{n}_{j\bar{\sigma}}(t')\hat{c}_{j\sigma}^\dagger(t')\rangle. \tag{4.5}$$

The local doublon density $d_i(t)$ can thus be expressed using the self-energy and the one-particle Green's function

$$d_i(t) \equiv \langle \hat{n}_{i\uparrow}(t)\hat{n}_{i\downarrow}(t)\rangle_{H_{T,U}} \tag{4.6}$$
$$= \frac{-i}{U(t)}[\Sigma_{T,U} \circ G_{T,U}]_{ii\sigma}(t,t^+) = \frac{-i}{U(t)}[G_{T,U} \circ \Sigma_{T,U}]_{ii\sigma}(t,t^+).$$

Decomposition of the self-energy into its Lehmann representation

Using the formalism developed in Chapter 3, the self-energy $\Sigma_{T,U}$ can be decomposed into its Lehmann representation. This yields the unitary completion $O_{T,U}$ of the Q-matrix as well as the effective Hamiltonian

$$H_{T,U}^{\text{eff}}(t) = \sum_{xy\sigma}[h_{T,U}]_{xy\sigma}(t)a_{x\sigma}^\dagger a_{y\sigma} \tag{4.7}$$

and a corresponding Green's function $[F_{T,U}]_{xy\sigma}(t,t')$ (cf. Sec. 3.2). We recall that both quantities span the physical as well as the virtual sector and that $F_{T,U}$ is constructed such

that it coincides with $G_{T,U}$ in the former, cf. Eq. (3.14). Inspired by the fact that higher-order correlation functions can be accessed by means of simple matrix-matrix products (cf. Sec. 3.2.1) we define

$$[\eta_{T,U}]_{ix\sigma}(t) \equiv \sum_{mn} z_{(m,n)} \langle m | \hat{n}_{i\bar{\sigma}}(t)\hat{c}_{i\sigma}(t) | n \rangle [O_{T,U}]^{\dagger}_{(m,n)x\sigma}(t), \tag{4.8}$$

To avoid confusion about the virtual sector we further define $[\eta_{T,U}]_{ss'} = 0$, although we will never reference these elements. The two-particle Green's functions $G^{(2l)}_{T,U}$ and $G^{(2r)}_{T,U}$ are now given as

$$[G^{(2l)}_{T,U}]_{ij\sigma}(t,t') = i \sum_{x} [\eta_{T,U}]_{ix\sigma}(t)[F_{T,U}]_{xj\sigma}(t,t'), \tag{4.9}$$

$$[G^{(2r)}_{T,U}]_{ij\sigma}(t,t') = i \sum_{x} [F_{T,U}]_{ix\sigma}(t,t')[\eta_{T,U}]^{*}_{ix\sigma}(t'), \tag{4.10}$$

as readily follows from Eq. (3.26). Assuming $U(t) \neq 0$, a different route to access $[\eta_{T,U}]_{ix\sigma}(t)$ uses the matrix elements of the effective Hamiltonian:

$$[h_{T,U}]_{ij\sigma}(t) = U(t)[\eta_{T,U}]_{ij\sigma}(t) + T_{ij\sigma}(t) - \delta_{ij}\mu, \tag{4.11}$$
$$[h_{T,U}]_{is\sigma}(t) = U(t)[\eta_{T,U}]_{is\sigma}(t).$$

To be consistent with Eq. (3.19), $[\Sigma^{\mathrm{HF}}_{T,U}]_{ij\sigma}(t) = U(t)[\eta_{T,U}]_{ij\sigma}(t) = U(t)\delta_{ij}\langle \hat{n}_{i\bar{\sigma}}(t)\rangle_{H_{T,U}}$ must hold. This is indeed the case, as can be shown by evaluating Eq. (4.8) in the physical sector.

4.2. Self-energy-based formulation of the CPT

The idea of the CPT [107, 108] is to partition the lattice into clusters small enough to be treated exactly, e.g., using Krylov-space methods or full diagonalization, and to subsequently include the connections between the clusters perturbatively. On the level of the Hamiltonian one starts by partitioning the full hopping matrix T into the intra-cluster hopping T' and the inter-cluster hopping V so that T' only contains terms which connect lattice sites within the individual clusters, while V contains all remaining terms such that $T = T' + V$, see Fig. 4.1. Corresponding to the intra-cluster hopping, we define a cluster Hamiltonian $H_{T',U}(t)$ which describes the system of isolated clusters, also referred to as the reference system. Its Green's function and self-energy are denoted as $G_{T',U}$ and $\Sigma_{T',U}$, respectively.

For the equilibrium as well as for the nonequilibrium case [105, 110, 112], the CPT can be seen as an all-order perturbation theory in the inter-cluster hopping V which provides the one-particle Green's function of the original system by expanding around the cluster Green's function:

$$G^{\mathrm{CPT}} = G_{T',U} + G_{T',U} \circ V \circ G_{T',U} + \cdots = \frac{1}{G^{-1}_{T',U} - V}. \tag{4.12}$$
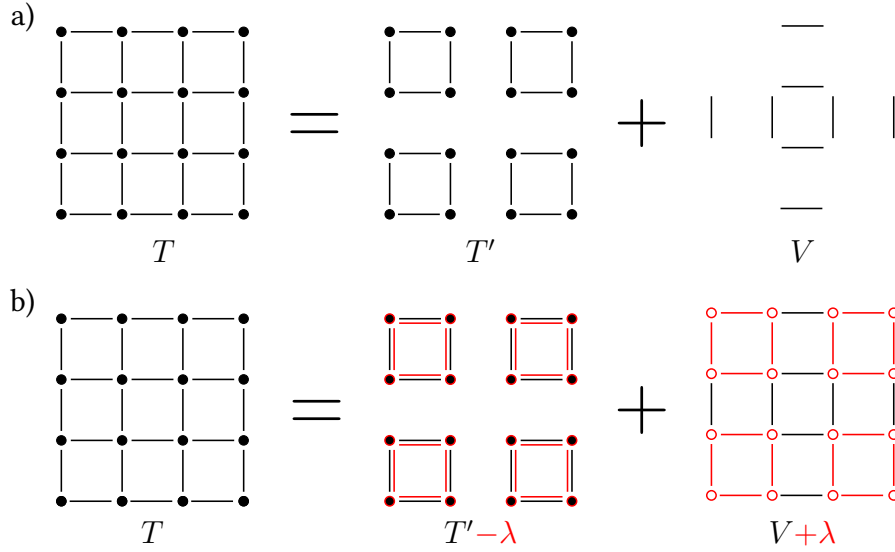
Figure 4.1.: Sketch of plain CPT (a) and conserving CPT (b). *Plain CPT:* the hopping matrix T is decomposed $T = T' + V$ into the intra-cluster (T') and the inter-cluster hopping V. The problem defined by T' (and the local Hubbard-type interaction) is solved exactly. V is treated by all-order perturbation theory (neglecting vertex corrections), see Eq. (4.12). *Conserving CPT:* the same as plain CPT but with "renormalized" intra- ($T' - \lambda$) and inter-cluster hopping $V + \lambda$, where the time-dependent renormalization λ (indicated in red) is used to enforce conservation laws. Note that λ may also comprise the on-site energies.

We also have:

$$G^{\text{CPT}} = \frac{1}{G_{T,0}^{-1} - \Sigma_{T',U}}. \tag{4.13}$$

In the noninteracting case, this is exact since $\Sigma_{T',0} = 0$. For finite $U(t)$, however, the CPT Green's function G^{CPT} represents an approximation of the exact Green's function $G_{T,U}$.

Eq. (4.13) defines the standard, *plain* CPT approach. A closer look, however, reveals that the CPT is not unique since one may consider a different starting point for the all-order perturbation theory in V. To this end, consider a starting point with a renormalized intra-cluster hopping, $T' \to T' - \lambda$, resulting in a renormalized cluster Green's function $G_{T'-\lambda,U}$ and self-energy $\Sigma_{T'-\lambda,U}$. Correspondingly, also the inter-cluster hopping V must be renormalized as $V \to V + \lambda$. Summation of the geometrical series yields

$$G^{\text{CPT}}[\lambda] = \frac{1}{G_{T'-\lambda,U}^{-1} - (V + \lambda)} = \frac{1}{G_{T,0}^{-1} - \Sigma_{T'-\lambda,U}}, \tag{4.14}$$

where we emphasized the special role of the renormalization parameter λ by square brackets. For $U(t) = 0$, we have $G^{\text{CPT}}[\lambda] = G_{T,0}$ for any λ. For an interacting system, however, the choice for λ is crucial, i.e., the resulting CPT Green's function does depend on the starting point of the all-order perturbation theory in the inter-cluster hopping. Finally, plain CPT at finite interaction is recovered as $G^{\text{CPT}}[0]$, i.e., the special role of the parameter λ is ignored in this case for simplicity.

This ambiguity in the definition of the CPT seems to be problematic on first sight, yet it can be turned into an advantage by interpreting the renormalization λ as an optimization parameter. This has been worked out systematically in the context of the (nonequilibrium) self-energy functional theory (SFT) [76, 78, 113, 120], where the optimal λ is derived from a variational principle based on the self-energy. In the following Chapter 5, we will take a slightly different route and use the freedom in λ to enforce local constraints on the spin-dependent particle and the doublon density which in turn will guarantee the otherwise violated macroscopic conservation laws. Physically, the parameter set λ must be interpreted as a nonlocal mean-field and the resulting conserving CPT as a cluster mean-field theory.

4.3. Hamiltonian-based formulation of the CPT

Let us now discuss how the CPT Green's function can be obtained from an effective one-particle Hamiltonian and how to set up a Markovian time-propagation scheme [105], As discussed in Sec. 4.2, we have $T = T' + V$ where $T' - \lambda$ is the renormalized intra-cluster and $V + \lambda$ the renormalized inter-cluster hopping. For each set of parameters λ, an effective one-particle CPT Hamiltonian can be defined by adding the inter-cluster hopping to the effective Hamiltonian (4.7) of the reference system:

$$H^{\mathrm{CPT}}[\lambda](t) = H^{\mathrm{eff}}_{T'-\lambda,U}(t) + \sum_{ij\sigma}[V_{ij\sigma}(t) + \lambda_{ij\sigma}(t)]c^\dagger_{i\sigma}c_{j\sigma} \tag{4.15}$$

$$\equiv \sum_{xy\sigma} h^{\mathrm{CPT}}_{xy\sigma}(t)c^\dagger_{x\sigma}c_{y\sigma}.$$

The CPT Green's function, as computed from $H^{\mathrm{CPT}}[\lambda](t)$,

$$G^{\mathrm{CPT}}[\lambda]_{xy\sigma}(t,t') = -i\langle \mathcal{T}_C \hat{c}_{x\sigma}(t)\hat{c}^\dagger_{y\sigma}(t')\rangle_{H^{\mathrm{CPT}}[\lambda]} \tag{4.16}$$

then coincides with the original definition in Eq. (4.14) if only the physical sector is considered, i.e., $(x,y) = (i,j)$. This can be verified easily by integrating out the virtual, s degrees of freedom from H^{CPT}. Eq. (4.15) reflects the freedom we have in the CPT construction as the λ-terms cancel in the physical sector. λ only enters implicitly through the hybridization strengths $h'_{is\sigma}(t)$, through the on-site energies $h'_{ss\sigma}$ (where $h' \equiv h_{T'-\lambda,U}$) and through the Hartree-Fock term $\Sigma^{\mathrm{HF}}_{T'-\lambda,U}$ of the reference system's Hamiltonian $H_{T'-\lambda,U}$. Similarly to the self-energy-based formulation, plain CPT is recovered as $H^{\mathrm{CPT}}[0]$.

For each set of parameters λ, the two-particle correlation function $G^{(2l)}$ is approximated within the context of the CPT as

$$G^{(2l)}[\lambda]_{ij\sigma}(t,t') = i\sum_x \eta'[\lambda]_{ix\sigma}(t)G^{\mathrm{CPT}}[\lambda]_{xj\sigma}(t,t'), \tag{4.17}$$

where we have defined

$$\eta'[\lambda] \equiv \eta_{T'-\lambda,U}. \tag{4.18}$$

Eq. (4.17) corresponds to the exact expression given by Eq. (4.9) and is in particular consistent with the standard approximation $G^{(2l)}[\lambda](t,t') = \frac{i}{U(t)}\left[\Sigma_{T'-\lambda,U} \circ G^{\mathrm{CPT}}[\lambda]\right](t,t')$.
$G^{(2r)}[\lambda]$ is defined analogously, and thus the symmetry relation

$$G^{(2r)}[\lambda]_{ji\sigma}(t,t^+) = \left[G^{(2l)}[\lambda]_{ij\sigma}(t,t^+)\right]^* \tag{4.19}$$

is ensured within the CPT independently of λ. We note that this symmetry is not sufficient to allow for an unambiguous definition of the doublon density based on Eq. (4.6). In addition, the diagonal elements must be independent of σ and their imaginary part must vanish. As will be discussed in detail in Chapter 5, both relations can be enforced through the renormalization parameter λ. In case of an arbitrary, non-conserving set of parameters λ and thus in particular for the plain CPT, the ambiguity needs to be circumvented by defining the doublon density as an average

$$d_i[\lambda](t) = -\frac{1}{4}\sum_\sigma \left[G^{(2l)}[\lambda]_{ii\sigma}(t,t^+) + G^{(2l)}[\lambda]_{ii\sigma}(t,t^+)\right]. \tag{4.20}$$

As an important observable of interest, the total energy is expressed as

$$\begin{aligned} E_{\mathrm{tot}}[\lambda](t) &= E_{\mathrm{kin}}[\lambda](t) + E_{\mathrm{int}}[\lambda](t) \\ &= -i\sum_{ij\sigma} T_{ij\sigma}(t)G^{\mathrm{CPT}}[\lambda]_{ij\sigma}(t,t^+) + U(t)\sum_i d_i[\lambda](t), \end{aligned} \tag{4.21}$$

within cluster perturbation theory.

4.4. Numerical example: An inhomogeneous setup in the 2D-Hubbard model

To showcase the potential of our time-local formulation of the CPT, we consider a concrete test scenario in this section: The dynamics of a local magnetic moment after an interaction quench in the 2D-Hubbard model. Measuring time in units of the inverse hopping, we are able to propagate the system up to a maximal time of $t_{\mathrm{max}} = 10^4$ in comparison to $t_{\mathrm{max}} = 10\text{--}20$ inverse hoppings that where reached in previous simulations using the nonequilibrium CPT (e.g., Refs. 110, 112).

We emphasized in Sections 4.2 and 4.3 that the CPT features an intrinsic degree of freedom, namely, the starting point $T' - \lambda$ of the all order perturbation theory. As this is a proof of concept calculation, we will consider *plain* CPT in this Section, i.e., $\lambda = 0$, for simplicity. A more advanced theory, which involves a self-consistent determination of λ by means of local constraints derived from the macroscopic conservation laws, is presented in Chapter 5.

4.4.1. Prethermalization

The study of real-time dynamics initiated by an interaction quench in the Hubbard model has attracted much attention recently [17, 79, 121–125]. Here, the system is prepared

in a thermal (usually noninteracting) initial state and then, after a sudden change of the interaction parameter U, evolves in time as prescribed by the interacting Hamiltonian. While the setup is apparently simple, the search for universal properties of the time evolution remains notoriously difficult due to the non-integrability of the Hubbard model in two and higher dimensions. Apart from the general assumption that non-integrable models feature thermalization and thus lose memory of the initial state in the long-time limit [126], only the time evolution after quenches to a weak, finite Hubbard U seems to be well understood so far. Here, it could be shown by means of weak-coupling perturbation theory [124, 125, 127, 128] that observables initially relax to non-thermal, quasistationary values (the system prethermalizes) before the significantly slower relaxation towards the thermal values sets in.

It was later worked out [129] that the mechanism which traps the system in a quasi-stationary prethermal state is quite similar to the mechanism that hinders noninteracting systems from thermalizing. In the latter case the integrability of the Hamiltonian leads to a large number of constants of motion that highly constrain the dynamics of the system. In case of weakly interacting systems it is the proximity to the integrable point that introduces approximate constants of motion and hinders relaxation beyond the prethermalization plateau on short timescales $t \lesssim T/U^2$ (here, T is the nearest-neighbor hopping). Relaxation towards the thermal average is delayed until later times ($t \gtrsim T^3/U^4$).

As a proof of concept of our formalism we use nonequilibrium CPT to investigate the short- and long-time dynamics of an inhomogeneous initial state after an interaction quench in the Hubbard model. In particular we will study if and to what extent the CPT is able to describe prethermalization and the subsequent relaxation to a thermal state.

4.4.2. Setup

We consider the Hubbard model at zero temperature ($\beta \to \infty$) and half-filling ($\mu = U/2$) on a square lattice of $L = 10 \times 10$ sites with periodic boundary conditions. The system is cut into 25 clusters of size 2×2. The hopping is restricted to nearest neighbors and we set $T = 1$ to fix energy and time units. Translational invariance of the initial state is broken by applying a local magnetic field of strength B to an arbitrarily chosen "impurity site" (here, site 0 in cluster 0):

$$T_{ij\sigma}(t) = \delta_{\langle i,j\rangle}T - z_\sigma \delta_{i,j}\delta_{i,0}\,B(t) \,, \tag{4.22}$$

where $\delta_{\langle\dots\rangle}$ is non-zero and unity for nearest neighbors only and where $z_\uparrow = +1$ and $z_\downarrow = -1$. Initially, the magnetic field is switched on with strength $B(0) = 10$ to induce a (nearly) fully polarized magnetic moment on the impurity site and then switched off for times $t > 0$:

$$B(t) = B(0)(1 - \Theta(t)). \tag{4.23}$$

Here, $\Theta(t)$ is the Heaviside step function. Furthermore, the interaction $U(t)$ is switched off initially and then switched on to a non-zero value U_{fin}

$$U(t) = U_{\text{fin}}\,\Theta(t). \tag{4.24}$$

Hence, in the quantum quench considered here, two parameters are changed simultaneously. The initial Hamiltonian H_{ini} features no interactions but is inhomogeneous due to the local magnetic field, the final Hamiltonian H_{fin} is translationally invariant due to the absence of the magnetic field but has a finite interaction $U_{\text{fin}} > 0$.

To apply nonequilibrium CPT, we use exact diagonalization to solve the 25 independent cluster problems and to construct the Hamiltonian of the effective medium (for details on the numerical implementation see Section 3.3). Finally, Eq. (4.15) is used to account for the inter-cluster hopping (we recall that $\lambda = 0$ in our case since we consider *plain* CPT). The number of non-zero elements of a cluster's Q-matrix and therefore the computational effort of our approach increases quadratically with the number of active states in the density matrix $\rho_{\text{cluster}} = \sum_m \exp\left(-\beta E_m\right)|m\rangle\langle m| \; (H_{\text{cluster}}|m\rangle = E_m|m\rangle)$, i.e., states that contribute with a significant weight $\exp\left(-\beta E_m\right)$ to thermal averages. For convenience we have therefore chosen a zero-temperature initial state and consider a weak interaction $U = 10^{-4}$ to lift the ground-state degeneracy present in the noninteracting system (denoted as $U = 0^+$ in the following). The effective Hamiltonian $h^I(t)$ for each cluster is then of size 48×48 and the final CPT Hamiltonian of size 1200×1200. Exploiting its sparse form we are able to perform $1,000,000$ time steps with $\Delta t = 0.01$ to reach a maximal time $t_{\text{max}} = 10^4$ with modest computational effort.

The partitioning of the lattice into 2×2 clusters by CPT breaks rotational and reflection symmetries of the original problem. These are restored by averaging the resulting one-particle density matrix over the 4 possible ways to cut the lattice into 2×2 clusters. In the following we will show results for the time evolution of the local magnetic moment $m_i(t) = n_{i\uparrow}(t) - n_{i\downarrow}(t)$ at the impurity ($m_{\text{Imp}}(t)$) and at its nearest neighbors ($m_{\text{NN}}(t)$). Only the latter are affected by the averaging. It restores the equivalence of nearest neighbors that lie in the same and nearest neighbors that lie in a neighboring cluster of the impurity. The extensive quantities total energy $E_{\text{tot}}(t) = E_{\text{kin}}(t) + E_{\text{int}}(t)$ (cf. Eq. (4.21)) and total magnetization $M(t) = \sum_i m_i(t)$ are both unaffected by the averaging.

The initial state is the same for all quenches discussed in the following. We find a polarization of $m_{\text{Imp}}(0) \approx 0.97$ at the impurity which is partially screened (e.g., $m_{\text{NN}}(0) = -0.04$) so that the total magnetization amounts to $M(0) = \sum_i m_i(0) \approx 0.70$.

4.4.3. Noninteracting case

We first discuss the noninteracting case, i.e., a purely magnetic quench where $U_{\text{fin}} = 0^+$. Here, CPT predicts the exact time evolution (cf. the discussion below Eq. (4.12)) since the cluster self-energies $\Sigma_{T',0}$ vanish. Our results are shown in Fig. 4.2. For short times ($t \in [10^{-2}, 4 \times 10^0]$) the local magnetic moment at the impurity $m_{\text{Imp}}(t)$ (blue line) decays to a value slightly above zero. Subsequently ($t \in [4 \times 10^0, 10^4]$) the dynamics is governed by collapse-and-revival oscillations caused by the finite system size. In particular we find that $m_{\text{Imp}}(t)$ returns arbitrarily close to its initial value for large times. This is readily understood from the fact that the system's dynamics is governed by the one-particle propagator $\exp\left(-iT_{\text{fin}}t\right)$ where T_{fin} denotes the final hopping matrix (i.e., after the quench). T_{fin} involves only a small number of different one-particle energy levels and thus $U(t,0)$ returns arbitrarily close to the identity matrix over time.

For the noninteracting system it is possible to directly access the long-time average of

Figure 4.2.: Time evolution of the local magnetic moment at the impurity ($m_{\mathrm{Imp}}(t)$, blue line) and its nearest neighbors ($m_{\mathrm{NN}}(t)$, orange line). The dark-blue (dark-orange) arrow, which is pointing from right to left, indicates the long time average of the blue (orange) curve. The light-blue (light-orange) arrow, which is pointing from left to right, indicates the analytical average, Eq. (4.25). The long time average was taken over $500,000$ data points in the interval $[0.5 \times 10^4, 10^4]$.

the one-particle density matrix. One finds

$$
\begin{aligned}
\rho_{ij\sigma}^{\mathrm{avg}} &= \lim_{t_{\max}\to\infty} \frac{1}{t_{\max}} \int_0^{t_{\max}} \mathrm{d}t \langle \hat{c}_{i\sigma}^\dagger(t) \hat{c}_{j\sigma}(t) \rangle \\
&= \frac{1}{L} \sum_{\vec{k}\vec{k}'} \delta_{\varepsilon_{\vec{k}},\varepsilon_{\vec{k}'}} e^{i(\vec{k}\cdot\vec{R}_i - \vec{k}'\cdot\vec{R}_j)} \langle \hat{c}_{\vec{k}\sigma}^\dagger(0) \hat{c}_{\vec{k}'\sigma}(0) \rangle,
\end{aligned}
\tag{4.25}
$$

where we used that H_{fin} can be diagonalized by a Fourier transformation involving the reciprocal lattice vectors $\vec{k}$ ($\vec{R}_i$ denotes the lattice vector to site i). This yields the expression $H_{\mathrm{fin}} = \sum_{\vec{k}\sigma} \varepsilon_{\vec{k}} \hat{c}_{\vec{k}\sigma}^\dagger \hat{c}_{\vec{k}\sigma}$ and $\hat{c}_{i\sigma}(t) = \frac{1}{\sqrt{L}} \sum_{\vec{k}} e^{-i\vec{k}\cdot\vec{R}_i} e^{-i\varepsilon_{\vec{k}} t} \hat{c}_{\vec{k}\sigma}(0)$, where L is the system size. In Fig. 4.2 this prediction is compared with the numerical time average and indeed shows perfect agreement. It is interesting to note that for non-degenerate energy levels ε_k one would have $\rho_{ii\sigma}^{\mathrm{avg}} = N_\sigma/L$, where N_σ is the total number of particles with spin σ, and therefore $m_i^{\mathrm{avg}} = M(0)/L$. We conclude that degeneracy of energy levels is required to find memory of the initial state encoded in the average local magnetic moments m_i^{avg}.

4.4.4. Quenches to finite U_{fin}

For finite U_{fin} the CPT becomes an approximation and it is a priori unclear what kind of phenomena it is able to describe. In Fig. 4.3 we show the long-time evolution for quenches to different U_{fin}. For weak $U_{\mathrm{fin}} \lesssim 0.5$ we find a (prethermalization-like) separation into
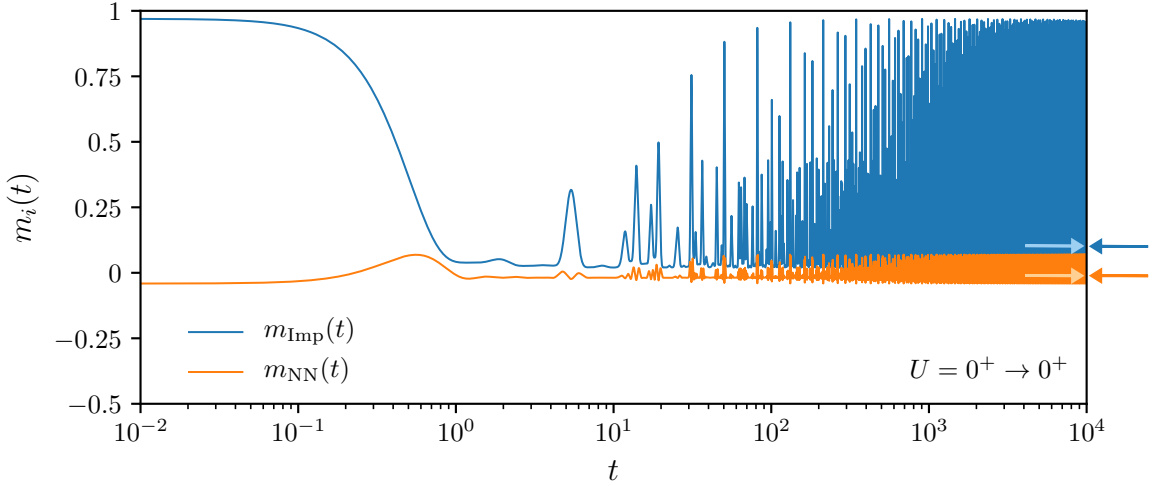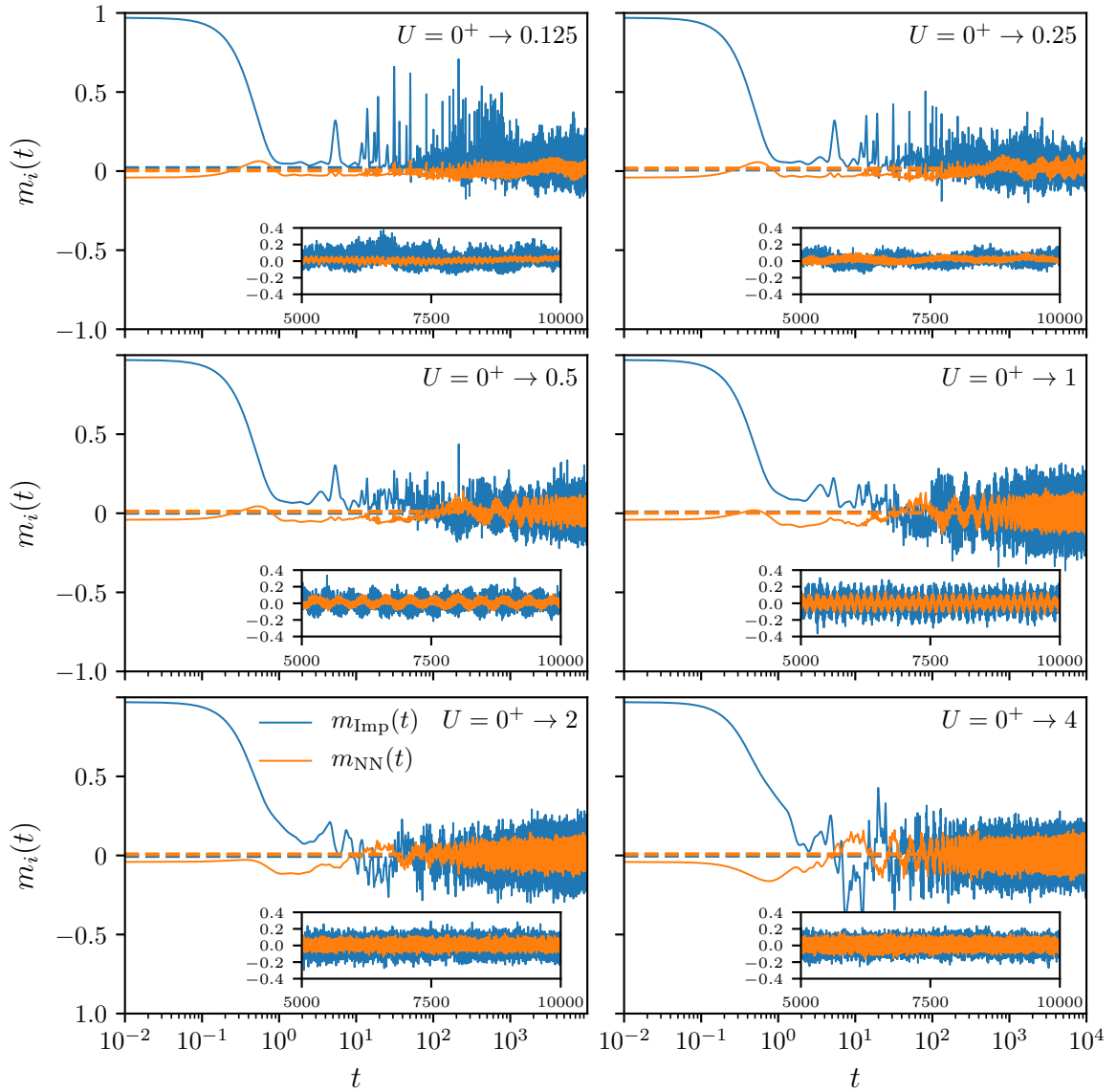
Figure 4.3.: CPT results for the time evolution of the local magnetic moment at the impurity ($m_{\text{Imp}}(t)$, blue line) and at its nearest neighbors ($m_{\text{NN}}(t)$, orange line) for quenches from the limit of vanishing interaction $U = 0^+$ (numerically implemented by setting $U = 0.0001$) to finite U_{fin}. In the insets the long-time behavior ($t \in [5 \times 10^3, 10^4]$) is plotted on a linear scale. The interval consists of $500,000$ data points and was also used to calculate the long-time average (straight dashed lines). In total 1,000,000 time steps were performed with $\Delta t = 0.01$ on a $L = 10 \times 10$ lattice (cut into 25 clusters of size 2×2 by CPT).

two different time scales. Initially the time evolution qualitatively follows the noninteracting case, i.e., we see a fast decay of the local moment at the impurity site (blue line) followed by a quasi-stationary region of collapse-and-revival oscillations. For larger times these oscillations decay and the system relaxes into a state characterized by quasi-periodic fluctuations around its long-time average (dashed blue line) which are driven by different frequencies. Taking a look at the U_{fin} dependence of the dynamics we notice that the region of collapse-and-revival oscillations shrinks with increasing U_{fin} and finally vanishes for $U_{\mathrm{fin}} \gtrsim 1$. The system then directly relaxes into a state with fluctuations around its long-time average.

For comparison, also the magnetic moment at the neighbouring sites $m_{\mathrm{NN}}(t)$ is plotted. While its dynamics for short times must naturally be different from $m_{\mathrm{Imp}}(t)$ due to the inhomogeneous initial state, we would expect a qualitative agreement in the long-time limit if the system thermalizes. However, this is not the case. There remains a clear difference in the amplitude of the fluctuations around the long-time average up to the largest simulated times. Hence we conclude that the system still keeps memory of the initial state and thus does not thermalize.

Having in mind the general discussion on prethermalization in Sec. 4.4.1, one can give an intuitive interpretation of these observations based on the effective-medium approach: While the noninteracting system is isolated and its dynamics is constrained through many constants of motion, there is a large number of virtual orbitals coupled to the system in the interacting case. These virtual orbitals act like a surrounding bath. For weak U_{fin} the virtual orbitals are only weakly coupled to the system and their influence is delayed to large times, while initially the dynamics is constrained similar to the noninteracting case. For strong U_{fin}, on the other hand, the coupling is strong and affects the dynamics of the system considerably. However, the number of virtual sites is still too small to allow for a complete dissipation of the information on the initial state into the bath. Therefore, a thermalized state is not reached. For an exact calculation the number of virtual sites would scale exponentially in system size. For CPT, on the other hand, it scales exponentially only in cluster size but linearly in the number of clusters and thus in the system size. Memory of the initial state is therefore retained within the one-particle density matrix and leaves its traces in the magnetic moments as seen in our calculations.

4.4.5. Violation of conservation laws

CPT as an approximation lacks any kind of self-consistency and is thus unable to respect the fundamental continuity equations and their corresponding conservation laws [76]. Therefore, one has to expect a violation of energy- or particle-number conservation, for example. Furthermore, in contrast to the equilibrium case where CPT interpolates between the exact limits $U = 0$ and $T = 0$, it yields exact results only for quenches to $U_{\mathrm{fin}} = 0$. The dynamics after a quench to the atomic limit $T_{\mathrm{fin}} = 0$ (with finite $U_{\mathrm{fin}} > 0$) cannot be described exactly due to the non-local entanglement of the initial state. We thus generally expect that the quality of the CPT results degrades with increasing interaction strength.

The numerical results for the total energy, see Fig. 4.4, confirm this expectation. Energy conservation is respected for $U_{\mathrm{fin}} = 0$, where CPT is exact. With $U_{\mathrm{fin}} > 0$ and increasing,
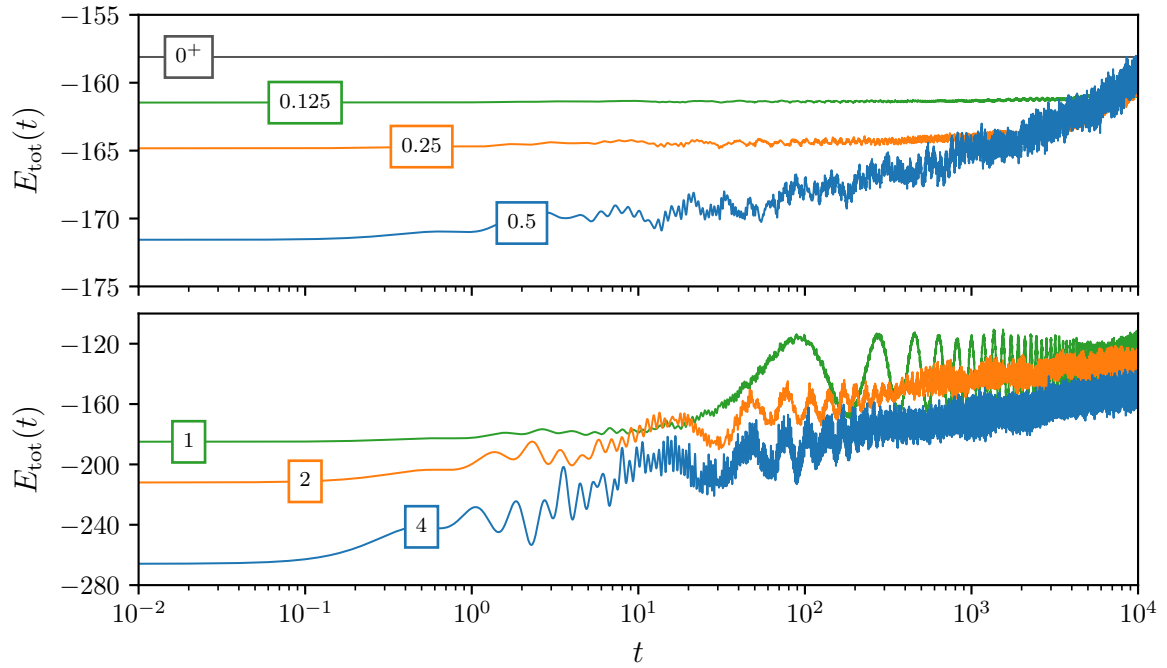
Figure 4.4.: Violation of energy conservation by the CPT. The numbers indicate the respective value of U_{fin}. Energy conservation is respected for $U_{\text{fin}} = 0^+$ where the CPT is exact (black line). An increasingly significant violation of energy conservation is seen for larger U_{fin}.
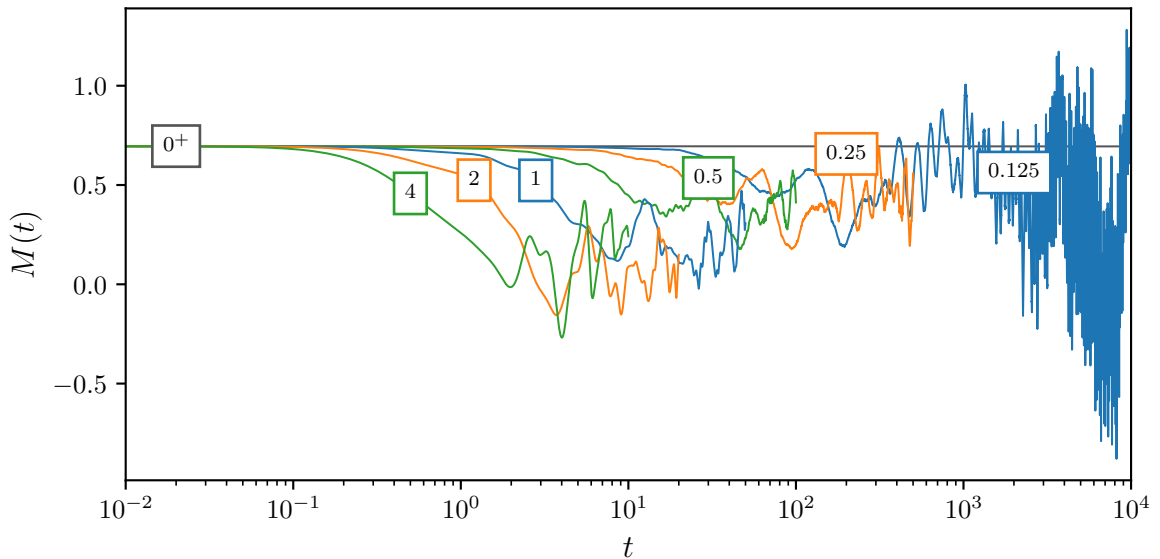
Figure 4.5.: Violation of conservation of the total magnetization M by the CPT. The numbers indicate the value of U_{fin}. Curves for $U_{\text{fin}} \geq 0.25$ are only partially plotted for better visibility.

however, a significant time dependence of the total energy sets in earlier and earlier. For $U_{\text{fin}} \gtrsim 1$ energy conservation is violated already for $t \lesssim 10$. Similar results are found for the total magnetization $M = \sum_i (n_{i\uparrow} - n_{i\downarrow})$, cf. Fig. 4.5. While the magnetization should be constant for all times since neither hopping nor interaction (cf. Eqs. (4.22) and (4.24)) involve spin-flip terms, we find such behavior only for short times. For longer times oscillations arise and the conservation of total magnetization is violated. For increasing U_{fin} the oscillations set in earlier indicating again that the quality of CPT is best for values of U_{fin} close to zero.

We note that the total particle number $N = N_\uparrow + N_\downarrow$, however, is conserved during the time evolution. This holds true for a half-filled and homogeneously charged system and is due to the fact that CPT preserves particle-hole symmetry. This can easily be understood as follows: Each cluster Hamiltonian is particle-hole symmetric and since each cluster is solved exactly within CPT the corresponding effective Hamiltonian $H^{\text{eff}}_{T',U}(t)$ is also particle-hole symmetric. The CPT Hamiltonian is now given by Eq. (4.15) which additionally includes the inter-cluster hopping. However, the inter-cluster hopping is clearly particle-hole symmetric and so is the final CPT Hamiltonian.

4.5. Summary

In this chapter, we have recalled the standard, self-energy-based viewpoint on the cluster perturbation theory and have derived an equivalent time-local Hamiltonian-based formulation. In the course of this, we have put special emphasis on an important property intrinsic to the CPT approach: The one-particle part of the intra-cluster Hamiltonian, which forms the starting point of the all-order perturbation theory [110] in the inter-cluster hopping, can be chosen freely. The simplest choice is to determine it directly from the full hopping matrix which yields the standard, plain CPT.

To emphasize the essential advantage of the Hamiltonian-based formulation – its Markovian (i.e., memory-kernel-free) propagation algorithm – we have used plain CPT to investigate the time evolution of local magnetic moments in the fermionic Hubbard model after an interaction quench. Indeed, our formalism allowed to avoid the solution of an inhomogeneous Dyson equation on the Keldysh contour and we were able to propagate the one-particle density matrix up to times $t_{\text{max}} = 10^4$. For comparison let us note that prior studies based on the nonequilibrium CPT (e.g., Refs. 110, 112) have been limited to $t_{\text{max}} = 10$–20 inverse hoppings.

On the physical side, quenches to weak U_{fin} turned out to be most interesting. In agreement with the predictions of general perturbative considerations [124, 125, 127–129], we found a separation of the dynamics into two time scales. While the system qualitatively follows the constrained dynamics of the noninteracting $U_{\text{fin}} = 0$ limit, the constraints are broken up for large times due to the interaction and the system shows signs of relaxation. However, memory of the initial state persists in the density matrix up to the largest simulated times clearly indicating the absence of thermalization.

While the simple treatment of correlations by nonequilibrium CPT has shown to be enough to cover the mentioned two-stage relaxation dynamics, it also leads to a violation of the fundamental conservation laws of energy and total magnetization. The natural

way to fix this is by additionally imposing a self-consistency condition as it is done in nonequilibrium DMFT or in self-energy functional theory. Due to the significant, additional complexity of these approaches, however, simulations would again be restricted to short time scales. A simpler, more pragmatic approach might thus be preferable where, for example, local continuity equations are enforced to ensure energy, total magnetization and particle-number conservation [76]. Such a "conserving cluster perturbation theory" is derived in the next Chapter.

5. Enforcing conservation laws in cluster perturbation theory

From the numerical example in Section 4.4 it was seen that plain CPT suffers from conceptional difficulties. While it is the drawback of *any* mean-field theory that the feedback of certain correlations on the dynamics of the observables of interest is missing, such as, e.g., the missing feedback of nonlocal spatial correlations on the local self-energy in the case of the DMFT, the situation is even worse in case of plain CPT: There is no feedback at all. In particular, plain CPT calculations cannot be expected to respect the macroscopic conservation laws emerging from the symmetries of the underlying Hamiltonian. This can be traced back to the lack of any element of self-consistency in the plain CPT. Indeed, we observed a violation of the conservation laws of total energy and magnetization in a numerical example (cf. Section 4.4.5).

In this chapter we give a proof of principle that this drawback can be overcome. We make use of the fact that the CPT can be viewed as an all-order perturbation theory [110] in the inter-cluster hopping around a system of decoupled clusters, where the starting point, i.e., the intra-cluster Hamiltonian, is not at all predetermined. The idea is to formulate the macroscopic conservation laws as local constraints on the spin-dependent particle and doublon density. These equations are then used to fix the intra-cluster one-particle parameters and thereby to optimize the starting point for the cluster perturbation expansion. This defines a novel "conserving cluster perturbation theory." The theory is conserving by construction, it is nonperturbative, and in principle controlled by the inverse cluster size as a small parameter. In practice, however, the accessible cluster size is limited by the exponential growth of the cluster Hilbert space. Hence, conserving CPT must be seen as a typical cluster mean-field theory which correctly accounts for nonlocal correlations up to the linear scale of the cluster. Opposed to standard mean-field theories, the "mean-field" or the renormalization of the one-particle parameters is determined by imposing local constraints expressing conservation laws, i.e., it is finally the symmetries of the lattice model which dictates the time-dependent cluster embedding. As the theory relies on *local* self-consistency or conditional equations, it can easily be extended to inhomogeneous models or inhomogeneous initial states.

While the underlying idea is conceptually simple, its practical realization requires a couple of new theoretical concepts which are discussed here in detail. In particular, the implementation of a causal time-stepping algorithm requires a careful analysis to which

order the renormalization of the intra-cluster parameters at a certain time slice enters the conditional equations. We are able to demonstrate that an efficient numerical implementation of the theory is possible and discuss first results for weak interaction quenches in a two-dimensional Hubbard model. The algorithm scales linearly with the propagation time and exponentially in the cluster size. Conservation laws are satisfied with numerical accuracy. Yet, long time scales cannot be achieved with the present implementation due to singular points which are found to evolve during the time propagation.

In this chapter, we make substantial use of the previous groundwork on the Hubbard model and the cluster perturbation theory as presented in Sections 4.1 – 4.3. As highly relevant quantities, let us explicitly recall the intra-cluster hopping $T'(t)$, the inter-cluster hopping $T(t)$, the Hubbard interaction $U(t)$ and the renormalization parameter $\lambda(t)$. Also, we pick up on the introduced convention to explicitly denote the dependence of the Green's function and other quantities on $T(t)$ and $U(t)$ using subscripts where convenient (e.g., $G_{T,U}$, $\Sigma_{T,U}$, etc.).

The macroscopic conservation laws are expressed by local constraints in Section 5.1. The main theoretical work addresses the solution of the local constraints for the optimal starting point of the all-order perturbation theory. This is presented in Sec. 5.2. Numerical results are discussed in Sec. 5.3. We summarize the main results in Sec. 5.4.

5.1. Formulation of the conservation laws as local constraints

While conservation laws like particle-number or energy conservation are naturally fulfilled if one is able to treat a physical problem exactly, this is not necessarily the case when working with approximate methods. For Green's-function-based methods it was shown by Baym and Kadanoff [130, 131] that respecting certain symmetry relations for the two-particle Green's function is sufficient to ensure that an approximation is conserving. Here, we build on an equivalent formulation of the macroscopic conservation laws for the particle number, spin and energy and reformulate them as local constraints for the spin-dependent particle density and the doublon density, respectively. This is in the spirit of expressing conservation laws of a classical field theory as continuity equations and follows the work of Baym and Kadanoff [130, 131]. One should note, however, that in our case the local constraints cannot be written in the standard form of continuity equations, as here we aim at an approach for a discrete lattice model.

To discuss the local constraints, we first consider the exact time evolution of a system described by the Hubbard Hamiltonian $H_{T,U}(t)$. We write $G \equiv G_{T,U}$, $G^{(2l)} \equiv G^{(2l)}_{T,U}$ and $G^{(2r)} \equiv G^{(2r)}_{T,U}$ in this subsection to keep the notation simple. The exact time evolution of the system will preserve the total particle number and the z-component of the total spin as can be expressed by the following local constraint for the spin-dependent density:

$$0 = \partial_t \langle \hat{n}_{i\sigma}(t) \rangle_{H_{T,U}} - [G \circ T - T \circ G]_{ii\sigma}(t, t^+),$$
$$\Leftrightarrow \quad F_{i\sigma}(t) \equiv G^{(2l)}_{ii\sigma}(t, t^+) - G^{(2r)}_{ii\sigma}(t, t^+) = 0 \,, \tag{5.1}$$

as can be verified directly using Eq. (4.6). The first line of Eq. (5.1) constitutes the discrete-lattice analog of the continuity equation for the spin-dependent particle density. Opposed to a continuum theory, however, the divergence of the spin-dependent particle-current density is replaced by the commutator. The second line of Eq. (5.1) is an equivalent formulation of the same constraint as has originally been mentioned by Baym and Kadanoff [130, 131]. Next, we consider the following local constraint for the doublon density [cf. Eq. (4.6)]:

$$C_{i\sigma}(t) \equiv i\partial_t \left[G_{ii\sigma}^{(2l)}(t,t^+) + G_{ii\sigma}^{(2r)}(t,t^+) \right] \tag{5.2}$$
$$- 2\sum_{j\sigma} \left[T_{ij\sigma}(t)G_{ji\sigma}^{(2r)}(t,t^+) - G_{ij\sigma}^{(2l)}(t,t^+)T_{ji\sigma}(t) \right] = 0.$$

In the exact theory, this constraint together with the above constraint $F_{i\sigma}(t) = 0$ expresses the necessity that the doublon density can be derived consistently from either $G^{(2l)}$ or $G^{(2r)}$ and for each spin component σ in Eq. (4.6). More important, in case of a time-independent Hamiltonian, i.e., if $H_{T,U}(t) = \text{const.}$ for $t > t_0$, Eq. (5.2) implies total-energy conservation. This is explicitly shown in the Appendix A.1 where, for completeness, also a formal derivation of Eq. (5.2) is carried out.

While in the exact theory the equations $F_{i\sigma}(t) = 0$ and $C_{i\sigma}(t) = 0$ must hold necessarily, this is no longer guaranteed in an approximate approach. In particular, the equations are usually violated within the conventional CPT. The important point is that via Eqs. (4.2) and (4.4) both, $G^{(2l)}$ and $G^{(2r)}$, can be expressed in terms of the single-particle Green's function and the self-energy and thus both equations $F_{i\sigma}(t) = 0$ and $C_{i\sigma}(t) = 0$ can be expressed in terms of the central quantities of the CPT. Furthermore, as we have shown in Sec. 4.3, they can be incorporated in the Markovian time-propagation scheme based on the Hamiltonian formulation of the CPT. The latter is essential for the numerical treatment.

Our main idea is thus to enforce the local constraints $F_{i\sigma}(t) = 0$ and $C_{i\sigma}(t) = 0$ within the context of the CPT by exploiting the above-discussed freedom in the choice of the CPT starting point, i.e., by choosing an appropriate renormalization $\lambda = \lambda^{\text{opt}}$. If λ^{opt} can be found, this automatically ensures the conservation of particle number, spin and energy.

The final forms of the conditional equations for λ^{opt} are obtained by replacing $G^{(2r)}$ and $G^{(2l)}$ by their CPT approximations $G^{(2l)}[\lambda]$ and $G^{(2r)}[\lambda]$ in the expressions for F and C given by Eqs. (5.1) and (5.2):

$$F[\lambda^{\text{opt}}]_{i\sigma}(t) \overset{!}{=} 0, \quad C[\lambda^{\text{opt}}]_{i\sigma}(t) \overset{!}{=} 0. \tag{5.3}$$

We note that the number of free parameters λ must be chosen to match the number of linear independent constraints defined by Eq. (5.3) to ensure the existence of a unique solution λ^{opt}.

5.2. Solving the self-consistency equations

Having formulated the self-consistency conditions, Eq. (5.3), it remains to explicitly solve these equations for λ^{opt}. An important simplification arises from the fact that the CPT

is by construction a causal theory, i.e., the time-local elements $G^{\mathrm{CPT}}(t, t^+)$ of the CPT Green's function at time t, for example, only depend on quantities at earlier times. The same holds for $G^{(2l)}(t, t^+)$ and for $h^{\mathrm{CPT}}_{xy\sigma}(t)$. This allows us to construct a strategy for the solution of Eq. (5.3) in the form of a time-propagation algorithm. Let us therefore assume that λ^{opt} is known for all time points on a discrete time grid and that only the parameters $\lambda^{\mathrm{opt}}(t)$ at the latest point of time t are unknown.

Therewith, the actual task is to solve Eq. (5.3) for $\lambda^{\mathrm{opt}}(t)$ *only at the given latest point of time t*. To this end we have to analyze at time t the $\lambda(t)$ dependence of the relevant quantities, i.e., of $G^{(2l)}(t, t^+)$ and $G^{(2r)}(t, t^+)$, see Eqs. (5.1) and (5.2). First of all, the dependence of $G^{(2l)}(t, t^+)$ (and $G^{(2r)}(t, t^+)$) on $\lambda(t)$ at time t is due to the CPT Hamiltonian $h^{\mathrm{CPT}}_{xy\sigma}(t)$ [see Eq. (4.15) and see Eqs. (4.16) and (4.17)]. The $\lambda(t)$-dependence of the latter is exclusively due to the time-evolution operator $\mathcal{U}'[\lambda] \equiv \mathcal{U}_{T'-\lambda,U}$ of the reference system. The detailed construction of $h^{\mathrm{CPT}}_{xy\sigma}(t)$ is not important here, and we refer to Ref. 105 for a comprehensive discussion. Finally, the functional dependence of $U'[\lambda](t, 0)$ on λ is through an integration over all times between 0 and t. With this information at hand, we are in fact able to characterize the dependence on $\lambda(t)$ at time t of the quantities $G^{(2l)}(t, t^+)$ and $G^{(2r)}(t, t^+)$ which enter the local constraints (5.3) that serve to enforce the conservation laws.

The most important point for the following discussion is the fact that, in the limit of vanishing time step $\Delta t \to 0$, the parameter set $\lambda(t)$ at the latest point of time enters basically all central quantities as a null set only: Consider, for example, $G^{(2l)}(t, t^+)$. Its first-order response due to a variation of $\lambda(t)$ at time t *vanishes* (as shown below). On the one hand, this missing sensitivity implies a complication of the theory since one has to account for this mathematical property explicitly when setting up a numerical implementation. On the other hand, once one has recognized the property, it actually helps to the solve Eqs. (5.3). Consider a given arbitrary causal functional $M[\lambda](t)$. The main trick is to enhance the sensitivity of $M[\lambda](t)$ to variations of $\lambda(t)$ at time t by taking its time derivative. Typically, if the first-order response of $M[\lambda](t)$ vanishes, $\partial_t M[\lambda](t)$ is a *linear* function of $\lambda(t)$ at time t. Clearly, this is the key to solve an equation like $M[\lambda](t) = 0$ for $\lambda^{\mathrm{opt}}(t)$.

In the following subsections Secs. 5.2.1 and 5.2.2 the above-sketched ideas are worked out on a more technical level. Finally, the Section 5.2.4 addresses the initial state at time $t = 0$.

5.2.1. Time-local variations

Assume that we have found the optimal renormalization $\lambda^{\mathrm{opt}}(t)$ for $t \leq t_n \equiv n\,\Delta t$. We introduce a variation δ^n_{loc} which affects the current (the n-th) time step only:

$$\delta^n_{\mathrm{loc}}\lambda_{ij\sigma}(t) = \delta\lambda_{ij\sigma}(t)\Theta^n_{\mathrm{loc}}(t), \quad \Theta^n_{\mathrm{loc}}(t) = \begin{cases} 1 & \text{if } t \in [t_n, t_{n+1}], \\ 0 & \text{else.} \end{cases} \tag{5.4}$$

For simplicity, we require the variations to be symmetric, i.e., $\delta\lambda_{ij\sigma}(t) = \delta\lambda_{ji\sigma}(t)$. This implies a restriction to symmetric solutions λ^{opt}. Consider now an arbitrary, causal functional $M[\lambda](t)$, i.e., a functional that at time t only depends on $\lambda(t')$ with $t' \leq t$. For such

an object, the variational operator δ_{loc}^n is related to the conventional functional derivative through

$$\delta_{\mathrm{loc}}^n M[\lambda](t) = \sum_\sigma \sum_{i \geq j} \int_{t_n}^t \mathrm{d}t' \frac{\delta M[\lambda](t)}{\delta \lambda_{ij\sigma}(t')} \delta \lambda_{ij\sigma}(t'), \tag{5.5}$$

where the restriction $i \geq j$ is necessary because of the symmetry requirement $\lambda_{ij\sigma} = \lambda_{ji\sigma}$.

We now take the combined limit $n \to \infty$, $\Delta t \to 0$ such that we always have $t \in [t_n, t_{n+1}]$ to define the time-local variation δ_{loc} in the continuum limit

$$\delta_{\mathrm{loc}} M[\lambda](t) = \lim_{\substack{\Delta t \to 0 \\ n \to \infty}} \delta_{\mathrm{loc}}^n M[\lambda](t), \tag{5.6}$$

with the corresponding variational quotient

$$\frac{\delta_{\mathrm{loc}} M[\lambda](t)}{\delta_{\mathrm{loc}} \lambda_{ij\sigma}(t)} \equiv \lim_{\substack{\Delta t \to 0 \\ n \to \infty}} \int_{t_n}^t \mathrm{d}t' \frac{\delta M[\lambda](t)}{\delta \lambda_{ij\sigma}(t')}. \tag{5.7}$$

This variational quotient describes the linear response of $M[\lambda](t)$ when varying the parameters at the latest time step:

$$\delta_{\mathrm{loc}} M[\lambda](t) = \sum_\sigma \sum_{i \geq j} \frac{\delta_{\mathrm{loc}} M[\lambda](t)}{\delta_{\mathrm{loc}} \lambda_{ij\sigma}(t)} \delta \lambda_{ij\sigma}(t). \tag{5.8}$$

5.2.2. Integrated quantities in λ

With the appropriate variation for our purposes at hand, we can study the effect of the variation on the main quantities within the CPT framework. We first consider the time-evolution operator ("propagator") of the reference system $\mathcal{U}'[\lambda] \equiv \mathcal{U}_{T'-\lambda,U}$. It is instructive to study the effect of the operator δ_{loc}^n first, i.e., the effect of a time-local variation with finite time step Δt. Keeping only terms of the order $O(\Delta t)$ one finds

$$\delta_{\mathrm{loc}}^n \mathcal{U}'[\lambda](t, 0) = -i \left[\sum_{ij\sigma} \int_{t_n}^t \delta \lambda_{ij\sigma}(t') \hat{c}_{i\sigma}^\dagger \hat{c}_{j\sigma} \mathrm{d}t' \right] \mathcal{U}'[\lambda](t_n, 0) + O(\Delta t^2). \tag{5.9}$$

In lowest order we thus have $\delta_{\mathrm{loc}}^n \mathcal{U}_{T'-\lambda,U}(t, 0) \propto \Delta t \, \delta \lambda(t)$. This means that the linear response vanishes identically in the limit $\Delta t \to 0$. This property originates from the fact that $\lambda(t)$ is integrated over time within the propagator $\mathcal{U}_{T'-\lambda,U}(t, 0)$, and that the contribution of a single time step, $t \in [t_n, t_{n+1}]$, to this integral is of zero measure in the limit $\Delta t \to 0$.

A finite time-local variation is obtained for the first time derivative of the propagator rather than for the propagator itself. Namely, the corresponding time-local variational quotient remains non-zero in the continuum limit:

$$\frac{\delta_{\mathrm{loc}}[i\partial_t \mathcal{U}'[\lambda](t, 0)]}{\delta_{\mathrm{loc}} \lambda_{ij\sigma}(t)} = -\left[c_{j\sigma}^\dagger c_{i\sigma} + c_{i\sigma}^\dagger c_{j\sigma} - \delta_{ij} c_{i\sigma}^\dagger c_{i\sigma} \right] \mathcal{U}'[\lambda](t, 0). \tag{5.10}$$

Multiplying this equation with $\lambda_{ij\sigma}(t)$, summing over i, j, σ and comparing with the standard equation of motion $i\partial_t \mathcal{U}'[\lambda](t, 0) = H_{T'-\lambda, U}(t)\mathcal{U}'[\lambda](t, 0)$, shows that the time derivative of the propagator is of the general form

$$i\partial_t \mathcal{U}'[\lambda](t, 0) = \sum_\sigma \sum_{i \geq j} \frac{\delta_{\text{loc}}[i\partial_t \mathcal{U}'[\lambda](t, 0)]}{\delta_{\text{loc}}\lambda_{ij\sigma}(t)}\lambda_{ij\sigma}(t) + \xi_{\mathcal{U}'}[\lambda](t), \qquad (5.11)$$

where $\xi_{\mathcal{U}'}[\lambda](t) = H_{T', U}(t)\mathcal{U}'[\lambda](t, 0)$. Note that the dependence on $\lambda_{ij\sigma}(t)$ at time t is strictly *linear* in the limit $\Delta t \to 0$.

With this definition and with Eq. (5.10), it is obvious that the variational derivative and $\xi_{\mathcal{U}'}[\lambda](t)$ on the right-hand side of Eq. (5.11) depend on $\lambda(t)$ only through an integration over time within the propagator $\mathcal{U}'[\lambda](t, 0)$. We will call such quantities *integrated* quantities in λ. Integrated quantities in λ inherit an important property from the cluster propagator $\mathcal{U}'[\lambda]$, see Eq. (5.9): Their time-local variation vanishes in the limit $\Delta t \to 0$.

Furthermore, the time derivative of any quantity $M[\lambda]$ that is integrated in λ, i.e., the time derivative of a functional of the form $M[\lambda](t) = M(\mathcal{U}'[\lambda](t, 0))$, can be brought into a form analogous to Eq. (5.11). This follows immediately from the chain rule in calculus as $i\partial_t M[\lambda](t) = \frac{i\partial M(\mathcal{U}')}{\partial \mathcal{U}'}\frac{\partial \mathcal{U}'[\lambda](t, 0)}{\partial t}$. Explicitly this result reads

$$i\partial_t M[\lambda](t) = \sum_\sigma \sum_{i \geq j} \frac{\delta_{\text{loc}}[i\partial_t M[\lambda](t)]}{\delta_{\text{loc}}\lambda_{ij\sigma}(t)}\lambda_{ij\sigma}(t) + \xi_M[\lambda](t), \qquad (5.12)$$

where $\frac{\delta_{\text{loc}}[i\partial_t M[\lambda](t)]}{\delta_{\text{loc}}\lambda_{ij\sigma}(t)}$ and $\xi_M[\lambda]$ are again integrated quantities in λ. We furthermore conclude that a time-local variation of the time derivative of an integrated quantity in λ is non-zero in general.

The main idea in the following is to combine the conditional equations (5.3) into a single equation $\Gamma[\lambda^{\text{opt}}](t) \overset{!}{=} 0$ such that $\Gamma[\lambda]$ is of the form $\Gamma[\lambda](t) = J[\lambda](t)\lambda(t) + \xi_\Gamma[\lambda](t)$ where $J[\lambda]$ and $\xi_\Gamma[\lambda]$ are integrated quantities in λ. This is formally easily solved for $\lambda^{\text{opt}}(t)$ by matrix inversion and allows to derive an efficient propagation scheme for numerical purposes.

λ-**dependence of** $G^{(2l)}$ **and** $G^{(2r)}$

The main building blocks of the local constraints on the spin-dependent density, Eq. (5.1), and the doublon density, Eq. (5.2), are given by the two-particle correlation functions $G^{(2l)}$ and $G^{(2r)}$. Within the CPT approximation they are defined through Eq. (4.17). We therefore have to understand the λ dependence of $\eta'[\lambda] \equiv \eta_{T'-\lambda, U}$ and $G^{\text{CPT}}[\lambda]$.

One can easily see that $\eta'[\lambda]$ is an integrated quantity in λ. Consider, for example, the physical sector. From Eq. (4.11) we have $\eta'_{ij\sigma}[\lambda](t) = \delta_{ij}\langle\hat{n}_{i\bar{\sigma}}(t)\rangle_{H_{T'-\lambda, U}}$. The only λ-dependence of this expression indeed stems from the propagator $\mathcal{U}'[\lambda]$. To obtain a non-vanishing time-local variation we thus have to consider the first derivative with respect to time. This is worked out in Appendix A.2:

$$\delta_{\text{loc}}[i\partial_t \eta'_{ij\sigma}(t)] = \eta'_{ii\sigma}(t)\delta\lambda_{ij\sigma}(t) - \sum_{l\sigma'}[\delta\lambda_{il\sigma'}(t)]\gamma^{l\sigma'}_{ij\sigma}(t),$$

$$\delta_{\text{loc}}[i\partial_t \eta'_{is\sigma}(t)] = -\sum_{l\sigma'}[\delta\lambda_{il\sigma'}(t)]\gamma^{l\sigma'}_{is\sigma}(t), \qquad (5.13)$$

where the newly introduced tensor $\gamma[\lambda]^{l\sigma'}_{is\sigma}(t)$ is cluster-diagonal, i.e., $\gamma[\lambda]^{l\sigma'}_{is\sigma}(t) \neq 0$ if and only if i and l refer to lattice sites within the same cluster. It furthermore follows that $i\partial_t\eta'[\lambda](t)$ can be brought into the form specified by Eq. (5.12), where the variational derivative $\frac{\delta_{\text{loc}}[i\partial_t\eta'[\lambda]_{ix\sigma}(t)]}{\delta\lambda_{jl\sigma}(t)}$, as given by Eq. (5.13), and $\xi_{\eta'}[\lambda]_{ix\sigma}(t)$ are integrated quantities in λ. An explicit expression for the latter is not needed for our purposes.

Let us now take a look at the CPT Green's function. It depends on λ through the Hamiltonian $H^{\text{CPT}}[\lambda]$, which in turn depends on λ through the hybridization strengths $h'[\lambda]_{is\sigma}(t) = U(t)\eta'[\lambda]_{is\sigma}(t)$ and the Hartree-Fock term $\Sigma'[\lambda]^{\text{HF}}_{ij\sigma}(t) = U(t)\eta'[\lambda]_{ij\sigma}(t)$. The Hamiltonian $H^{\text{CPT}}(t)$ is therefore an integrated quantity in λ. As the propagator $\mathcal{U}^{\text{CPT}}[\lambda](t,0) = T\exp\left(-i\int_0^t dt' H^{\text{CPT}}[\lambda](t')\right)$ involves a second integral over time, we conclude that $\delta^n_{\text{loc}}G^{\text{CPT}}(t,t^+) \propto \Delta t^2\,\delta\lambda(t)$. In this sense, G^{CPT} must be seen as an integrated quantity in λ of second order. Consequently, the time-local variation of its first derivative with respect to time vanishes:

$$\delta_{\text{loc}}[i\partial_t G^{\text{CPT}}[\lambda](t,t^+)] = 0. \tag{5.14}$$

We note that the time derivative involves the product of the matrix elements of the CPT Hamiltonian, Eq. (4.15), with $G^{\text{CPT}}[\lambda](t,t^+)$, i.e., the product of an integrated quantity in λ with an integrated quantity in λ of second order, respectively. Obviously, the product scales like an ordinary integrated quantity in λ when a time-local variation is applied, i.e., $\delta^n_{\text{loc}}h^{\text{CPT}}(t)G^{\text{CPT}}(t,t^+) \propto \Delta t\delta\lambda(t)$ in lowest order in Δt.

Concluding, to get a non-vanishing time-local variation, one must consider the first time derivative of the two-particle Green's functions $G^{(2l)}$ and $G^{(2r)}$. We find

$$\delta_{\text{loc}}\left[i\partial_t G^{(2l)}_{ij\sigma}(t,t^+)\right] = \sum_x \left(\delta_{\text{loc}}[i\partial_t\eta'_{ix\sigma}(t)]\right)G^{\text{CPT}}_{xj\sigma}(t,t^+) \tag{5.15}$$

and an analogous expression for $G^{(2r)}$. Only the η'-term contributes to the variation, cf. Eq. (5.13), while the variation of the CPT Green's function vanishes, cf. Eq. (5.14). We also note that Eq. (5.13) may be used at this point and that $i\partial_t G^{(2l)}(t,t^+)$ [and analogously $i\partial_t G^{(2r)}(t,t^+)$] is of the form

$$i\partial_t G^{(2l)}_{ij\sigma}(t,t^+) = \sum_{\sigma'}\sum_{k\geq l}\frac{\delta_{\text{loc}}G^{(2l)}_{ij\sigma}(t,t^+)}{\delta_{\text{loc}}\lambda_{kl\sigma'}(t)}\lambda_{kl\sigma'}(t) + [\xi_{G^{(2l)}}]_{ij\sigma}(t), \tag{5.16}$$

where both, the variational derivative $\frac{\delta_{\text{loc}}G^{(2l)}(t,t^+)}{\delta_{\text{loc}}\lambda(t)}$, as given by Eq. (5.15), and the quantity $\xi_{G^{(2l)}}(t)$, which is not needed in explicit form for our purposes, scale like integrated quantities in λ under time-local variations. This follows from the fact that $i\partial_t G^{\text{CPT}}(t,t^+)$ scales like an integrated quantity in λ under time-local variations and the related discussion above.

λ-dependence of the local constraints

The local constraint on the spin-dependent density, Eq. (5.1), is formulated in terms of the difference between $G^{(2l)}$ and $G^{(2r)}$. Therefore its first derivative with respect to time must

be considered to obtain a non-vanishing time-local variation:

$$\delta_{\text{loc}}[i\partial_t F[\lambda]_{i\sigma}(t)] = \delta_{\text{loc}}\left[i\partial_t G^{(2l)}[\lambda]_{ii\sigma}(t,t^+) - i\partial_t G^{(2r)}[\lambda]_{ii\sigma}(t,t^+)\right], \tag{5.17}$$

For the time-local variation of the local constraint on the doublon density, Eq. (5.2), on the other hand, one finds

$$\delta_{\text{loc}}C[\lambda]_{i\sigma}(t) = \delta_{\text{loc}}\left[i\partial_t G^{(2l)}[\lambda]_{ii\sigma}(t,t^+) + i\partial_t G^{(2r)}[\lambda]_{ii\sigma}(t,t^+)\right], \tag{5.18}$$

since $\delta_{\text{loc}}[T \circ G^{(2r)} - G^{(2l)} \circ T](t,t^+) = 0$, where we made use of the fact that $T = T' + V$ is the hopping of the original system and thus independent of λ.

To treat both constraints in a combined formal frame, we define the functional $\Gamma[\lambda]$:

$$\Gamma[\lambda]_a(t) = \begin{cases} i\partial_t F[\lambda]_{i\sigma}(t) & \text{if} \quad 0 \leq a < 2L, \\ C[\lambda]_{i\sigma}(t) & \text{if} \quad 2L \leq a < 4L, \end{cases} \tag{5.19}$$

where L is the number of lattice sites. With this, the conditional equation for the optimal renormalization reads $\Gamma[\lambda^{\text{opt}}] \overset{!}{=} 0$. From the previous discussion and Eq. (5.16) it follows that $\Gamma[\lambda]_a(t)$ is of the form

$$\Gamma[\lambda]_a(t) = \sum_b J[\lambda]_{ab}(t)\lambda_b(t) + \xi_\Gamma[\lambda]_a(t), \tag{5.20}$$

where we introduced the super-index b which labels the set of free parameters: $\lambda_b = \lambda_{ij\sigma}$, $i \geq j$. Both $J[\lambda]$ and $\xi_\Gamma[\lambda]$ scale like integrated quantities in λ under time-local variations. The Jacobian matrix J is defined as

$$J[\lambda]_{ab}(t) \equiv \frac{\delta_{\text{loc}}\Gamma_a[\lambda](t)}{\delta_{\text{loc}}\lambda_b(t)}. \tag{5.21}$$

The matrix $J[\lambda](t)$ is quadratic if the number of free parameters λ_b is chosen such that it equals the number of conditional equations [see Eq. (5.19)]. Assuming that $J[\lambda](t)$ is regular, one can formally solve the conditional equation for the optimal renormalization:

$$\Gamma[\lambda^{\text{opt}}](t) \overset{!}{=} 0 \quad \Leftrightarrow \quad \lambda^{\text{opt}}(t) = -\left[J[\lambda^{\text{opt}}](t)\right]^{-1}\xi_\Gamma[\lambda^{\text{opt}}](t), \tag{5.22}$$

see Eq. (5.20). This completes our derivation.

Let us emphasize that the single point $\lambda^{\text{opt}}(t)$ represents a null set with respect to the time-integrations in $J[\lambda^{\text{opt}}](t)$ and $\xi_\Gamma[\lambda^{\text{opt}}](t)$. This can be exploited to derive an efficient numerical scheme to obtain $\lambda^{\text{opt}}(t)$ step by step on the time axis as detailed in the next subsection 5.2.3. There we also argue why finding an explicit expression for $\xi_\Gamma[\lambda](t)$ can in fact be circumvented. An explicit expression for $J[\lambda](t)$ in terms of known quantities, on the other hand, is available via Eqs. (5.13), (5.15), (5.17) and (5.18).

5.2.3. High-order time propagation scheme

Finally, we like to set up an efficient numerical scheme to determine $\lambda^{\mathrm{opt}}(t)$. This should be based on a time-propagation algorithm where the error is of high order in the basic time step Δt. Let us assume that for each time step the Taylor expansion of $\lambda^{\mathrm{opt}}(t)$ is well defined. For each time interval and for arbitrary $t \in [t_n, t_{n+1}]$ we then have

$$
\lambda^{\mathrm{opt}}(t) = \begin{cases} \lambda^{(0)}(t) = \displaystyle\sum_{p=0}^{n_p} \frac{\lambda_{0,p}}{p!} t^p + O(\Delta t^{n_p+1}) & \text{if } t \in [0, t_1[, \\[2ex] \lambda^{(1)}(t) = \displaystyle\sum_{p=0}^{n_p} \frac{\lambda_{1,p}}{p!} (t - t_1)^p + O(\Delta t^{n_p+1}) & \text{if } t \in [t_1, t_2[, \\[2ex] \dots \end{cases}
\tag{5.23}
$$

where each λ-term must be considered as a tuple with components labelled by the superindex b, e.g., $\lambda_{n,p} = ([\lambda_{n,p}]_b)$, where n refers to the n-th time interval, and where p runs from $p = 0$ up to the maximum order of the polynomial n_p. During the time propagation, the polynomial approximation must be updated after each time step. This is done by fixing the coefficients at each interfacing time t_n such that $\Gamma[\lambda^{\mathrm{opt}}](t_n) = 0$. For times $t \neq t_n$ we then have $\Gamma[\lambda^{\mathrm{opt}}](t) = O(\Delta t^{n_p+1})$. Writing $J(t) \equiv J[\lambda^{\mathrm{opt}}](t)$ and $\xi_\Gamma(t) \equiv \xi_\Gamma[\lambda^{\mathrm{opt}}](t)$ for short and applying the product rule to $J(t)\lambda^{\mathrm{opt}}(t) = \xi_\Gamma(t)$, the self-consistency condition (5.22) is readily rewritten in terms of the Taylor coefficients:

$$
\lambda_{n,p} = J^{-1}(t_n) \left(\sum_{r=0}^{p-1} \binom{p}{r} [\partial_t^{p-r} J(t)]_{t=t_n} \lambda_{n,r} - [\partial_t^p \xi_\Gamma(t)]_{t=t_n} \right).
\tag{5.24}
$$

Suppose that $\lambda^{(q)}(t)$ is known for all $q < n$, i.e., suppose that the propagation has been completed over the interval $[0, t_n[$. The next step is to update the coefficients. At this point we can exploit that $J(t)$ and $\xi_\Gamma(t)$ scale like integrated quantities in λ under time-local variations which implies $\delta_{\mathrm{loc}} J(t) = 0$ and $\delta_{\mathrm{loc}} \xi_\Gamma(t) = 0$. Hence, at $t = t_n$, both are independent of $\lambda^{\mathrm{opt}}(t_n)$. We define

$$
\tilde{\lambda}(t) = \begin{cases} \lambda^{\mathrm{opt}}(t) & \text{if } t < t_n, \\ 0 & \text{else.} \end{cases}
\tag{5.25}
$$

Then,

$$
\xi_\Gamma(t_n) = \Gamma[\tilde{\lambda}](t_n),
\tag{5.26}
$$

and we are now able to solve Eq. (5.24) for $\lambda_{n,0}$. The first derivatives $\partial_t J(t)\big|_{t=t_n}$ and $\partial_t \xi_\Gamma(t)\big|_{t=t_n}$ explicitly depend on $\lambda^{\mathrm{opt}}(t_n) = \lambda_{n,0}$, which is now known, but are integrated quantities in the first derivative $\partial_t \lambda^{\mathrm{opt}}(t)$, i.e., they are independent of $\partial_t \lambda^{\mathrm{opt}}(t)\big|_{t=t_n} = \lambda_{n,1}$. Therefore, the same idea can be applied and in fact be repeated again and again until finally $\lambda^{(n)}(t)$ is known up to the desired order. We emphasize that the presented algorithm gives a fully converged $\lambda^{\mathrm{opt}}(t) = \lambda^{(n)}(t) + O(\Delta t^{n_p+1})$ for $t \in [t_n, t_{n+1}[$ within a single iteration.

5.2.4. The equilibrium initial state

Initially, at time $t = 0$ the system is assumed to be in a thermal state. The CPT approximation for the initial thermal state suffers from the fact that the starting point of the all-order perturbation theory in the inter-cluster hopping is not unique. This is completely analogous to the CPT description of the real-time dynamics. Unlike the real-time dynamics, however, the local constraints cannot be used to fix the renormalization parameters $\lambda_{\mathrm{eq}} \equiv \lambda(0)$ for the initial state, and thus a nontrivial self-consistency condition is not available, unfortunately.

This can be seen as follows: Let us assume that the hopping matrix T, and consequently T' and V, are real and symmetric. Consider $G^{(2l)}$ at times $t = t' = 0$. Via Eq. (4.17) this is given as $G^{(2l)}[\lambda]_{ij\sigma}(0, 0^+) = i \sum_x \eta'[\lambda]_{ix\sigma}(0) G^{\mathrm{CPT}}[\lambda]_{xj\sigma}(0, 0^+)$. Taking a look at η' first we find that its imaginary part vanishes. To this end we note that the Hamiltonian $H_{T,U}(0)$ is symmetric and therefore has real eigenvectors $|m\rangle$. Similarly, the Q-matrix is real at time $t = 0$ and completion to a unitary matrix $O(0)$ yields the special case of an orthogonal, i.e., real $O(0)$. It then follows that $\mathrm{Im}\{\eta'_{ix\sigma}(0)\} = 0$ from Eq. (4.8). Hence, Eq. (4.11) implies that $H^{\mathrm{CPT}}[\lambda](0)$ is real and symmetric, and therefore $G^{\mathrm{CPT}}[\lambda]_{xy\sigma}(0, 0^+) = i\langle \hat{c}^\dagger_{y\sigma}(0)\hat{c}_{x\sigma}(0)\rangle_{H^{\mathrm{CPT}}[\lambda]}$ is purely imaginary. Consequently, $G^{(2l)}[\lambda](0, 0^+)$ is real. Finally, we conclude with Eq. (4.19) that

$$G^{(2l)}[\lambda]_{ij\sigma}(0, 0^+) = G^{(2r)}[\lambda]_{ji\sigma}(0, 0^+). \tag{5.27}$$

This directly proves that $F[\lambda]_{i\sigma}(0) = 0$. Furthermore, causality requires λ_{eq} to be independent of $H_{T,U}(t > 0)$. We are therefore free to choose $H_{T,U}(t) = H_{T,U}(0) = \mathrm{const.}$ such that

$$C[\lambda]_{i\sigma}(0) = 2 \sum_{j\sigma} T_{ij\sigma}(0) \left[G^{(2r)}[\lambda]_{ji\sigma}(0, 0^+) - G^{(2l)}[\lambda]_{ij\sigma}(0, 0^+) \right] = 0 \tag{5.28}$$

irrespective of λ_{eq}. Thus, both constraints hold trivially.

For the concrete numerical calculations we circumvent this issue and consider a noninteracting initial state. The initial value λ_{eq} is then fixed by requiring λ to be continuous so that $\lambda_{\mathrm{eq}} = \lambda(0^+)$. This does not violate causality since the CPT is exact in this case independently of λ_{eq}.

5.3. Numerical results

The conserving CPT has been implemented numerically. First results are discussed for the two-dimensional Hubbard model on an $L = 10 \times 10$ square lattice with periodic boundary conditions. As these results shall serve as a proof of concept only, we restrict ourselves to the most simple approximation, i.e., to the smallest meaningful cluster as the building block of the reference system, namely a cluster consisting of 2×1 sites. Hence, the entire system is partitioned into 50 clusters in total, see Fig. 5.1.

Initially, the system is prepared in its noninteracting ground state at half-filling by choosing $\mu = 0$. Note that the CPT description of this initial state is exact (and independent of the renormalization). The hopping of the original system is restricted to
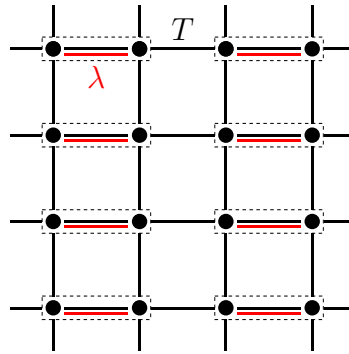
Figure 5.1.: Partitioning of the Hubbard model with nearest-neighbor hopping on the two-dimensional square lattice used for the numerical calculations. Original system: $L = 10 \times 10$ lattice with periodic boundary conditions. Reference system: 50 clusters of size 2×1. The figure shows a 4×4 excerpt. Clusters are indicated by dashed rectangles. Nearest-neighbor hopping T and optimization parameter $\lambda(t)$ are indicated by black and red lines. The time-dependent renormalization $\lambda(t)$ is employed to enforce the conservation of energy in the real-time dynamics following an interaction quench.

nearest neighbors, and we set the nearest-neighbor hopping $T = 1$ to fix energy and time units. To drive the system out of equilibrium we consider an interaction quench where the Hubbard-U is suddenly, at time $t = 0$, switched on to a finite value U_{fin}:

$$U(t) = \Theta(t) U_{\text{fin}}. \tag{5.29}$$

Here, $\Theta(t)$ denotes the Heaviside step function. For times $t > 0$ the interaction strength is constant. To maintain particle-hole symmetry and half-filling, the chemical potential is quenched as well, from $\mu = 0$ to $\mu = U/2$ in the final state.

Studying the model at the particle-hole symmetric point is convenient since the conservation of the total particle number is trivially respected in this case [112]. For a spin-independent parameter quench, as considered here, the CPT also trivially respects the conservation of the total spin. Total-energy conservation, on the other hand, is violated in a conventional CPT approach as has been explicitly demonstrated recently [105]. For the present setup we will therefore employ the nearest-neighbor hopping within the 2×1 reference system to enforce the energy-conservation law. This specifies the time-dependent renormalization parameter $\lambda(t)$ (see Fig. 5.1).

We note that the computational effort to self-consistently evaluate the presented theory numerically is essentially determined by the underlying solver for the conventional nonequilibrium CPT with little overhead. Here, we use the time-local, Hamiltonian-based solver developed in Ref. 105 which constructs the effective Hamiltonian of each cluster by exact diagonalization. For the 2×1 reference system under consideration, only two virtual sites are needed for an exact mapping. This gives us four sites per cluster so that the CPT-Hamiltonian comprises 200 sites in total. Furthermore, regarding computational demands, our approach inherits a constant memory consumption from the CPT solver as well as the linear scaling in the maximum propagation time. In particular, we have used

a time step of $\Delta t = 0.001$ to propagate the system up to $26,500$ steps up to a maximum propagation time of $t_{\mathrm{max}} = 26.5$. For each such time step t_n, the scheme developed in Section 5.2.3 has been employed with $n_p = 1$, i.e., we have calculated the Taylor coefficients $\lambda_{n,0}$ and $\lambda_{n,1}$.

While the required computational resources are very moderate, accessing longer time scales has turned out to be hindered by mathematical complications. As is obvious from Eq. (5.22), an inversion of the Jacobian matrix $J(t)$ is necessary to obtain $\lambda^{\mathrm{opt}}(t)$ at each time step. However, with increasing U_{fin} this matrix exhibits singular points of non-invertibility at earlier and earlier times. In fact, one finds numerically that also the starting point $t = 0^+$ is singular, namely the Jacobian matrix vanishes: $J(0^+) = 0$. Fortunately, one also has $\xi_\Gamma(0^+) = 0$, such that this problem is fixed by applying L'Hôpital's rule. At time $t = 0^+$, the defining equation for $\lambda^{\mathrm{opt}}(0^+)$ becomes

$$\lambda^{\mathrm{opt}}(0^+) = - \left[\partial_t J[\lambda^{\mathrm{opt}}](0^+) \right]^{-1} \left[\partial_t \xi_\Gamma[\lambda^{\mathrm{opt}}](0^+) \right]. \tag{5.30}$$

While this solves the problem at time $t = 0^+$, finding a systematic and convenient way to propagate beyond the singular points of the Jacobian matrix at *finite* times remains topic for future investigations.

Apart from this technical problem, the suggested scheme works as expected. Results for the time evolution of the doublon density are shown in Fig. 5.2. It is evident that the renormalization λ has a strong influence on the dynamics and leads to qualitatively different results when comparing the plain unoptimized CPT calculation with the novel conserving CPT. While the dynamics is characterized by ongoing oscillations when using plain CPT, there is a monotonous decay of the doublon density in case of the conserving CPT. The longest maximum propagation time is achieved for the quench $U = 0 \to 0.5$. Here, the first singular point of the Jacobian shows up at $t_{\mathrm{max}} \approx 26.5$. On this time scale, the doublon density seems to relax to a stationary state with little to no oscillations.

The qualitatively different time dependence of the doublon density reflects the qualitatively different behavior found for the total energy in the plain and the conserving CPT: This is shown in the inset of Fig. 5.3. For the conserving CPT, the total energy is perfectly conserved within numerical accuracy—by construction of the approach. In the plain CPT calculation, however, the total energy shows unphysical oscillations. Here, maxima and minima of $E_{\mathrm{tot}}(t)$ nicely correspond to maxima and minima in the plain-CPT doublon density seen in Fig. 5.2. It must be concluded that those are artifacts of the plain CPT approach. We also note that small unphysical oscillations of the total energy *density* $E_{\mathrm{tot}}(t)/L$ (with $L = 100$) with amplitudes less than 0.01 lead to much stronger oscillations in the doublon density with amplitudes of about 0.04.

The main part of Fig. 5.3 displays the results for the time evolution of the renormalization parameter $\lambda(t)$. Its dependence on U_{fin} turns out to be rather weak on a time scale of a few inverse hoppings. Irrespective to the final interaction strength U_{fin}, the initial equilibrium value is found as $\lambda_{\mathrm{eq}} \approx -0.86$. For $t > 0$ and for all U_{fin}, the renormalization parameter rapidly increases to $\lambda \approx 0.6$ within a very short time $t \approx 0.7$. This corresponds to the rapid initial drop of the doublon density (cf. Fig. 5.2). Results for longer times are again only available for the quench $U = 0 \to 0.5$. On the time scale up to $t_{\mathrm{max}} \approx 26.5$, we observe a subsequent slow relaxation of $\lambda(t)$ toward an average final value $\lambda_\infty \approx 1.0$ with
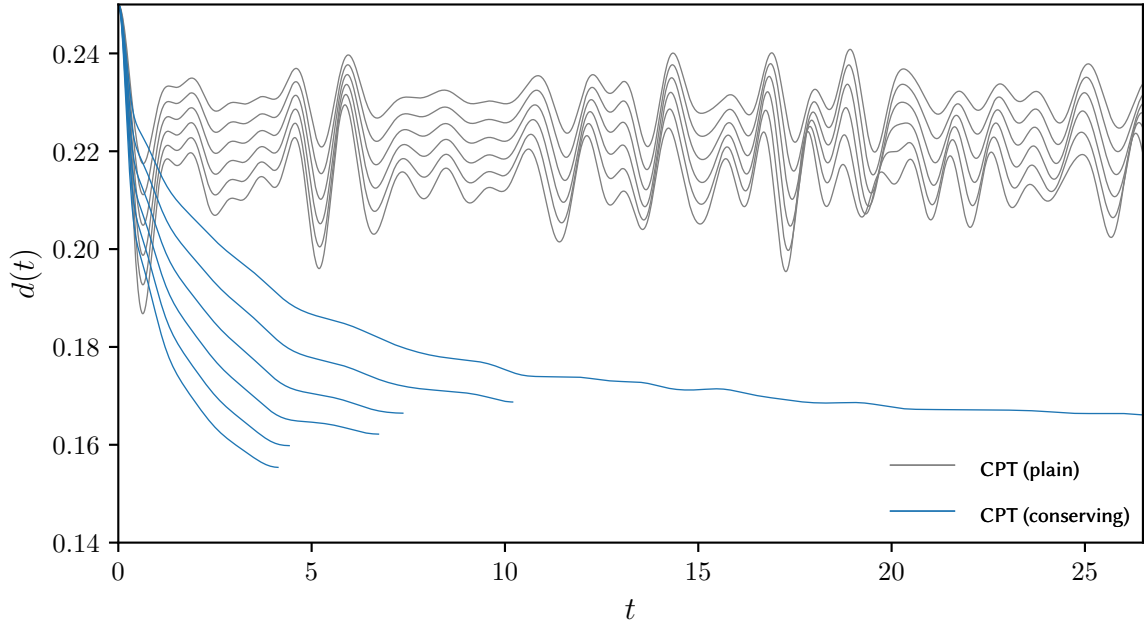
Figure 5.2.: Time evolution of the local doublon density after an interaction quench $U = 0 \rightarrow U_{\text{fin}}$. Grey lines: plain CPT. Blue lines: conserving CPT. Results for different U_{fin} ranging from $U_{\text{fin}} = 0.5$ (top curve) to $U_{\text{fin}} = 1.0$ (bottom) with equidistant steps $\Delta U_{\text{fin}} = 0.1$. For the conserving CPT calculations, propagation times are limited by singular Jacobians.
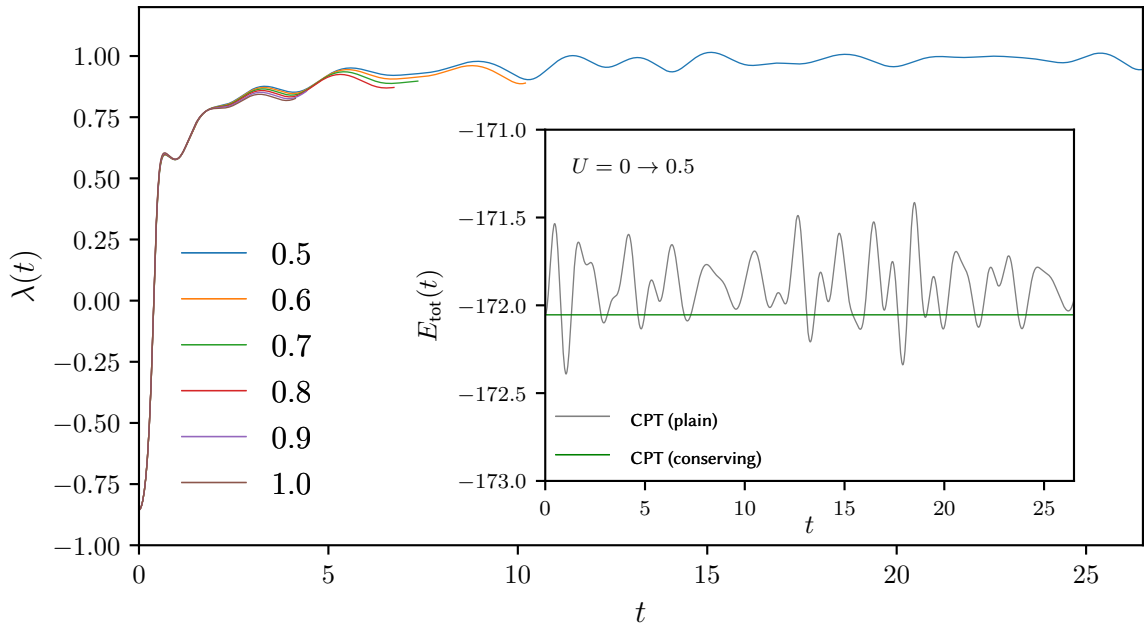
Figure 5.3.: Time evolution of the optimal renormalization parameter $\lambda^{\text{opt}}(t)$ for different U_{fin} as indicated and corresponding to Fig. 5.2. Inset: time dependence of the total energy (plain and conserving CPT).

small superimposed oscillations. It seems reasonable to assume that a similar behavior would also be found for the other quenches, given that the short-time dynamics is very similar for the different U_{fin}.

One should note that $\lambda_\infty = 1$ amounts $T' - \lambda_\infty = 0$, i.e., a vanishing renormalized intra-cluster hopping. Apart from the remaining oscillations of the renormalization parameter around $\lambda_\infty = 1$, this means that the system "chooses" the atomic limit of the Hubbard model as the optimal starting point for the all-order perturbation theory in the inter-cluster hopping for long times. This may be interpreted as follows: First of all, the remaining oscillations are understood as being necessary to keep the total energy constant within the conserving CPT. Disregarding the oscillations, the value $\lambda_\infty = 1$ means that, on the level of the reference system, the doublon density becomes a conserved quantity for long times. This, however, is in fact a plausible starting point if the doublon density of the full lattice model approaches a constant in the course of time. As is seen in Fig. 5.2, this is almost the case. The remaining time dependence of the doublon density of the lattice model is weak and would be exclusively due to the inter-cluster hopping (if $\lambda(t) = \lambda_\infty = 1$ exactly).

Let us compare the CPT result for the doublon density with the results of previous calculations for the one-dimensional Hubbard model [58] using the density-matrix renormalization group (DMRG) and for the model in infinite dimensions using the dynamical mean-field theory (DMFT) [79]. In both cases, a very fast relaxation of the doublon density on a time scale of one inverse hopping has been found in fact. Typically, however, the doublon density first develops a minimum before it saturates to an almost constant value. This minimum is absent in the conserving CPT calculations (see Fig. 5.2). Note, that for weak quenches and on the intermediate time scale discussed here and in the DMRG and DMFT studies, the doublon density does not relax to its thermal value due to kinematic constraints becoming active after the ultrashort initial relaxation step. [124, 132] Indeed, one expects a subsequent relaxation on a much longer time scale. Let us emphasize that while our data in Fig. 5.2 are compatible with these expectations, serious predictions using the conserving CPT are not yet possible. This would require a much more systematic study involving different and in particular larger clusters, an analysis of the dependence on the cluster shape and also a systematic discussion of the different possibilities to choose renormalization parameters for the self-consistent procedure.

5.4. Summary

Cluster perturbation theory, as proposed originally, represents the most simple way to construct a mean-field theory which incorporates to some extent the effects of short-range correlations. In Chapter 4 we had emphasized that the starting point of the perturbational expansion in the inter-cluster hopping is by no means predetermined and that the according freedom in the choice of the intra-cluster hopping parameters can be exploited to "optimize" the mean-field theory. There are different conceivable optimization schemes. One way is to add an additional self-consistency condition as, for example, a self-consistent renormalization of the on-site energies which would be very much in the spirit of the Hubbard-I approximation. The disadvantage of such ideas is their *ad hoc* char-

acter. An optimization following a general variational principle is much more satisfying and physically appealing. This is the route that is followed up by self-energy-functional theory [75, 76]. Unfortunately, total-energy conservation is not straightforwardly implemented within the SFT context. An appealing idea is thus to use the above-mentioned freedom to *enforce* energy conservation, and actually any conservation law dictated by the symmetries of the problem at hand. This leads to the conserving CPT proposed here.

As we have argued (see Sec. 5.2.4), this idea can exclusively be used to constrain the CPT real-time dynamics while other concepts must be invoked for the initial thermal state. On the other hand, there is an urgent need for numerical approaches, even for comparatively simple cluster mean-field concepts, which are able to address the real-time dynamics of strongly correlated lattice fermion models beyond the more simple extreme limits of one and infinite lattice dimension.

In this chapter we could give a proof of principle that a nonequilibrium conserving cluster perturbation theory is possible and can be evaluated numerically in practice. An highly attractive feature of this approach is the linear scaling with the propagation time, while the exponential scaling with the cluster size is the typical bottleneck of any cluster mean-field theory.

The mapping of the original nonequilibrium CPT onto an effective auxiliary problem specified by a noninteracting Hamiltonian with additional virtual ("bath") degrees of freedom is crucial for the practical implementation of the approach. One should note that the number of virtual sites is related to the number of one-particle excitations and thus grows exponentially with the original cluster size. Hence, any practical calculation is limited to a few (say, at most 10) cluster sites only. This implies that a systematic finite-size scaling analysis will be problematic if long-range correlations dominate the essential physical properties – this is the above-mentioned drawback that is shared with any available cluster-mean-field theory. We therefore expect that the field of applications of conserving CPT is limited to problems with possibly strong but short-ranged correlations.

Due to its formulation in terms of Green's functions with time arguments on the Keldysh contour, the CPT has an inherently causal structure. Our results in particular demonstrate how to exploit this causality for an efficient time-stepping algorithm where updates of the parameter renormalization can be limited to the respective last time slice during time propagation. The essential problem that had to be solved here consists in controlling the order (in the sense of a Taylor series) at which the parameter renormalization on a single time slice enters other physical quantities, such as the basic time-evolution operator, Green's functions, etc. This has allowed us to set up a highly accurate numerical algorithm where conservation laws are respected with machine precision.

For convenience, first numerical results have been generated for interaction quenches of the two-dimensional Hubbard model on a square lattice at half-filling, where particle-number and spin conservation are respected trivially. Energy conservation has been enforced by time-dependent renormalization of the intra-cluster hopping in the 2×1 reference cluster. It is worth pointing out that even with this simple approximation (small cluster) the impact of the self-consistency condition is substantial. Comparing the conserving against plain CPT, there is a qualitative change of the time-dependence of the doublon density which is plausible and improves the theory: Artificial oscillations due to the finite cluster size are almost completely suppressed, and an ultrafast relaxation to a

(prethermal) state with nearly constant doublon density is predicted as might be expected from previous computations for one- and infinite-dimensional lattices.

Let us emphasize once more that our purpose has been to formally develop the very idea of a constrained CPT and to provide a proof of principle for its practicability. There are a couple of future tasks that suggest themselves immediately but are beyond the scope of this chapter: First of all, a more systematic study of the dependence on the cluster size and shape is needed. Note that this also includes the necessity to take into account more than a single optimization parameter as there are four local constraints to be satisfied in the present formulation of the theory [see Eq. (5.3)], corresponding to the conservation of spin and particle density as well as two constraints for the doublon density (implying energy conservation). Hence, for a cluster consisting of L_c sites, at most $4L_c$ parameters are needed. In addition, both the number of constraints and the optimization parameters depend on the spatial symmetries and other symmetries, e.g., particle-hole symmetry, of the original and the reference system. If necessary, more degrees of freedom and correspondingly more parameters can be generated by coupling uncorrelated "bath" sites to the physical sites in the reference system in the spirit of (cluster) dynamical mean-field theory. Systematic studies addressing the mentioned issues are necessary before a systematic and quantitative comparison with other approaches or with experiments is meaningful.

Interestingly, the conditional equations for the renormalization parameters feature singular points of non-invertibility. Technically, this currently restricts our investigations to quenches with small final interaction and short propagation times. It is not clear at the moment whether or not a physical meaning can be attributed to those singular points; also this requires further systematic studies. According to our present experience, it is well conceivable that, with a suitable regularization scheme, time propagation through a singularity of the Jacobian is possible and has no apparent impact on the time dependence of physical observables. Developing such a regularization scheme is the next task for future studies and the most important issue to make the conserving CPT a powerful numerical tool to address, e.g., real-time magnetization dynamics, even of inhomogeneous models and on long time scales.

6. Nonequilibrium two-pole approximation

In a first attempt to deal with the complexity of electronic correlations described by the Hubbard model, Hubbard himself proposed a scheme to decouple the hierarchy that arises from the equation of motion of the one-particle Green's function [27]. Nowadays known as Hubbard-I, his approach is equivalent to self-consistently approximating the self-energy using the exact expression of the atomic limit. Following the review of Gebhard [23], the resulting expression for the equilibrium Green's function reads

$$
G_{\vec{k}\sigma}(\omega) = \frac{Z_\sigma^+(\vec{k})}{\omega - E_\sigma^+(\vec{k})} + \frac{Z_\sigma^-(\vec{k})}{\omega - E_\sigma^-(\vec{k})},
\tag{6.1}
$$

where $\vec{k}$ refers to quasi-momenta exploiting the lattice periodicity. Quasi-particle dispersion and spectral weight are given as

$$
E_\sigma^\pm(\vec{k}) = \frac{1}{2}\left[\epsilon(\vec{k}) + U \pm \sqrt{(\epsilon(\vec{k}) - U)^2 + 4U n_{\bar\sigma}\epsilon(\vec{k})}\right],
\tag{6.2}
$$

$$
Z_\sigma^\pm(\vec{k}) = \pm\frac{E^\pm(\vec{k}) - U(1 - n_{\bar\sigma})}{E^+(\vec{k}) - E^-(\vec{k})},
$$

with $\epsilon(\vec{k}) = \sum_{\vec{R}} T(\vec{R}) e^{-i\vec{k}\cdot\vec{R}}$ being the Fourier transform of the time-independent hopping $T_{ij\sigma} = T(\vec{R}_i - \vec{R}_j)$, with $\vec{R}_i$ denoting a lattice vector, and $n_\sigma = \frac{1}{L}\sum_i\langle n_{i\sigma}\rangle$ as the spin-dependent density which is self-consistently determined from the lattice Green's function.

By design, Hubbard-I is exact in the noninteracting limit, $U = 0$, and the atomic limit $\epsilon(\vec{k}) = 0$. In the intermediate regime, it includes important effects characteristic for a many-body system: There is a dynamic shifting of spectral weight between the two poles, which correspond to the lower (E_σ^-) and the upper (E_σ^+) Hubbard bands, by tuning of the interaction U and the particle density $n_{\bar\sigma}$. In his original paper [27], Hubbard further showed that for a constant density of states, $\rho_0(\omega) = \frac{1}{\Delta}$, for $|\omega| \leq \frac{\Delta}{2}$, $\rho_0(\omega) = 0$ otherwise, a Mott transition is found at $U = 0^+$ at half-filling. Of course, one should also note that, due to its simplicity and rather ad hoc decoupling scheme, the theory has a number of severe defects [23]. First of all, a Mott transition at $U = 0^+$ is by no means generic. Although correct in one dimension [59], this seems more like a random coincidence since Hubbard-I lacks feedback of non-local correlations, i.e., the self-energy is $\vec{k}$-independent. This is far from true in low-dimensional systems but becomes accurate only in the opposite limit of infinite lattice dimension [39], where DMFT studies have shown, however,

that the Mott transition happens at finite critical interaction [133]. As another problematic aspect, Hubbard-I gives an insufficient description of the weak-coupling limit $U/W \ll 1$ (with W as the bandwidth). In particular, it does not reduce to the Hartree-Fock solution, i.e., there is no Fermi-liquid phase. This cannot hold in general. Lastly let us mention a problem that is shared with any two-pole approximation: The two distinct poles form a poor approximation of the branch cut of the Green's function at the real axis. This implies the lack of quasi-particle damping.

Necessary improvements to Hubbard-I can be derived from a number of different viewpoints. A non-comprehensive list includes the decoupling scheme by Roth [81, 82], the spectral density approach (SDA) [83], Mori-Zwanzig-like projection techniques [84, 85], or the composite operator method (COM) [134]. The resulting broad spectrum of possible applications is rather impressive: It reaches as far as the study of high-temperature superconductivity [135], ab initio electronic structure calculations [136], magnetic ordering [137, 138], the interplay of disorder and strong correlations [139], and, of course, the Mott transition which was already investigated as part of Hubbard's original series [27, 140], cf. Ref. 141 for a recent discussion. Even an extension to the classical Heisenberg ferromagnet has been put forward [142].

Targeted at nonequilibrium steady states, a generalization of the spectral density approach (SDA) has been developed [143, 144] and has been used to study the current-induced switching of the magnetization in magnetic tunnel junctions. A systematic framework for arbitrary time-dependent setups, however, is still lacking. Within this chapter, we develop such an approach for fermionic lattice models. Our starting point is a main result from Chapter 3, namely, that any interacting, fermionic lattice model can be mapped onto a noninteracting model by introducing virtual degrees of freedom. In Sec 6.1 we show, that these virtual degrees of freedom have a counterpart in the original system from which the effective medium can be derived without the need of calculating the Q-matrix (cf. Chapter 3). A systematic scheme to construct such operators parallels the Lanczos algorithm [145] and is presented in Sec. 6.2. It leads us very naturally to a nonequilibrium continued fraction representation of Green's function and self-energy thus generalizing Mori's famous result [88] to Keldysh-Matsubara Green's functions. Finally, in Sec. 6.3, we employ our results to construct a nonequilibrium two-pole approximation to the Hubbard model. A summary is given in Sec. 6.4.

6.1. Prerequisites

Within this section we heavily build upon the results proven in Chapter 3. To recapitulate an important insight recall that any interacting fermionic lattice model can be mapped to an appropriately chosen effective medium. In Sec. 3.2 we have constructed this effective medium to feature a diagonal virtual sector. By integrating out the virtual sites, this lead us to the self-energy in its Lehmann representation. Let us emphasize, however, that a diagonal virtual sector is by no means the only choice. Considering an arbitrary fermionic lattice model, $H(t)$ as given by Eq. (2.4), we drop this requirement for the effective medium, $h(t)$, in this section: $h_{ss'}(t) \neq \delta_{ss'} h_{ss'}(0)$. This restores the full freedom in choosing the generating O-matrix, $h(t) = [i\partial_t O(t)]O(t)$ (cf. Sec. 3.2). Nevertheless,

the main feature of the effective medium approach still holds: One-particle expectation values taken with respect to the effective Hamiltonian, $H^{\text{eff}}(t) = \sum_{xy} h_{xy}(t)\hat{a}_x^\dagger \hat{a}_y$, and the original Hamiltonian, $H(t)$, are equivalent, cf. Sec. 3.2.

In Section 6.1.1 we show that each choice for the O-matrix comes accompanied with a set of operators acting in the original many-body Fock space. By definition, these operators give direct access to the effective medium and thus suggest a new recipe for its construction (Sec. 6.1.2). Furthermore, together with the physical creation (annihilation) operators, they span an inner product space of operators (Sec. 6.1.3). Considering the time-evolution of a creation (annihilation) operator in the exact case and in effective-medium-based approximations, we show in Sec. 6.1.4 that it is restricted to a reduced subspace, which we call the *active* subspace. Exploiting the existence of an inner product, we use this property to derive a completeness relation (Sec. 6.1.5) which directly leads us to the decoupling scheme by Roth [81, 82].

6.1.1. One-to-one correspondence of virtual operators

Within the physical sector, there is an obvious one-to-one correspondence between the operators $\hat{a}_i$ [$\hat{a}_j^\dagger$] and the operators $\hat{c}_i$ [$\hat{c}_j^\dagger$]: $\langle \mathcal{T}_C \hat{a}_i(t)\hat{a}_j^\dagger(t') \rangle_{H^{\text{eff}}} = \langle \mathcal{T}_C \hat{c}_i(t)\hat{c}_j^\dagger(t') \rangle_H$, i.e., one-particle expectation values taken with respect to the effective Hamiltonian and the original Hamiltonian are equivalent, cf. Sec. 3.2. Let us emphasize though that this equivalence is restricted to one-particle Green's functions. This is due to the fact that, in contrast to the original system, higher-order Green's functions in the effective system decouple by Wick's theorem, e.g.,

$$\langle \hat{a}_i^\dagger(t_1)\hat{a}_j^\dagger(t_2)\hat{a}_k(t_3)\hat{a}_l(t_4) \rangle_{H^{\text{eff}}} = \langle \hat{a}_i^\dagger(t_1)\hat{a}_l(t_4) \rangle_{H^{\text{eff}}} \langle \hat{a}_j^\dagger(t_2)\hat{a}_k(t_3) \rangle_{H^{\text{eff}}} \tag{6.3}$$
$$- \langle \hat{a}_i^\dagger(t_1)\hat{a}_k(t_3) \rangle_{H^{\text{eff}}} \langle \hat{a}_j^\dagger(t_2)\hat{a}_l(t_4) \rangle_{H^{\text{eff}}}$$
$$\neq \langle \hat{c}_i^\dagger(t_1)\hat{c}_j^\dagger(t_2)\hat{c}_k(t_3)\hat{c}_l(t_4) \rangle_H.$$

It is, however, possible to define operators $\hat{c}_s$ [$\hat{c}_{s'}^\dagger$] that extend the one-to-one correspondence to the virtual sector. Interestingly, these can be chosen such that certain higher-order correlation functions become easily accessible. A concrete example will be studied in Sec. 6.3.1. We start by defining $I_\beta = \left\{ (m,n) : z_{(m,n)} > 0 \right\}$ where $z_{(m,n)} = \sqrt{e^{-\beta E_m} + e^{-\beta E_n}}/Z$ as defined in Section 2.3. Here, it is important to note that $z_{(m,n)}$ can only be zero if $\beta \to \infty$. I_β thus only distinguishes between zero and finite temperature and will be used to rigorously take care of a number of subtleties that arise in the zero temperature limit. Let further $O(t)$ be an arbitrary (in the sense of a possibly non-diagonal virtual sector, cf. the introduction Sec. 6.1), sufficiently smooth completion of the Q-matrix (cf. Sec. 3.2) such that

$$\sum_x O_{(m,n)x}(t)O_{(m',n')x}^*(t) = \delta_{mm'}\delta_{nn'}, \quad (m,n), (m',n') \in I_\beta. \tag{6.4}$$

6. Nonequilibrium two-pole approximation

Using the eigenbasis of the initial Hamiltonian, $H_{\text{ini}}|m\rangle = E_m|m\rangle$, we define the matrix elements of the virtual operators for $(m, n) \in I_\beta$ as

$$\hat{c}_s(t) \equiv \sum_{(m,n)\in I_\beta} \frac{1}{z_{(m,n)}} O_{s(m,n)}(t)|m\rangle\langle n|, \tag{6.5}$$

For $(m, n) \in I_\beta$, this is consistent with the relation $\langle m|\hat{c}_i(t)|n\rangle = \frac{1}{z_{(m,n)}} O_{i(m,n)}(t)$ that trivially holds in the physical sector. Corresponding to the O-matrix, we obtain an effective Hamiltonian $H^{\text{eff}}(t) = \sum_{xy} h_{xy}(t)\hat{a}_x^\dagger\hat{a}_y$ from Eq. (3.6) such that the one-particle Green's function of the original system can be extended to the virtual sector:

$$G_{xy}(t, t') \equiv -i\langle \mathcal{T}_C \, \hat{c}_x(t)\hat{c}_y^\dagger(t')\rangle_H = -i\langle \mathcal{T}_C \, \hat{a}_x(t)\hat{a}_y^\dagger(t')\rangle_{H^{\text{eff}}} = F_{xy}(t, t'). \tag{6.6}$$

In the context of one-particle expectation values, the operators $\hat{c}_x$ $[\hat{c}_x^\dagger]$ and $\hat{a}_x$ $[\hat{a}_x^\dagger]$ are therefore equivalent.

6.1.2. Accessing the effective medium

Exploiting the one-to-one correspondence, a number of relations can be generalized from the effective to the original system. First of all, there exists an analog to the fermionic anticommutation relation $\{\hat{a}_x(t), \hat{a}_y^\dagger(t)\} = \delta_{xy}$:

$$\langle \{\hat{c}_x(t), \hat{c}_y^\dagger(t)\}\rangle_H = \delta_{xy}. \tag{6.7}$$

We emphasize that it is essential to take the expectation value $\langle\cdot\rangle_H$ if calculating the anticommutator in Eq. (6.7). The anticommutator itself is not fermionic [except, of course, in the physical sector]. In general, we thus have

$$\{\hat{c}_i(t), \hat{c}_s^\dagger(t)\} \neq 0, \quad \{\hat{c}_s(t), \hat{c}_i^\dagger(t)\} \neq 0, \quad \{\hat{c}_s(t), \hat{c}_{s'}^\dagger(t)\} \neq \delta_{ss'}. \tag{6.8}$$

Furthermore, one can easily show that the operators $\hat{c}_x(t)$ $[\hat{c}_y^\dagger(t)]$ are subject to the same equation of motion as the operators $\hat{a}_x(t)$ $[\hat{a}_y^\dagger(t)]$

$$i\partial_t\hat{c}_x(t) = \sum_y h_{xy}(t)\hat{c}_y(t), \tag{6.9}$$

which, in general, is not consistent with Heisenberg's equation of motion (for the subset of physical operators $\hat{c}_i(t)$, see Sec. 6.1.3).[1] Together with the anticommutation relation,

---

[1] Considering only virtual operators, Eq. (6.9) is consistent with Heisenberg's equation of motion for operators with an explicit time-dependence in the Schrödinger picture. By defining $c_s(t) = \mathcal{U}(t, 0)\hat{c}_s(t)\mathcal{U}^\dagger(t, 0)$ as the Schrödinger picture version of $\hat{c}_s(t)$, we get the equation of motion $i\partial_t\hat{c}_s(t) = \sum_y h_{sy}(t)\hat{c}_y(t) = [\hat{c}_s(t), \hat{H}(t)] + \mathcal{U}^\dagger(t, 0)[i\partial_t c_s(t)]\mathcal{U}(t, 0)$. The explicit time-dependence of $c_s(t)$ originates from time-dependent orthonormalization coefficients which ensure $\langle\{\hat{c}_x(t), \hat{c}_y(t)\}\rangle_H = \delta_{xy}$ at every time t. In equilibrium, it is thus possible to enforce $i\partial_t c_s(t) = 0$ such that Heisenberg's equation of motion is restored in its well known form. To this end, one simply chooses $O_{s(m,n)}(t) = O_{s(m,n)}(0)e^{-i\epsilon_{(m,n)}t}$ when completing the Q-matrix, cf. Sec. 3.2.

Eq. (6.7), it follows that the matrix elements of the effective Hamiltonian can be accessed from the operators $\hat{c}_x(t)$ $[\hat{c}_y^\dagger(t)]$ as well

$$h_{xy}(t) = \langle\{[i\partial_t\hat{a}_x(t)], \hat{a}_y^\dagger(t)\}\rangle_{H^{\text{eff}}} = \langle\{[i\partial_t\hat{c}_x(t)], \hat{c}_y^\dagger(t)\}\rangle_H, \tag{6.10}$$

with the associated propagator $\mathcal{U}$ being given as

$$\mathcal{U}_{xy}(t) = \left[\mathcal{T}\exp\left(-i\int_0^t \mathrm{d}t' h(t')\right)\right]_{xy} = \sum_{mn} O_{x(m,n)}(t)O_{(m,n)y}^\dagger(0). \tag{6.11}$$

While all these results are in principle straightforward, they suggest a new recipe to construct the effective medium: Instead of completing the Q-matrix to a unitary transform, which requires the knowledge of all eigenstates of the initial Hamiltonian as well as their time-evolution, we can focus on constructing virtual operators $\hat{c}_s(t)$ $[\hat{c}_{s'}^\dagger(t)]$ that satisfy the anticommutation relation, Eq. (6.7), and give rise to the effective medium via Eq. (6.10). In this context we recall that the unitary completion $O(t)$ of the Q-matrix and as such the effective medium $h_{xy}(t)$ is not unique, cf. Chapter 3. As is evident from Eq. (6.5), this non-uniqueness transfers to the equivalent formulation using the virtual operator operators. It implies that the *virtual* operators $\hat{c}_s(t)$ $[\hat{c}_{s'}^\dagger(t)]$ are only fixed up to a time-dependent unitary transform. Note that such a transformation *must not* involve the physical degrees of freedom, i.e., $\hat{c}_i(t)$ $[\hat{c}_j^\dagger(t)]$, but has to be limited to the virtual sector.

6.1.3. Inner product space of operators

It is worthwhile to realize that the expression $\langle\{\cdot, \cdot^\dagger\}\rangle_H$ can be interpreted as a scalar product. To this end, we trivially have linearity in the first and semilinearity in the second argument for any operator A. To establish positive definiteness, however, one must define the underlying vector space differently in case of zero and finite temperature. Consider the following:

$$\langle\{A, A^\dagger\}\rangle_H = \sum_{nm} z_{(m,n)}^2 |\langle n|A|m\rangle|^2 \geq 0, \tag{6.12}$$

While we have $z_{(m,n)} = \sqrt{e^{-\beta E_m} + e^{-\beta E_n}}/Z > 0$ at any finite temperature, the quantity vanishes for many combinations (m, n) in the limit $\beta \to \infty$ implying that $\langle\{\cdot, \cdot^\dagger\}\rangle_H$ is only *semi*-definite at zero temperature (cf. the remark below Eq. (6.3)). To establish definiteness also in this case, we define the vector space as:

$$\mathcal{O} \equiv \left\{\sum_{(m,n)\in I_\beta} \alpha_{(m,n)}|m\rangle\langle n| : \alpha_{(m,n)} \in \mathbb{C}\right\}, \qquad I_\beta = \left\{(m,n) : z_{(m,n)} > 0\right\}. \tag{6.13}$$

Correspondingly, we define a projection operator $\mathcal{P}_\beta[\cdot]$ such that $\mathcal{P}_\beta[A] \in \mathcal{O}$ for any operator A. It can be interpreted to project out the thermally suppressed matrix elements at zero temperature. At finite temperature $\beta < \infty$, it is equal to the identity, i.e., $\mathcal{P}_\beta[A] = A$. In practice, it can of course also make sense to neglect certain combinations with $z_{(m,n)} < \epsilon \ll 1$ assuming we are at low-enough temperatures (cf. Section 3.3.3). Finally let us note that, by definition, the set of operators $\{\mathcal{P}_\beta[\hat{c}_x(t)]\}$ forms an orthonormal basis of $\mathcal{O}$ with respect to the scalar product $\langle\{\cdot, \cdot^\dagger\}\rangle_H$ at every time t.

Time-evolution of the physical operators

The difference between zero and finite temperature has an important consequence if we consider the time-evolution of the physical operators $\hat{c}_i(t)$. At finite temperature, their time-evolution as generated by Heisenberg's equation of motion is completely consistent with the time-evolution that follows from the effective medium:

$$\beta < \infty: \quad i\partial_t \hat{c}_i(t) = \left[\hat{H}(t)\hat{c}_i(t) - \hat{c}_i(t)\hat{H}(t) \right] \overset{(6.9)}{=} \sum_x h_{ix}(t)\hat{c}_x(t). \tag{6.14}$$

At zero temperature, however, this holds only true if we restrict ourselves to non-suppressed matrix elements. Using the projection operator $\mathcal{P}_\beta$, the following general equation can be formulated:

$$i\partial_t \mathcal{P}_\beta[\hat{c}_i(t)] = \mathcal{P}_\beta \left[\hat{H}(t)\hat{c}_i(t) - \hat{c}_i(t)\hat{H}(t) \right] \overset{(6.9)}{=} \sum_x h_{ix}(t)\mathcal{P}_\beta \left[\hat{c}_x(t) \right]. \tag{6.15}$$

The difference between zero and finite temperature can be traced back to the fact that the Q-matrix (cf. Eq. (2.16)) does not hold information on matrix elements $\langle n|\hat{c}_i(t)|m\rangle$ for which $z_{(m,n)} = 0$. Only elements $(m,n) \in I_\beta$, which fulfill $z_{(m,n)} > 0$, are stored and thus described by the effective medium. As a consequence, if considering two arbitrary operators A, B, we are always allowed to write $\langle \hat{c}_i(t)B\rangle = \sum_x \mathcal{U}_{ix}(t)\langle \hat{c}_i(0)B\rangle$, with $\mathcal{U}_{xy}(t)$ from Eq. (6.11), since only matrix elements with $z_{(m,n)} > 0$ are referenced. However, the evaluation of the time-evolution in a more general expression, e.g., $\langle A\hat{c}_i(t)B\rangle = \sum_x \mathcal{U}_{ix}(t)\langle A\hat{c}_i(0)B\rangle$, where all matrix elements $\langle m|\hat{c}_i(t)|n\rangle$ are referenced, is only valid at finite temperature.

6.1.4. The active subspace

While the possibility to neglect certain matrix elements of the operators $\hat{c}_x(t)$ at zero temperature is an important simplification, it is likely that we are interested in neglecting even more degrees of freedom. Either, because the problem can be simplified by exploiting certain symmetries of the Hamiltonian, or because the basis is by far too large, e.g., for non-integrable systems. Of course, a further basis reduction in the latter case must be carefully motivated since it leads into the realm of approximations. After having truncated the basis to a small enough, tractable set, its resulting dynamics are confined to a vector space $\mathcal{A}$ which is much smaller than $\mathcal{O}$ and which we call the *active subspace*.

To give a proper definition, we consider a full basis of operators $\hat{c}_x(t)$ as given. We further assume that, by having performed a basis reduction (either exactly or approximately), we have divided the basis into two subsets: A small, tractable subset $I_\mathcal{A}$ of basis vectors which includes the physical degrees of freedom $\hat{c}_i(t)$ and a large subset $I_\mathcal{A}^\perp$ that we neglect. For both subsets, the dynamics shall be unitary, i.e.,

$$i\partial_t \hat{c}_x(t) = \langle \{ [i\partial_t \hat{c}_x(t)], \hat{c}_y^\dagger(t) \} \rangle_H, \quad x, y \in I_\mathcal{A} \quad (x, y \in I_\mathcal{A}^\perp) \tag{6.16}$$

and thus in particular $h_{xy}(t) = 0$ if $x \in I_\mathcal{A}, y \in I_\mathcal{A}^\perp$. The matrix elements of the corresponding O-matrix are defined via Eq. (6.5). We note that in case of an approximate basis reduction, our assumption implies that Eq. (6.15) is violated.

We now define the active subspace $\mathcal{A}$ of operators as:

$$\mathcal{A} \equiv \left\{ \sum_{x \in I_{\mathcal{A}}} \alpha_x \mathcal{P}_\beta[\hat{c}_x(0)] : \alpha_x \in \mathbb{C} \right\}, \qquad (6.17)$$

with an associated projection operator $\mathcal{P}_{\mathcal{A}}[\cdot]$ such that $\mathcal{P}_{\mathcal{A}}[\mathcal{O}] = \mathcal{A}$. With respect to the eigenbasis of the initial Hamiltonian H_{ini}, $\mathcal{P}_{\mathcal{A}}$ can be stated explicitly as

$$[\mathcal{P}_{\mathcal{A}}]_{(m',n')}^{(m,n)} = \sum_{x \in I_{\mathcal{A}}} O_{x(m,n)}(t) O_{(m',n')x}^\dagger(t), \qquad (m,n), (m',n') \in I_\beta, \qquad (6.18)$$

where the time t can be chosen arbitrarily due to $\mathcal{P}_\beta[\hat{c}_x(t)] \in \mathcal{A}$ because of the unitary time evolution. Furthermore, we define by $\mathcal{A}^\perp$ the orthogonal complement space of $\mathcal{A}$ with respect to $\mathcal{O}$ [i.e., $\mathcal{O} = \mathcal{A} \oplus \mathcal{A}^\perp$, with "$\oplus$" being the direct sum].

The division into a set of tractable, $x \in \mathcal{I}_{\mathcal{A}}$, and intractable, $x \in \mathcal{I}_{\mathcal{A}}^\perp$, degrees of freedom is quite analogous to the Mori-Zwanzig projection technique [86–88]. Following Mori's original paper [87], the equation of motion of a set of dynamical variables $A(t)$ (in our case this is given by the set of operators $\hat{c}_x$) is considered. For a time-independent Hamiltonian, $H(t) = H$, the equation of motion $i\partial_t A(t) = [A(t), H]$ is restated as

$$\partial_t A(t) - i\hat{\omega} A(t) + \int_0^t \varphi(t - s) A(s) \mathrm{d}s = f(t), \qquad (6.19)$$

where $(f(t), A^*) = 0$, $(f(t_1), f^*(t_2))) = \varphi(t_1 - t_2)(A, A^*)$ for a scalar product $(\cdot, \cdot^*)$ and $A \equiv A(0)$. His projection operator onto the A-axis, $P(\cdot) = (\cdot, A^*)(A, A^*)^{-1} A$, is analog to our projection operator onto the active subspace, $\mathcal{P}_{\mathcal{A}}[\cdot]$. A minor difference is found in the property that our degrees of freedom are normalized. His $\hat{\omega}$ corresponds to our effective medium $h(t)$. Since Eq. (6.19) is exact, it highlights the information discarded in the context of an approximate basis truncation: $f(t)$ must be discarded, which amounts to contributions of the orthogonal complement space $\mathcal{A}^\perp$. Furthermore, a bit more subtle, $\varphi(t)$ is also discarded. It quantifies the amount of back scattering, i.e., processes of the form $A \to f \to A$.

6.1.5. Completeness of the active subspace

The restriction of the dynamics to the linear subspace $\mathcal{A}$, either exactly due to symmetries of the Hamiltonian or approximately due to neglecting a certain subset of basis vectors, allows for the statement of a completeness relation. Let "$\bullet$" denote an arbitrary product of fermionic creation and annihilation operators. One finds

$$\langle \bullet \, \hat{c}_i(t) \rangle_H = \sum_{mn} z_{(m,n)} \langle n | \bullet | m \rangle f(\epsilon_{(m,n)}) O_{i(m,n)}(t) \qquad (6.20)$$

$$= \sum_x \sum_{m'n'} \sum_{mn} z_{(m,n)} \langle n | \bullet | m \rangle O_{x(m,n)}(t') O_{(m',n')x}^\dagger(t') f(\epsilon_{(m',n')}) O_{i(m',n')}(t)$$

$$= \sum_x \langle \{ \bullet, \hat{c}_x(t') \} \rangle_H \langle \hat{c}_x^\dagger(t') \hat{c}_i(t) \rangle_H$$

$$= \sum_{x \in I_{\mathcal{A}}} \langle \{ \bullet, \hat{c}_x(t') \} \rangle_H \langle \hat{c}_x^\dagger(t') \hat{c}_i(t) \rangle_H$$

6. Nonequilibrium two-pole approximation

The last equality exploits the unitarity of the time-evolution, i.e., Eq. (6.16). Correlation functions of the form

$$\langle \hat{c}_x^\dagger(t)\hat{c}_i(t)\rangle_H = 0, \quad x \in I_{\mathcal{A}}^\perp, \tag{6.21}$$

must therefore vanish, as the two subspaces $\mathcal{A}$ and $\mathcal{A}^\perp$ are not connected through the effective medium. Relation (6.20) proves that the evaluation of $\langle \bullet\, \hat{c}_i(t)\rangle_H$ involves a projection of "$\bullet$" onto the active subspace. Its time-independent, equilibrium variant lies at the heart of the famous Roth approximation, cf. Eq. (32) in Ref. 82. It should be emphasized though, that the *approximate* nature of the Roth approximation does not stem from the application of Eq. (6.20) which is an exact relation. The single approximation made is the usage of a truncated basis, cf. Sec. 6.1.4. Let us further note that, by slightly adapting the proof, one can show the following variations

$$\langle \hat{c}_i(t) \bullet \rangle_H = \sum_{x \in I_{\mathcal{A}}} \langle \hat{c}_i(t)\hat{c}_x^\dagger(t')\rangle_H \langle \{\hat{c}_x(t'), \bullet\} \rangle_H, \tag{6.22}$$

$$\langle \hat{c}_i^\dagger(t) \bullet \rangle_H = \sum_{x \in I_{\mathcal{A}}} \langle \hat{c}_i^\dagger(t)\hat{c}_x(t')\rangle_H \langle \{\hat{c}_x^\dagger(t'), \bullet\} \rangle_H,$$

$$\langle \bullet\, \hat{c}_i^\dagger(t)\rangle_H = \sum_{x \in I_{\mathcal{A}}} \langle \{\bullet, \hat{c}_x^\dagger(t')\} \rangle_H \langle \hat{c}_x(t')\hat{c}_i^\dagger(t)\rangle_H.$$

In combination with the completeness relations, Eq. (6.20) and Eq. (6.22), a second relation will prove to be useful. Let $\mathcal{U}_{xy}(t)$, $x, y \in I_{\mathcal{A}}$ denote the matrix elements of the propagator $\mathcal{U}(t) = \mathcal{T}\exp\left(-i\int_0^t dt' h(t')\right)$ in the active subspace. Let further M be an arbitrary operator. Then:

$$\sum_{x \in I_{\mathcal{A}}} \hat{c}_x(t)M\hat{c}_x^\dagger(t) = \sum_{x,y_1,y_2 \in I_{\mathcal{A}}} \mathcal{U}_{xy_1}(t)\mathcal{U}_{y_2x}^*(t)\hat{c}_{y_1}(0)M\hat{c}_{y_2}^\dagger(0) = \sum_{x \in I_{\mathcal{A}}} \hat{c}_x(0)M\hat{c}_x^\dagger(0), \tag{6.23}$$

where we exploited the unitarity of the propagator. One easily veryfies that the proof holds independent of the order of $\hat{c}_x^\dagger(t), \hat{c}_x(t)$, i.e.,

$$\sum_{x \in I_{\mathcal{A}}} \hat{c}_x^\dagger(t)M\hat{c}_x(t) = \sum_{x \in I_{\mathcal{A}}} \hat{c}_x^\dagger(0)M\hat{c}_x(0) \tag{6.24}$$

holds as well.

Non-interacting systems and Wick's Theorem

For a noninteracting system, one can easily show that Wick's Theorem follows from Eqs. (6.20) and (6.23). To this end, let $H(t) = H_0(t)$ be an arbitrary one-particle Hamiltonian. The active subspace follows as $\mathcal{A} = \{\sum_i \alpha_i[\mathcal{P}_\beta \hat{c}_i(0)] : \alpha_i \in \mathbb{C}\}$, i.e., dynamics is restricted to the physical one-particle degrees of freedom. Let us now consider an arbitrary, two-

particle expectation value:

$$\langle \hat{c}_i^\dagger(t_1)\hat{c}_j^\dagger(t_2)\hat{c}_k(t_3)\hat{c}_l(t_4)\rangle \overset{(6.20)}{=} \sum_{j'}\langle\left\{\hat{c}_i^\dagger(t_1)\hat{c}_j^\dagger(t_2)\hat{c}_k(t_3), \hat{c}_{j'}(t')\right\}\rangle\langle\hat{c}_{j'}^\dagger(t')\hat{c}_l(t_4)\rangle \qquad (6.25)$$

$$= \sum_{j'}\langle\hat{c}_i^\dagger(t_1)\hat{c}_j^\dagger(t_2)\left\{\hat{c}_k(t_3), \hat{c}_{j'}(t')\right\}\rangle\langle\hat{c}_{j'}^\dagger(t')\hat{c}_l(t_4)\rangle$$

$$- \sum_{j'}\langle\left[\hat{c}_i^\dagger(t_1)\hat{c}_j^\dagger(t_2), \hat{c}_{j'}(t')\right]\hat{c}_k(t_3)\rangle\langle\hat{c}_{j'}^\dagger(t')\hat{c}_l(t_4)\rangle$$

$$\overset{(6.23)}{=} \langle\hat{c}_j^\dagger(t_2)\hat{c}_k(t_3)\rangle\langle\hat{c}_i^\dagger(t_1)\hat{c}_l(t_4)\rangle - \langle\hat{c}_i^\dagger(t_1)\hat{c}_k(t_3)\rangle\langle\hat{c}_j^\dagger(t_2)\hat{c}_l(t_4)\rangle.$$

In the last step we exploited Eq. (6.23) by setting $t' = t_3$, so that $\{\hat{c}_k(t_3), \hat{c}_{j'}(t_3)\} = 0$. The commutator in the remaining term is easily evaluated and yields the final result after taking again advantage of Eq. (6.23) by setting $t' = t_1$ and $t' = t_2$, respectively. Let us emphasize that for a two-particle expression with a different order of the operators, e.g., $\langle\hat{c}_k(t_3)\hat{c}_i^\dagger(t_1)\hat{c}_l(t_4)\hat{c}_j^\dagger(t_2)\rangle$, one can apply the same idea by using one of the variants of the completeness relation and the time-shift argument, i.e., Eqs. (6.22) and Eq. (6.24). Considering finally an arbitrarily ordered n-particle expectation value, the same steps can be performed repeatedly such that in the end an expression involving only one-particle expectation values is obtained. This proves Wick's Theorem.

6.2. Analytical scheme to construct the effective medium

In Section 6.1.2 we have argued that the possibility to extend the one-to-one correspondence to the virtual sector suggests the following construction scheme for the effective Hamiltonian: Assume that only the operators in the physical sector, i.e., $\hat{c}_i(t)$ [$\hat{c}_j^\dagger(t)$], and the Hamiltonian $H(t)$ are given. By completing the set of virtual operators $\hat{c}_s(t)$ [$\hat{c}_{s'}^\dagger(t)$] we enable ourselves to obtain $h_{xy}(t)$ from Eq. (6.10). An intuitive way to work this out largely parallels the Lanczos algorithm [145] and is presented in Section 6.2.1. The resulting effective medium is found to be block-tridiagonal. Its relation to the effective medium that we have used for the Lehmann representation, which features a diagonal virtual sector (cf. Fig. 3.1), is worked out as part of Section 6.2.2. There we also show that the block-tridiagonal structure of the effective medium translates to a representation of the two-time Green's function as a continued fraction within the Keldysh-Matsubara formalism.

6.2.1. Lanczos-like algorithm for obtaining the virtual operators

Our construction is based on the property that $\langle\{\cdot, \cdot^\dagger\}\rangle$ forms a scalar product on $\mathcal{O}$, i.e., our main idea is to apply Gram-Schmidt orthonormalization. A systematic scheme can be based on a repeated calculation of the derivative with respect to time of the physical operators $\hat{c}_i(t)$ which yields linear independent operators due to the commutation with

the Hamiltonian. Consider, for example, the first step:

$$\hat{\Gamma}_i^{(1)}(t) \equiv i\partial_t \hat{c}_i(t) - \sum_j \langle \{ i\partial_t \hat{c}_i(t), \hat{c}_j^\dagger(t) \} \rangle \hat{c}_j(t) - \sum_{j<i} \langle \{ i\partial_t \hat{c}_i(t), [\hat{c}_j^{(1)}(t)]^\dagger \} \rangle \hat{c}_j^{(1)}(t),$$

$$\hat{c}_i^{(1)}(t) \equiv \frac{\hat{\Gamma}_i^{(1)}(t)}{\sqrt{\langle \{ \hat{\Gamma}_i^{(1)}(t), [\hat{\Gamma}_i^{(1)}]^\dagger(t) \} \rangle}}. \tag{6.26}$$

Assuming $0 \leq i < L$, with L denoting the total number of single-particle degrees of freedom, this provides us with L virtual operators denoted as $\hat{c}_i^{(1)}(t)$. With $\hat{c}_i^{(n)}(t) \equiv \hat{\Gamma}_i^{(n)}(t)/\langle \{ \hat{\Gamma}_i^{(n)}(t), [\hat{\Gamma}_i^{(n)}(t)]^\dagger \} \rangle$, we iteratively define

$$\hat{\Gamma}_i^{(n+1)}(t) = i\partial_t \hat{c}_i^{(n)}(t) - \sum_{m \leq n} \sum_j \langle \{ i\partial_t \hat{c}_i^{(n)}(t), [\hat{c}_j^{(m)}(t)]^\dagger \} \rangle \hat{c}_j^{(m)}(t)$$

$$- \sum_{j<i} \langle \{ i\partial_t \hat{c}_i^{(n)}(t), [\hat{c}_j^{(n+1)}(t)]^\dagger \} \rangle \hat{c}_j^{(n+1)}(t) \tag{6.27}$$

for all n. The matrix elements of the effective Hamiltonian can be classified according to our construction scheme. We set $\hat{c}_i^{(0)}(t) \equiv \hat{c}_i(t)$ and define

$$h_{ij}^{(n,m)}(t) \equiv \langle \{ i\partial_t \hat{c}_i^{(n)}(t), [\hat{c}_j^{(m)}(t)]^\dagger \} \rangle, \tag{6.28}$$

which is non-zero only for $n-1 \leq m \leq n+1$, i.e., the hopping is limited to neighbouring sectors. This follows from Eq. (6.27) and the from the effective Hamiltonian being Hermitian. Consequently, we obtain a block-tridiagonal form:

$$h^{\setminus}(t) = \begin{pmatrix} h^{(0,0)} & h^{(0,1)} & 0 & 0 & \cdots \\ h^{(1,0)} & h^{(1,1)} & h^{(1,2)} & 0 & \cdots \\ 0 & h^{(2,1)} & h^{(2,2)} & h^{(2,3)} & \cdots \\ 0 & 0 & h^{(3,2)} & h^{(3,3)} & \cdots \\ \vdots & \vdots & \vdots & \vdots & \ddots \end{pmatrix}. \tag{6.29}$$

Similarly, the virtual sector can be subdivided according to this scheme such that $h^{(n,n)}(t)$ is a linear map in the n-th virtual sector. Consequently, $h^{(n,n+1)}$ maps from the $n+1$-th to the n-th virtual sector. Let us note that $h^{\setminus}(t)$ coincides with the effective medium $h(t)$, as defined in Eq. (3.9), only in the physical sector. Finally, Eq. (6.29) implies that $\hat{c}_i^{(n+1)}$ can be stated by means of a recursion formula

$$\hat{\Gamma}_i^{(n+1)}(t) = h_{ii}^{(n,n+1)}(t)\hat{c}_i^{(n+1)}(t) = i\partial_t \hat{c}_i^{(n)}(t) - \sum_{j \geq i} h_{ij}^{(n,n-1)} \hat{c}_j^{(n-1)}(t) \tag{6.30}$$

$$- \sum_{j<i} h_{ij}^{(n,n+1)}(t)\hat{c}_j^{(n+1)}(t) - \sum_j h_{ij}^{(n,n)}(t)\hat{c}_j^{(n)}(t).$$

A closer look reveals that the block-tridiagonal shape as well as the recursion formula were results to be expected by design. In its essence, the construction largely parallels

the Lanczos algorithm [145] which yields an orthonormal basis [here: $\hat{c}_i^{(n)}(t)$] of a corresponding Krylov subspace [146] [here: $\mathcal{A}$, see below]. It should also be noted, that a similar algorithm appears in the context of the Mori-Zwanzig projection technique [86–88]. It is thus to no surprise that it is possible to derive a generalization of Mori's continued fraction expansion [88] to Keldysh-Matsubara Green's functions (cf. Sec. 6.2.2).

Termination of the iterative scheme

If we are dealing with finite systems, the maximal number of virtual operators is also finite and so the inductive scheme given by Eq. (6.27) must terminate after a finite number of iterations. In the simplest case, the time-evolution of all involved operators is smooth. Then, we find at every time t the same lowest order N_{it} such that $h^{(N_{it},N_{it}+1)}(t)$ vanishes. The associated active subspace reads:

$$\mathcal{A} = \left\{ \sum_{n=0}^{N_{it}} \sum_i \alpha_i [\mathcal{P}_\beta \hat{c}_i^{(n)}(0)] : \alpha_i \in \mathbb{C} \right\}. \tag{6.31}$$

Interestingly, it is the lowest-dimensional subspace that features $\mathcal{P}_\beta[\hat{c}_i(t)] \in \mathcal{A}$, i.e., any other subspace $\tilde{\mathcal{A}}$ with the same property must contain $\mathcal{A}$. This follows from its construction as a Krylov space with $i\partial_t$ as the generating operator. Based on this property, an upper bound for the required number of iterations N_{it} can be obtained by counting the number of non-vanishing elements of the Q-matrix (in complete analogy to Section 3.3.3): Exploiting known symmetries of the Hamiltonian and excluding thermally suppressed combinations (i.e., combinations with $z_{(m,n)} = 0$) we start with an upper bound N_{ct} for the number of contributing combinations (m, n). Based on this knowledge we can be sure that an exact description of the system using an O-matrix of dimension $N_{ct} \times N_{ct}$ is possible. Assuming L linear independent operators are obtained per iteration, the inductive procedure must terminate after $N_{it} \leq N_{ct}/L - 1$ steps.

A possible complication could be that we do not obtain L linear independent operators per iteration. This is most likely due to a special form of the Hamiltonian. For a single-impurity Anderson model, for example, we obtain per step only a single new virtual operator since interactions are restricted to the impurity site. Consequently, we have to perform $N_{ct} - L$ iterations in this case.

The situation is more complicated if the time-evolution is not smooth. An important scenario that falls into this category is an interaction quench: $H(t < t_q) = H_0(t)$, $H(t \geq t_q) = H_0(t) + H_{int}(t)$. In this case, we have $N_{it} = 0$ for times $t < t_q$ since the system can be completely described in terms of the physical degrees of freedom. For $t \geq t_q$, on the other hand, virtual degrees of freedom must be considered as well such that we have $N_{it} > 0$. A simple solution for this example is to include the missing virtual operators for $t < t_q$.

6.2.2. The nonequilibrium Green's function as a continued fraction

It is worthwhile to link our results back to the conventional, two-time Keldysh-Matsubara formalism. To this end, we integrate out the virtual degrees of freedom step by step for

each n. The block-tridiagonal form of the effective Hamiltonian leads to the emergence of a continued fraction. Consider the definition

$$g_{ij}^{(n)}(t,t') = \frac{1}{[g_0^{(n,n)}]^{-1} - \Lambda^{(n)}}, \quad [g_0^{(n,n)}]_{ij}^{-1}(t,t') = [\delta_{ij}i\partial_t - h_{ij}^{(n,n)}(t)]\delta_C(t,t'), \quad (6.32)$$

$$\Lambda_{ij}^{(n)}(t,t') = \sum_{kl} h_{ik}^{(n,n+1)}(t)g_{kl}^{(n+1)}(t,t')h_{lj}^{(n+1,n)}(t'), \quad (6.33)$$

which yields for the one-particle Green's function

$$G_{ij}(t,t') = \left[\frac{1}{[g_0^{(0,0)}]^{-1} - h^{(0,1)} \circ \frac{1}{[g_0^{(1,1)}]^{-1} - h^{(1,2)} \circ \frac{1}{[g_0^{(2,2)}]^{-1}-\dots} \circ h^{(2,1)}} \circ h^{(1,0)}} \right]_{ij} (t,t'). \quad (6.34)$$

In contrast to equilibrium expansions, cf. Ref. 88, the evaluation of every fraction requires a matrix inversion on the Keldysh-Matsubara contour. Due to this property, it seems much more convenient to refrain from integrating out the physical sectors in practice. Instead, one works with an enlarged single-particle Hilbert space which also comprises the virtual sector.

A continued fraction can also be stated for the nonequilibrium self-energy $\Sigma(t,t') = \delta_C(t,t')\Sigma^{\mathrm{HF}}(t) + \Sigma^C(t,t')$:

$$\Sigma_{ij}^C(t,t') = \left[h^{(0,1)} \circ \frac{1}{[g_0^{(1,1)}]^{-1} - h^{(1,2)} \circ \frac{1}{[g_0^{(2,2)}]^{-1}-\dots} \circ h^{(2,1)}} \circ h^{(1,0)} \right]_{ij} (t,t'). \quad (6.35)$$

Note that in this form, the correlated part of the self-energy is *not* given in form of a Lehmann representation. Even if we diagonalize $g^{(1)}(t,t')$ such that

$$\Sigma_{ij}^C(t,t') = \sum_{kk'} h_{ik}^{(0,1)}(t)g_{kk'}^{(1)}(t,t')h_{k'j}^{(1,0)}(t') = \sum_k \bar{h}_{ik}^{(0,1)}(t)\bar{g}_{kk}^{(1)}(t,t')\bar{h}_{kj}^{(1,0)}(t') \quad (6.36)$$

there is a mismatch with our definition, Eq. (3.15), since $\bar{g}^{(1,1)}(t,t')$ is not simply the solution of an isolated site, Eq. (2.17). Since it is quite instructive, we explicitly derive the Lehmann representation of the nonequilibrium self-energy starting from Eq. (6.32) in the following.

Lehmann representation of the nonequilibrium self-energy

The Green's function $g_{kl}^{(1)}(t,t')$ can be written as

$$g_{kl}^{(1)}(t,t') = i \left[\mathcal{U}^{(1)}(t,0) \left(f[h^{\geq(1,1)}(0)] - \Theta_C(t,t') \right) [\mathcal{U}^{(1)}(t',0)]^\dagger \right]_{kl}. \quad (6.37)$$

Here, $h^{\geq(1,1)}(t)$ is defined as equal to $h^{\backslash}(t)$ but with the first line and column removed, cf. Eq. (6.29). At time $t = 0$, it is diagonalized as $h^{\geq(1,1)}(0) = RDR^\dagger$, with $D_{ss'} = \delta_{ss'}D_{ss}$.

The propagator $\mathcal{U}^{(1)}$ is defined as $\mathcal{U}^{(1)}(t,0) = \mathcal{T}\exp\left(-i\int_0^t dt' h^{\geq(1,1)}(t')\right)$. Finally, the expression $f[\cdot]$ refers to the matrix Fermi distribution:

$$f[h^{\geq(1,1)}(0)] = f[RDR^\dagger] = Rf[D]R^\dagger, \quad \text{where} \quad f[D]_{ss'} = \delta_{ss'}f(D_{ss}), \qquad (6.38)$$

where $f(\epsilon)$ denotes the Fermi distribution. Let us emphasize that $\mathcal{U}^{(1)}(t,0)$, $h^{\geq(1,1)}(t)$, D and R are linear transformations in the full virtual sector. The corresponding indices are s, s', while the k, l indices label degrees of freedom in the first virtual sector only. Eq. (6.37) thus projects out the dynamics of all virtual sectors but the first. We proceed by defining

$$h_{is}(t) \equiv e^{iD_{ss}t}\sum_{ks'} h_{ik}^{(0,1)}(t)\mathcal{U}_{ks'}^{(1)}(t,0)R_{s's}, \qquad (6.39)$$

which in particular guarantees $h_{is}(-i\tau) = h_{is}(0)$ as is easily verified. This is necessary to use $h_{is}(t)$ as hopping parameter within a single-particle Hamiltonian. Inserting this definition into Eq. (6.36) yields the Lehmann representation

$$\Sigma_{ij}^{\mathrm{C}}(t,t') = \sum_s h_{is}(t)g(D_{ss};t,t')h_{js}^*(t') \qquad (6.40)$$

in formal agreement with our definition, Eq. 3.2, and with $g(\epsilon;t,t')$ as defined in Eq. (2.17). Note that formal agreement implies identity up to rotations in invariant subspaces due to the uniqueness of the Lehmann representation (cf. the discussion below Eq. (3.9)).

6.3. Application to the one-band Hubbard model

So far, our considerations are formally exact for arbitrary, fermionic lattice systems. In this section we take a look at a concrete model Hamiltonian, namely the time-dependent Hubbard model. In particular, since an exact solution is restricted to very small lattice sizes, we suggest a self-consistent approximation that can also be applied to larger systems. The main idea is rather simple: Taking advantage of the block-tridiagonal form of the effective medium, we decouple virtual sectors of second and higher order, i.e.,

$$h^{\backslash}(t) = \begin{pmatrix} h^{(0,0)} & h^{(0,1)} & 0 & 0 & \cdots \\ h^{(1,0)} & h^{(1,1)} & h^{(1,2)} & 0 & \cdots \\ 0 & h^{(2,1)} & h^{(2,2)} & h^{(2,3)} & \cdots \\ 0 & 0 & h^{(3,2)} & h^{(3,3)} & \cdots \\ \vdots & \vdots & \vdots & \vdots & \ddots \end{pmatrix} \approx \begin{pmatrix} h^{(0,0)} & h^{(0,1)} & 0 & 0 & \cdots \\ h^{(1,0)} & h^{(1,1)} & 0 & 0 & \cdots \\ 0 & 0 & h^{(2,2)} & h^{(2,3)} & \cdots \\ 0 & 0 & h^{(3,2)} & h^{(3,3)} & \cdots \\ \vdots & \vdots & \vdots & \vdots & \ddots \end{pmatrix}.$$
$$(6.41)$$

As $h^{(0,0)}$ is exactly given by the Hartree-Fock Hamiltonian, this can be considered as the simplest approximation possible within this scheme that goes beyond standard mean-field theory. From the viewpoint of the continued fraction expansion, it is equivalent to setting $\Lambda^{(1)} = 0$ within the expansion of the Green's function as a continued fraction. A

decoupling via Eq. (6.41) can therefore be interpreted as the nonequilibrium variant of a two-pole approximation [88].

The route to a self-consistent two-pole approximation first of all requires the explicit derivation of the matrix elements of the first virtual sector $h^{(1,1)}$ for the Hubbard model. This is worked out in Section 6.3.1. As a major complication we find, that this does not automatically lead to a closed set of equations, i.e., there is no obvious way to express $h^{(1,1)}$ in terms of $\langle [\hat{c}_i^{(n)}(t)]^\dagger \hat{c}_j^{(m)}(t) \rangle, n, m \leq 1$. This issue is investigated in Section 6.3.2 where we exploit the completeness of the active subspace to close the self-consistency without the need to resort to a further approximation. In Section 6.3.3, we discuss the resulting self-consistency cycle and argue that a violation of energy and particle number conservation must be expected during the propagation. Finally, we specialize the propagation to the time-local density matrix instead of the time-non-local Green's function which allows to enforce the conservation laws and their corresponding local constraints (Section 6.3.4).

For a leaner notation, we employ the shorthand notation $\hat{A} \equiv \hat{A}(t)$ for operators in the Heisenberg picture throughout this section where this is unambiguously possible. Expectation values are taken with respect to the Hubbard Hamiltonian, i.e., $\langle \cdot \rangle \equiv \langle \cdot \rangle_H$ with $H(t)$ as defined in Eq. (6.42).

6.3.1. Evaluating the first virtual sector for the Hubbard model

To give a self-contained presentation, we recall the Hubbard Hamiltonian as

$$H(t) = \sum_{ij\sigma} [T_{ij\sigma}(t) - \mu\delta_{ij}] c_{i\sigma}^\dagger c_{j\sigma} + U(t) \sum_i n_{i\uparrow} n_{i\downarrow}. \tag{6.42}$$

One readily calculates the time-derivative $i\partial_t \hat{c}_{i\sigma}$ as

$$i\partial_t \hat{c}_{i\sigma} = \left[\hat{c}_{i\sigma}, \hat{H} \right] = \sum_j (T_{ij\sigma}(t) - \delta_{ij}\mu)\hat{c}_{j\sigma} + U(t)\hat{n}_{i\bar{\sigma}}\hat{c}_{i\sigma} \tag{6.43}$$

Evaluation of Eq. (6.26) yields

$$\hat{\gamma}_{i\sigma} \equiv \hat{c}_{i\sigma}^{(1)} = \frac{\hat{n}_{i\bar{\sigma}} - \langle \hat{n}_{i\bar{\sigma}} \rangle}{\sqrt{\langle \hat{n}_{i\bar{\sigma}} \rangle - \langle \hat{n}_{i\bar{\sigma}} \rangle^2}} \hat{c}_{i\sigma} \tag{6.44}$$

It is instructive to verify that $\hat{\gamma}_{i\sigma}$ indeed fulfills the orthonormalization requirement, Eq. (6.7):

$$\langle \{ \hat{\gamma}_{i\sigma}, \hat{c}_{j\sigma}^\dagger \} \rangle \propto \langle \{ [\hat{n}_{i\bar{\sigma}} - \langle \hat{n}_{i\bar{\sigma}} \rangle] \hat{c}_{i\sigma}, \hat{c}_{j\sigma}^\dagger \} \rangle = \langle [\hat{n}_{i\bar{\sigma}} - \langle \hat{n}_{i\bar{\sigma}} \rangle] \{ \hat{c}_{i\sigma}, \hat{c}_{j\sigma}^\dagger \} \rangle = 0, \tag{6.45}$$

$$\langle \{ \hat{\gamma}_{i\sigma}, \hat{\gamma}_{j\sigma}^\dagger \} \rangle = \frac{\langle [\hat{n}_{i\bar{\sigma}} - \langle \hat{n}_{i\bar{\sigma}} \rangle][\hat{n}_{j\bar{\sigma}} - \langle \hat{n}_{j\bar{\sigma}} \rangle] \{ \hat{c}_{i\sigma}, \hat{c}_{j\sigma}^\dagger \} \rangle}{\sqrt{\langle \hat{n}_{i\bar{\sigma}} \rangle - \langle \hat{n}_{i\bar{\sigma}} \rangle^2} \sqrt{\langle \hat{n}_{j\bar{\sigma}} \rangle - \langle \hat{n}_{j\bar{\sigma}} \rangle^2}} = \delta_{ij} \frac{\langle [\hat{n}_{i\bar{\sigma}} - \langle \hat{n}_{i\bar{\sigma}} \rangle]^2 \rangle}{\langle \hat{n}_{i\bar{\sigma}} \rangle - \langle \hat{n}_{i\bar{\sigma}} \rangle^2} = \delta_{ij}.$$

We proceed by calculating explicit expressions for $h^\backslash(t)$. The physical sector is readily obtained from Eq. (6.43)

$$h_{ij\sigma}^{(0,0)}(t) = \langle \{ i\partial_t \hat{c}_{i\sigma}, \hat{c}_{j\sigma}^\dagger \} \rangle = T_{ij\sigma}(t) - \mu\delta_{ij} + U(t)\langle \hat{n}_{i\bar{\sigma}} \rangle \delta_{ij} \tag{6.46}$$

and identical to the Hartree-Fock Hamiltonian as expected. The hybridization elements between the physical and virtual sector follow as

$$
h_{ij\sigma}^{(0,1)}(t) = [h_{ji\sigma}^{(1,0)}(t)]^* = \langle \{i\partial_t \hat{c}_{i\sigma}, \hat{\gamma}_{j\sigma}^\dagger\}\rangle = U(t) \frac{\langle\{\hat{n}_{i\bar{\sigma}}\hat{c}_{i\sigma}, (\hat{n}_{j\bar{\sigma}} - \langle\hat{n}_{j\bar{\sigma}}\rangle)\hat{c}_{j\sigma}^\dagger\}\rangle}{\sqrt{\langle\hat{n}_{i\bar{\sigma}}\rangle - \langle\hat{n}_{i\bar{\sigma}}\rangle^2}}
$$

$$
= \delta_{ij}U(t)\sqrt{\langle\hat{n}_{i\bar{\sigma}}\rangle - \langle\hat{n}_{i\bar{\sigma}}\rangle^2}. \tag{6.47}
$$

The evaluation of $h_{ik\sigma}^{(1,1)}(t) = \langle\{i\partial_t\hat{\gamma}_{i\sigma}, \hat{\gamma}_{k\sigma}^\dagger\}\rangle$, on the other hand, turns out to be quite tedious. We refer to Appendix B.1 for the details. For the diagonal elements, one obtains the final expression

$$
h_{ii\sigma}^{(1,1)}(t) = T_{ii\sigma}(t) - \mu + U(t)(1 - \langle\hat{n}_{i\bar{\sigma}}\rangle) - \left(\frac{1}{2} - \langle\hat{n}_{i\sigma}\rangle\right)\sum_{j\neq i}\frac{\left[T_{ij\bar{\sigma}}(t)\langle\hat{c}_{i\bar{\sigma}}^\dagger\hat{c}_{j\bar{\sigma}}\rangle + \text{cc.}\right]}{\sqrt{\langle\hat{n}_{i\bar{\sigma}}\rangle - \langle\hat{n}_{i\bar{\sigma}}\rangle^2}}
$$

$$
+ \frac{\sqrt{\langle\hat{n}_{i\sigma}\rangle - \langle\hat{n}_{i\sigma}\rangle^2}}{\sqrt{\langle\hat{n}_{i\bar{\sigma}}\rangle - \langle\hat{n}_{i\bar{\sigma}}\rangle^2}}\sum_{j\neq i}\frac{\left[T_{ij\bar{\sigma}}(t)\langle\hat{\gamma}_{i\bar{\sigma}}^\dagger\hat{c}_{j\bar{\sigma}}\rangle + \text{cc.}\right]}{\sqrt{\langle\hat{n}_{i\bar{\sigma}}\rangle - \langle\hat{n}_{i\bar{\sigma}}\rangle^2}}, \tag{6.48}
$$

and for the off-diagonals ($i \neq k$)

$$
h_{ik\sigma}^{(1,1)}(t) = \frac{T_{ik\sigma}(t)(\langle\hat{n}_{i\bar{\sigma}}\hat{n}_{k\bar{\sigma}}\rangle - \langle\hat{n}_{i\bar{\sigma}}\rangle\langle\hat{n}_{k\bar{\sigma}}\rangle) - \langle\left[T_{ik\bar{\sigma}}(t)\hat{c}_{i\bar{\sigma}}^\dagger\hat{c}_{k\bar{\sigma}} + T_{ki\bar{\sigma}}(t)\hat{c}_{k\bar{\sigma}}^\dagger\hat{c}_{i\bar{\sigma}}\right]\hat{c}_{k\sigma}^\dagger\hat{c}_{i\sigma}\rangle}{\sqrt{\langle\hat{n}_{i\bar{\sigma}}\rangle - \langle\hat{n}_{i\bar{\sigma}}\rangle^2}\sqrt{\langle\hat{n}_{k\bar{\sigma}}\rangle - \langle\hat{n}_{k\bar{\sigma}}\rangle^2}}. \tag{6.49}
$$

So far no approximation has been made, i.e., the expressions stated for the hybridization elements, Eq. (6.47), and the first virtual sector of the effective Hamiltonian, Eqs. (6.48) and (6.49), are exact. Within in the two-time Keldysh-Matsubara framework, they prove the non-equilibrium self-energy of the Hubbard to be of the following structure

$$
\Sigma_{ij\sigma}(t, t') = \delta_C(t, t')\delta_{ij}U(t)\langle\hat{n}_{i\bar{\sigma}}(t)\rangle \tag{6.50}
$$

$$
+ U(t)\sqrt{\langle\hat{n}_{i\bar{\sigma}}(t)\rangle(1 - \langle\hat{n}_{i\bar{\sigma}}(t)\rangle)}g_{ij\sigma}^{(1,1)}(t, t')\sqrt{\langle\hat{n}_{j\bar{\sigma}}(t')\rangle(1 - \langle\hat{n}_{j\bar{\sigma}}(t')\rangle)}U(t'),
$$

where

$$
[g^{(1,1)}]_{ij\sigma}^{-1}(t, t') = \left(\delta_{ij}i\partial_t - h_{ij\sigma}^{(1,1)}(t)\right)\delta_C(t, t') - \Lambda_{ij\sigma}^{(1)}(t, t'). \tag{6.51}
$$

There are two obvious limits where our results yield a closed set of equations and thus allow for an instant solution of the Hubbard model. There first is trivially given by the noninteracting limit, i.e., $U(t) = 0$. A bit more interesting is the opposite, atomic limit, i.e., $T(t) = 0$. In this case one finds $\hat{\Gamma}_i^{(2)} = 0 \Rightarrow h^{(1,2)}(t) = 0$ (amounting to $\Lambda^{(1)}(t, t') = 0$ in the two-time Keldysh-Matsubara formalism), and furthermore $h_{ik\sigma}^{(1,1)} = \delta_{ik}h_{ii\sigma}^{(1,1)}$. We can thus setup a selfconsistency cycle and solve exactly for the one-particle Green's function in the physical as well as in the virtual sector. In addition, through $\langle\hat{\gamma}_{i\sigma}\hat{c}_{i\sigma}\rangle$, the latter provides us with an expression of the double occupation.

Interestingly, there is a third case where the physical and first virtual sector alone are sufficient to aim for an exact solution of the Hubbard model: The two-site cluster with a zero-temperature initial state. Assuming a non-degenerate ground state and exploiting conservation of the total spin, the O-matrix corresponding to this setup is maximally of dimension 4×4 per spin type as detailed in Section 3.3.3. Since the spin-dependent effective medium is of the same dimension, it must be sufficient for an exact description (cf. the discussion beneath Eq. (6.31) for more details). However, taking a look at the off-diagonal values of the effective medium we notice a severe difficulty: There is no obvious way to express the expectation values

$$\langle \hat{n}_{i\sigma}\hat{n}_{k\sigma}\rangle, \quad \langle \hat{c}^\dagger_{k\sigma}\hat{c}_{k\bar{\sigma}}\hat{c}^\dagger_{i\bar{\sigma}}\hat{c}_{i\sigma}\rangle, \quad \langle \hat{c}^\dagger_{k\sigma}\hat{c}^\dagger_{k\bar{\sigma}}\hat{c}_{i\bar{\sigma}}\hat{c}_{i\sigma}\rangle, \tag{6.52}$$

in terms of expectation values $\langle \hat{c}^\dagger_{i\sigma}\hat{c}_{j\sigma}\rangle, \langle \hat{\gamma}^\dagger_{i\sigma}\hat{c}_{j\sigma}\rangle, \langle \hat{\gamma}^\dagger_{i\sigma}\hat{\gamma}_{j\sigma}\rangle$ only. Of course, this also hinders to directly employ our expressions for the effective medium in the context of an approximation which truncates any but the first virtual sector. A possible way to proceed exploits the completeness of the active subspace, cf. Section 6.1.5. It is detailed in the next subsection.

6.3.2. Accessing arbitrary two-particle expectation values

By design, two-particle correlation functions of the form $\langle \hat{n}_{i\bar{\sigma}}\hat{c}^\dagger_{i\sigma}\hat{c}_{j\sigma}\rangle$ are easily expressed using the operators $\hat{\gamma}_{i\sigma}, \hat{c}_{j\sigma}$:

$$\langle \hat{n}_{i\bar{\sigma}}\hat{c}^\dagger_{i\sigma}\hat{c}_{j\sigma}\rangle = \sqrt{\langle \hat{n}_{i\bar{\sigma}}\rangle - \langle \hat{n}_{i\bar{\sigma}}\rangle^2}\langle \hat{\gamma}^\dagger_{i\sigma}\hat{c}_{j\sigma}\rangle + \langle \hat{n}_{i\bar{\sigma}}\rangle\langle \hat{c}^\dagger_{i\sigma}\hat{c}_{j\sigma}\rangle. \tag{6.53}$$

The idea to obtain expressions for the remaining two-particle correlation functions exploits that we are dealing with a four-dimensional active subspace

$$\mathcal{A} = \left\{ \sum_{i\sigma} \left[\alpha^{(0)}_{i\sigma}\mathcal{P}_\beta[\hat{c}_{i\sigma}(0)] + \alpha^{(1)}_{i\sigma}\mathcal{P}_\beta[\hat{\gamma}_{i\sigma}(0)] \right], \quad \alpha^{(0)}_{i\sigma}, \alpha^{(1)}_{i\sigma} \in \mathbb{C} \right\}. \tag{6.54}$$

As shown in Section 6.1.5, it comes accompanied by a completeness relation. For an arbitrary time-local two-particle correlation function it can be stated in the following way [using $\hat{c}^{(0)}_{i\sigma} = \hat{c}_{i\sigma}, \hat{c}^{(1)}_{i\sigma} = \hat{\gamma}_{i\sigma}$ for efficient notation]

$$\langle \hat{c}^\dagger_{i\sigma}\hat{c}^\dagger_{j\bar{\sigma}}\hat{c}_{k\bar{\sigma}}\hat{c}_{l\sigma}\rangle = \frac{1}{4}\sum_{j'\sigma'}\sum_{n=0}^{1}\left(\langle\{\hat{c}^\dagger_{i\sigma}\hat{c}^\dagger_{j\bar{\sigma}}\hat{c}_{k\bar{\sigma}}, \hat{c}^{(n)}_{j\sigma'}\}\rangle\langle[\hat{c}^{(n)}_{j'\sigma'}]^\dagger\hat{c}_{l\sigma}\rangle \right. \tag{6.55}$$

$$- \langle\{\hat{c}^\dagger_{i\sigma}\hat{c}^\dagger_{j\bar{\sigma}}\hat{c}_{l\sigma}, \hat{c}^{(n)}_{j\sigma'}\}\rangle\langle[\hat{c}^{(n)}_{j\sigma'}]^\dagger\hat{c}_{k\bar{\sigma}}\rangle$$

$$+ \langle\hat{c}^\dagger_{i\sigma}\hat{c}^{(n)}_{j\sigma'}\rangle\langle\{[\hat{c}^{(n)}_{j\sigma'}]^\dagger, \hat{c}^\dagger_{j\bar{\sigma}}\hat{c}_{k\bar{\sigma}}\hat{c}_{l\sigma}\}\rangle$$

$$\left. - \langle\hat{c}^\dagger_{j\bar{\sigma}}\hat{c}^{(n)}_{j\sigma'}\rangle\langle\{[\hat{c}^{(n)}_{j\sigma'}]^\dagger, \hat{c}^\dagger_{i\sigma}\hat{c}_{k\bar{\sigma}}\hat{c}_{l\sigma}\}\rangle \right).$$

In contrast to the original expression, Eq. (6.20), we have stated a symmetrized form by averaging over the four possible choices to single out an individual creation [annihilation]

operator. Within the context of an approximation, we might otherwise be faced with inconsistent results depending on our choice. This was already noted by Roth in her original paper, Ref. 82 below Eq. (56), who also suggested to cure this ambiguity by taking the average. The correlation functions considered by her lack invariance under spin flips "*and this points up an ambiguity in our method of evaluating the four operator averages (...), namely, that the division into the A and B of Eq. (32) is not unique. In the limits $U \to \infty$ and $U \to 0$, the two spin directions do give equivalent results. For intermediate values it would seem best to average them.*" Here, Roth's Eq. (32) is an equilibrium variant of our Eq. (6.20). The found ambiguity in splitting four operators into A and B is exactly the question which operator should be singled out if applying Eq. (6.20). As she also observes, an average is not necessary in exact cases, where all terms must give the same result.

Let us take a closer look now at one of the anticommutator terms, e.g., $\langle \{ \hat{c}_{i\sigma}^\dagger \hat{c}_{j\bar{\sigma}}^\dagger \hat{c}_{k\bar{\sigma}}, \hat{c}_{j\sigma'}^{(n)} \} \rangle$. If $n = 0$, the expression reduces to a one-particle expectation value. If $n = 1$, on the other hand, the anticommutation yields another two-particle expectation value. Within our theory, all one-particle expectation values as well as two-particle expectation values of the form $\langle \hat{\gamma}_{i\sigma}^\dagger \hat{c}_{j\sigma} \rangle$, cf. Eq. (6.53), are directly accessible. Eq. (6.55) therefore constitutes a linear equation that can be solved for the remaining two-particle correlation functions. We emphasize that the validity of Eq. (6.55) follows directly from the low-dimensional structure of the active subspace which only involves one virtual degree of freedom [$\gamma_{i\sigma}$]. If the low dimensionality is due to an approximation, Eq. (6.55) provides a natural way to access arbitrary time-local two-particle correlation functions which involves no additional approximation. If the low dimensionality is exact, e.g., the two-site Hubbard cluster at zero-temperature mentioned above Eq. (6.52), it is exact as well. In either case, it allows to close the self-consistency cycle as every matrix element of the effective medium can now be stated in terms of $\langle \hat{c}_{i\sigma}^\dagger \hat{c}_{j\sigma} \rangle$, $\langle \hat{\gamma}_{i\sigma}^\dagger \hat{c}_{j\sigma} \rangle$ and $\langle \hat{\gamma}_{i\sigma}^\dagger \hat{\gamma}_{j\sigma} \rangle$.

Although straightforward, it is quite cumbersome in practice to solve Eq. (6.55) for the operators necessary to close the self-consistency cycle, Eq. (6.52). We refer to Appendix B.2 for the details of the derivation. For an efficient notation, we suppress an explicit time-dependence not only for operators in the Heisenberg picture but for any quantity in the results below. For example, in Eqs. (6.56) and (6.57), $\xi_{k\sigma} \equiv \xi_{k\sigma}(t)$ is of course time-dependent. As an assuring check, we find that Wick's theorem is recovered in all cases if the limit $U(t) \to 0$ is taken. This follows from $h^{(0,1)}(t)$ vanishing in this limit such that $\langle \hat{\gamma}_{i\sigma}^\dagger \hat{c}_{j\sigma} \rangle = 0$. Finally, we note that $i \neq k$ is assumed for all results below.

Explicit solution of Eq. (6.55) for $\langle \hat{n}_{i\sigma} \hat{n}_{k\sigma} \rangle$

Density-density correlations are obtained as:

$$
\begin{pmatrix} \langle \hat{n}_{k\bar{\sigma}} \hat{n}_{i\bar{\sigma}} \rangle \\ \langle \hat{n}_{k\sigma} \hat{n}_{i\bar{\sigma}} \rangle \\ \langle \hat{n}_{k\bar{\sigma}} \hat{n}_{i\sigma} \rangle \\ \langle \hat{n}_{k\sigma} \hat{n}_{i\sigma} \rangle \end{pmatrix} = \frac{1}{2} \begin{pmatrix} 1 & -\frac{1}{2}\xi_{k\bar{\sigma}} & -\frac{1}{2}\xi_{i\bar{\sigma}} & 0 \\ -\frac{1}{2}\xi_{k\sigma} & 1 & 0 & -\frac{1}{2}\xi_{i\bar{\sigma}} \\ -\frac{1}{2}\xi_{i\sigma} & 0 & 1 & -\frac{1}{2}\xi_{k\bar{\sigma}} \\ 0 & -\frac{1}{2}\xi_{i\sigma} & -\frac{1}{2}\xi_{k\sigma} & 1 \end{pmatrix}^{-1} \begin{pmatrix} w_{ik\bar{\sigma}}^{(1)} + w_{ki\bar{\sigma}}^{(1)} \\ w_{ik\bar{\sigma}}^{(2)} + w_{ki\sigma}^{(2)} \\ w_{ik\sigma}^{(2)} + w_{ki\bar{\sigma}}^{(2)} \\ w_{ik\sigma}^{(1)} + w_{ki\sigma}^{(1)} \end{pmatrix}, \quad (6.56)
$$

6. Nonequilibrium two-pole approximation

where the coefficients are given by

$$w_{ik\bar{\sigma}}^{(1)} = -\langle\hat{n}_{k\sigma}\rangle\langle\hat{n}_{i\bar{\sigma}}\rangle\xi_{k\bar{\sigma}} + \langle\hat{n}_{i\bar{\sigma}}\rangle\langle\hat{n}_{k\bar{\sigma}}\rangle - \left|\langle\hat{c}_{i\bar{\sigma}}^\dagger\hat{c}_{k\bar{\sigma}}\rangle\right|^2 - \left|\langle\hat{\gamma}_{i\bar{\sigma}}^\dagger\hat{c}_{k\bar{\sigma}}\rangle\right|^2,\qquad(6.57)$$

$$w_{ik\bar{\sigma}}^{(2)} = -\langle\hat{n}_{k\bar{\sigma}}\rangle\langle\hat{n}_{i\bar{\sigma}}\rangle\xi_{k\sigma} + \langle\hat{n}_{i\bar{\sigma}}\rangle\langle\hat{n}_{k\sigma}\rangle,$$

$$\xi_{k\sigma} = \frac{1}{2}\frac{\langle\hat{c}_{k\sigma}^\dagger\hat{\gamma}_{k\sigma}\rangle + \langle\hat{\gamma}_{k\sigma}^\dagger\hat{c}_{k\sigma}\rangle}{\sqrt{\langle\hat{n}_{k\bar{\sigma}}\rangle - \langle\hat{n}_{k\bar{\sigma}}\rangle^2}}.$$

By construction, we find that Eq. (6.56) features the right symmetries: It is invariant under exchanges the of indices, $i \leftrightarrow k$, spin-flips, $\sigma \leftrightarrow \bar{\sigma}$, or complex conjugation.

Explicit solution of Eq. (6.55) for $\langle\hat{c}_{k\sigma}^\dagger\hat{c}_{k\bar{\sigma}}\hat{c}_{i\bar{\sigma}}^\dagger\hat{c}_{i\sigma}\rangle$

For the spin-flip correlation function we find the expression:

$$\langle\hat{c}_{k\sigma}^\dagger\hat{c}_{k\bar{\sigma}}\hat{c}_{i\bar{\sigma}}^\dagger\hat{c}_{i\sigma}\rangle = -\frac{1}{4}\left[1 + \frac{1}{4}\left(\zeta_{k\sigma} + \zeta_{k\bar{\sigma}}^* + \zeta_{i\bar{\sigma}} + \zeta_{i\sigma}^*\right)\right]^{-1} \times \left[w_{ik\bar{\sigma}}^{(3)} + w_{ki\sigma}^{(3)} + [w_{ik\sigma}^{(3)}]^* + [w_{ki\bar{\sigma}}^{(3)}]^*\right],$$

$$(6.58)$$

where the coefficients are given by

$$w_{ik\bar{\sigma}}^{(3)} = \langle\hat{c}_{i\bar{\sigma}}^\dagger\hat{c}_{k\bar{\sigma}}\rangle\langle\hat{c}_{k\sigma}^\dagger\hat{c}_{i\sigma}\rangle + \left[\frac{\sqrt{\langle\hat{n}_{i\sigma}\rangle - \langle\hat{n}_{i\sigma}\rangle^2}}{\sqrt{\langle\hat{n}_{i\bar{\sigma}}\rangle - \langle\hat{n}_{i\bar{\sigma}}\rangle^2}}\langle\hat{\gamma}_{i\bar{\sigma}}^\dagger\hat{c}_{k\bar{\sigma}}\rangle - \frac{\langle\hat{n}_{i\bar{\sigma}}\rangle - \langle\hat{n}_{i\sigma}\rangle}{\sqrt{\langle\hat{n}_{i\bar{\sigma}}\rangle - \langle\hat{n}_{i\bar{\sigma}}\rangle^2}}\langle\hat{c}_{i\bar{\sigma}}^\dagger\hat{c}_{k\bar{\sigma}}\rangle\right]\langle\hat{c}_{k\sigma}^\dagger\hat{\gamma}_{i\sigma}\rangle,$$

$$\zeta_{k\sigma} = \frac{\langle\hat{c}_{k\sigma}^\dagger\hat{\gamma}_{k\sigma}\rangle}{\sqrt{\langle\hat{n}_{k\bar{\sigma}}\rangle - \langle\hat{n}_{k\bar{\sigma}}\rangle^2}}.\qquad(6.59)$$

The right-hand side of Eq. (6.58) features indeed the right symmetries: The result is invariant if we replace $i \leftrightarrow k$ (or conjugate the equation) in combination with a spin flip, $\sigma \leftrightarrow \bar{\sigma}$.

Explicit solution of Eq. (6.55) for $\langle\hat{c}_{k\sigma}^\dagger\hat{c}_{k\bar{\sigma}}^\dagger\hat{c}_{i\bar{\sigma}}\hat{c}_{i\sigma}\rangle$

The last correlation function describes the movement of doublons on the lattice:

$$\langle\hat{c}_{k\sigma}^\dagger\hat{c}_{k\bar{\sigma}}^\dagger\hat{c}_{i\bar{\sigma}}\hat{c}_{i\sigma}\rangle = \frac{1}{4}\left[1 + \frac{1}{4}\sum_{\sigma'}\left[\zeta_{k\sigma'} + \zeta_{i\sigma'}^*\right]\right]^{-1} \times \left[w_{ik\bar{\sigma}}^{(4)} + w_{ik\sigma}^{(4)} + [w_{ki\sigma}^{(4)}]^* + [w_{ki\bar{\sigma}}^{(4)}]^*\right]\qquad(6.60)$$

where the coefficients are given by

$$w_{ik\bar{\sigma}}^{(4)} \equiv \langle\hat{c}_{k\bar{\sigma}}^\dagger\hat{c}_{i\bar{\sigma}}\rangle\langle\hat{c}_{k\sigma}^\dagger\hat{c}_{i\sigma}\rangle\qquad(6.61)$$

$$+ \left[\frac{(1 - \langle\hat{n}_{i\bar{\sigma}}\rangle - \langle\hat{n}_{i\sigma}\rangle)\langle\hat{c}_{k\bar{\sigma}}^\dagger\hat{c}_{i\bar{\sigma}}\rangle}{\sqrt{\langle\hat{n}_{i\bar{\sigma}}\rangle - \langle\hat{n}_{i\bar{\sigma}}\rangle^2}} - \frac{\sqrt{\langle\hat{n}_{i\sigma}\rangle - \langle\hat{n}_{i\sigma}\rangle^2}}{\sqrt{\langle\hat{n}_{i\bar{\sigma}}\rangle - \langle\hat{n}_{i\bar{\sigma}}\rangle^2}}\langle\hat{c}_{k\bar{\sigma}}^\dagger\hat{\gamma}_{i\bar{\sigma}}\rangle\right]\langle\hat{c}_{k\sigma}^\dagger\hat{\gamma}_{i\sigma}\rangle.$$

Again, we note that symmetry relations are correctly reproduced by the right-hand side of Eq. (6.60): It is invariant under spin flips, $\sigma \leftrightarrow \bar{\sigma}$, as well as complex conjugation in combination with an index exchange, $i \leftrightarrow k$.
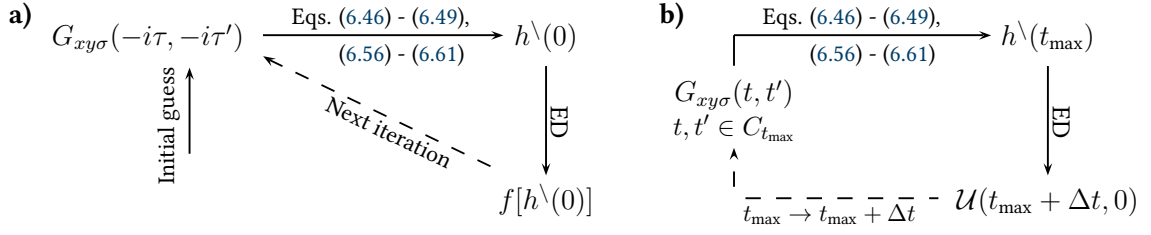
Figure 6.1.: a) Self-consistent determination of the initial state: Given a guess for the Green's function, the effective medium $h^{\backslash}(0)$ can be determined. By using exact diagonalization, we obtain the Fermi matrix $f[h^{\backslash}(0)]$ such that the Green's function can be updated via Eq. (6.62). b) Propagation scheme: Given $h^{\backslash}(t_{\max})$ and $\mathcal{U}(t_{\max}, 0)$, we can perform a single time-step Δt. The updated Green's function follows from Eq. (6.62) and gives rise to $h^{\backslash}(t_{\max} + \Delta t)$.

6.3.3. Self-consistency cycle for a time-non-local theory

With expressions for a self-consistent determination of the effective medium at hand, we can state a self-consistency cycle to obtain the equilibrium Green's function as well as a propagation scheme for finite times t, t'. Its precise form is detailed in Fig. 6.1. We emphasize that the propagation scheme allows for $t \neq t'$, i.e., time-non-local correlations are accessible by our approximation. This property is ensured by design since we have access to the time-evolution operator $\mathcal{U}(t, 0) = \mathcal{T} \exp\left(-i \int_0^t dt' h^{\backslash}(t')\right)$. The Green's function is then given as

$$G_{xy\sigma}(t, t') = -i\langle \mathcal{T}_C \hat{c}_{x\sigma}(t) \hat{c}_{y\sigma}^{\dagger}(t') \rangle = i \left[\mathcal{U}(t, 0) \left(f[h^{\backslash}(0)] - \Theta_C(t, t') \right) \mathcal{U}^{\dagger}(t', 0) \right]_{xy\sigma},$$

$$\text{where} \quad \hat{c}_{x\sigma}(t) = \begin{cases} \hat{c}_{i\sigma}(t) & \text{if} \quad x \in \{0, \dots, L-1\}, \\ \hat{\gamma}_{i\sigma}(t) & \text{if} \quad x \in \{L, \dots, 2L-1\}. \end{cases} \tag{6.62}$$

Here, $f[\cdot]$ refers to the matrix Fermi distribution, cf. Eq. (6.38). We recall that the obtained dynamics are exact in the following limits: (1) No interactions, i.e., $U(t) = 0$, (2) single-site cluster, $T_{ij\sigma}(t) = \delta_{ij} T_{ii\sigma}(t)$ and (3) two-site cluster with the initial state being non-degenerate and at zero-temperature.

In the approximate case, on the other hand, we note an important restriction. Despite the completely self-consistent design, we must expect a violation of conservation laws, or more general, their corresponding local constraints derived in Section 5.1. To understand what is missing, we take a closer look at the double occupation. The ambiguity that arises from Eq. (6.53) is dealt with by taking the average, which is in particular consistent with Eq. (6.55). The explicit expression reads

$$\langle \hat{n}_{i\bar{\sigma}} \hat{n}_{i\sigma} \rangle = \frac{1}{4} \sum_{\sigma} \left(\sqrt{\langle \hat{n}_{i\bar{\sigma}} \rangle - \langle \hat{n}_{i\bar{\sigma}} \rangle^2} \left[\langle \hat{\gamma}_{i\sigma}^{\dagger} \hat{c}_{i\sigma} \rangle + \langle \hat{c}_{i\sigma}^{\dagger} \hat{\gamma}_{i\sigma} \rangle \right] + 2 \langle \hat{n}_{i\bar{\sigma}} \rangle \langle \hat{n}_{i\sigma} \rangle \right). \tag{6.63}$$

In the exact case, its time-derivative simplifies considerably since the interaction term commutes with the double occupation:

$$i\partial_t \langle \hat{n}_{i\bar{\sigma}} \hat{n}_{i\sigma} \rangle = \langle \left[\hat{n}_{i\bar{\sigma}} \hat{n}_{i\sigma}, \hat{H}_0 \right] \rangle. \tag{6.64}$$

Within our approximation, on the other hand, we explicitly take into account only simplifications that arise in calculating $[\hat{c}_{i\sigma}, \hat{H}]$ and $[\hat{n}_{i\bar{\sigma}}\hat{c}_{i\sigma}, \hat{H}]$ separately (in the context of calculating $h_{ij\sigma}^{(n,m)}(t)$, cf. Sec. 6.3.1). As a result, a violation of the local constraint of the doublon density must be expected. From an analog argumentation the same follows for the local constraint of the spin-dependent density. In practice, this poses a severe issue, since it implies violation of energy as well as particle number conservation. However, the problem can be cured by specializing the theory to be purely time-local. This is detailed in the following.

6.3.4. Conservation laws: Specialization to a time-local theory

In a purely time-local context, it is possible to specialize the self-consistency cycle such that conservation laws are respected by the time-evolution. The idea is linked to the Pauli principle, which poses a constraint on some of the matrix elements of $G(t, t^+)$:

$$\langle\hat{\gamma}_{i\sigma}^{\dagger}\hat{c}_{i\sigma}\rangle = \frac{\langle\hat{n}_{i\bar{\sigma}}\hat{n}_{i\sigma}\rangle - \langle\hat{n}_{i\bar{\sigma}}\rangle\langle\hat{n}_{i\sigma}\rangle}{\sqrt{\langle\hat{n}_{i\bar{\sigma}}\rangle - \langle\hat{n}_{i\bar{\sigma}}\rangle^2}} = \langle\hat{c}_{i\sigma}^{\dagger}\hat{\gamma}_{i\sigma}\rangle, \tag{6.65}$$

$$\langle\hat{\gamma}_{i\sigma}^{\dagger}\hat{\gamma}_{i\sigma}\rangle = \frac{\langle\hat{n}_{i\bar{\sigma}}\hat{n}_{i\sigma}\rangle\left(1 - 2\langle\hat{n}_{i\sigma}\rangle\right) + \langle\hat{n}_{i\bar{\sigma}}\rangle^2\langle\hat{n}_{i\sigma}\rangle}{\langle\hat{n}_{i\bar{\sigma}}\rangle - \langle\hat{n}_{i\bar{\sigma}}\rangle^2}, \tag{6.66}$$

Within our time-non-local (Roth-like) approach, these constraints are known to be violated [147], i.e., incompatible values for the double occupation are obtained from Eqs. (6.65) and (6.66). In the following we fix this issue and, in the course of this, furthermore enforce conservation laws.

The overall scheme is easiest to understand if we set aside the initial state problem for a moment and only focus on the dynamics. To this end, let us assume that the initial one-particle density matrix, $G_{xy\sigma}(0, 0^+)$, is given such that Eqs. (6.65) and (6.66) are fulfilled. To derive the dynamics of $G(t, t^+)$, we need an equation of motion for each of its matrix elements. To ensure the Pauli principle, we define the equation of motion of $\langle\hat{\gamma}_{i\sigma}^{\dagger}\hat{c}_{i\sigma}\rangle$ and $\langle\hat{\gamma}_{i\sigma}^{\dagger}\hat{\gamma}_{i\sigma}\rangle$ as the time-derivate of Eqs. (6.65) and (6.66). To become able to evaluate it selfconsistently, we need expression for $i\partial_t\langle\hat{n}_{i\bar{\sigma}}\hat{n}_{i\sigma}\rangle$ as well as $i\partial_t\langle\hat{n}_{i\sigma}\rangle$ in terms of matrix elements of $G(t, t^+)$. Considering the time-derivative of the double occupation first, we define its equation of motion using the local constraint Eq. (5.2) for the doublon density. In the context of our theory it reads

$$i\partial_t\langle\hat{n}_{i\bar{\sigma}}\hat{n}_{i\sigma}\rangle = \sum_{j\sigma'}\sqrt{\langle\hat{n}_{i\bar{\sigma}'}\rangle - \langle\hat{n}_{i\bar{\sigma}'}\rangle^2}\left(T_{ij\sigma'}(t)\langle\hat{\gamma}_{i\sigma'}^{\dagger}\hat{c}_{j\sigma'}\rangle - \langle\hat{c}_{j\sigma'}^{\dagger}\hat{\gamma}_{i\sigma'}\rangle T_{ji\sigma'}(t)\right)$$

$$+ \sum_{j\sigma'}\langle\hat{n}_{i\bar{\sigma}'}\rangle\left(T_{ij\sigma'}(t)\langle\hat{c}_{i\sigma'}^{\dagger}\hat{c}_{j\sigma'}\rangle - \langle\hat{c}_{j\sigma'}^{\dagger}\hat{c}_{i\sigma'}\rangle T_{ji\sigma'}(t)\right). \tag{6.67}$$

The crucial point is here that Eq. (6.67) automatically ensures energy conservation as we have previously discussed in Section 5.1. The equation of motion of all remaining matrix elements of $G(t, t^+)$ (therefore including $i\partial_t\langle\hat{n}_{i\sigma}\rangle$) is now readily defined via the effective

medium:

$$i\partial_t G_{xy\sigma}(t, t^+) = \left[h^{\backslash}(t), G(t, t^+) \right]_{xy\sigma} \quad \text{for} \quad (x, y) \notin \mathcal{I}_d, \tag{6.68}$$
$$\mathcal{I}_d \equiv \{ (L + i, L + i), (i, L + i), (L + i, i) \} .$$

It remains to take a look at the local constraint for the spin-dependent density:

$$i\partial_t \langle \hat{n}_{i\sigma} \rangle = \sum_j \left[T_{ij\sigma}(t) \langle \hat{c}_{i\sigma}^\dagger \hat{c}_{j\sigma} \rangle - T_{ji\sigma}(t) \langle \hat{c}_{j\sigma}^\dagger \hat{c}_{i\sigma} \rangle \right] \tag{6.69}$$
$$+ U(t) \sqrt{\langle \hat{n}_{i\sigma} \rangle - \langle \hat{n}_{i\sigma} \rangle^2} \underbrace{\left(\langle \hat{c}_{i\sigma}^\dagger \hat{\gamma}_{i\sigma} \rangle - \langle \hat{\gamma}_{i\sigma}^\dagger \hat{c}_{i\sigma} \rangle \right)}_{=0, \text{ due to Eq. (6.65)}} .$$

Comparing to Eq. (5.1), we find it obeyed as well.

Concluding, let us emphasize once more that the through Eqs. (6.65) - (6.68) defined selfconsistent propagation scheme fulfills both, the Pauli exclusion principle as well as the macroscopic conservation laws. Nevertheless, a closer look also reveals that a price had to be paid: We have lost access to time-non-local states as there is no apparent way to define an effective Hamiltonian $H^{\text{tl}}(t)$ such that $G_{xy\sigma}(t, t^+) = i\langle \hat{c}_{y\sigma}^\dagger(t) \hat{c}_{x\sigma}(t) \rangle_{H^{\text{tl}}}$. Furthermore, and maybe more importantly, the initial state is not easily determined from Eqs. (6.65) - (6.68) alone, as discussed below.

Initial state

Apart from Eqs. (6.65) and (6.66), we have only stated equations of motion, i.e., the initial state $G_{xy\sigma}(0, 0^+)$ is undefined up to now. In the simple cases, it can be stated exactly. Important examples are given by the noninteracting initial state or the atomic limit which can both be treated rigorously. In particular, Eq. (6.65) is then trivially fulfilled. However, if one wants to start from arbitrary interaction, one runs into problems: While a selfconsistency cycle for the matrix elements unrelated to the double occupation, $G_{xy\sigma}(0, 0^+)$ for $(x, y) \notin \mathcal{I}_d$, is easily setup in complete analogy to the time-non-local case, it is rather unclear how to correctly incorporate Eqs. (6.65) and (6.66) or, equivalently, how to define the double occupation.

Coming from the time-non-local self-consistency cycle, a possible choice is to enforce Eq. (6.65) by averaging inconsistent results. The algorithm could look as follows: Given a density matrix $G_{xy\sigma}^{(N)}(0, 0^+)$ after the N-th iteration, we compute the effective medium $h_{(N)}^{\backslash}(0)$ in complete analogy to before. We then define $G_{xy\sigma}^{\text{tmp}}(0, 0^+) \equiv if[h_{(N)}^{\backslash}(0)]_{xy\sigma}$ which, in general, will violate Eqs. (6.65) and (6.66), i.e., it does not constitute a proper update $G^{(N+1)}(0, 0^+)$. It can be used, however, to update the double occupation alone. To avoid the instability of Eq. (6.66) at half-filling, we base the average on Eq. (6.63):

$$\langle n_{i\bar{\sigma}} n_{i\sigma} \rangle^{(N+1)} = \frac{1}{4} \sum_\sigma \left(\sqrt{\langle n_{i\bar{\sigma}} \rangle_t - \langle n_{i\bar{\sigma}} \rangle_t^2} \left[\langle \gamma_{i\sigma}^\dagger c_{i\sigma} \rangle_t + \langle c_{i\sigma}^\dagger \gamma_{i\sigma} \rangle_t \right] + 2 \langle n_{i\bar{\sigma}} \rangle_t \langle n_{i\sigma} \rangle_t \right), \tag{6.70}$$

where $\langle c_{x\sigma}^{\dagger} c_{y\sigma} \rangle_{\mathrm{t}} \equiv -i G_{xy\sigma}^{\mathrm{tmp}}(0, 0^+)$. With an update for the double occupation at hand, we define

$$\langle c_{x\sigma}^{\dagger} c_{y\sigma} \rangle^{(N+1)} = \langle c_{x\sigma}^{\dagger} c_{y\sigma} \rangle_{\mathrm{t}} \quad \text{if} \quad (x, y) \notin \mathcal{I}_d, \tag{6.71}$$

such that the remaining matrix elements $(x, y) \in \mathcal{I}_d$ follow from Eqs. (6.65) and (6.66).

A second option specific to zero-temperature initial states is adiabatic switching: Starting at time $t = -t_{\mathrm{ad}}$ from a noninteracting initial state, $U(-t_{\mathrm{ad}}) = 0$, the interaction is slowly turned on until the desired interaction, $U(0) = U_{\mathrm{eq}}$, is reached. The resulting one-particle density matrix, $G(0, 0^+)$, serves as the initial state for the subsequent nonequilibrium dynamics. Let us emphasize that, to ensure quasi-adiabatic dynamics during this process, it is crucial that the switch duration time, t_{ad}, is chosen long enough. Since the presented time-propagation algorithm for $G(t, t^+)$ is completely Markovian (i.e., memory-kernel-free), we expect that this important condition can be met with ease in numerical applications.

6.4. Summary

For the equilibrium case, Hubbard-I and its many improvements have proven to be a highly versatile method that can be formalized systematically in the framework of the Mori-Zwanzig projection technique [86–88]. Interestingly, this technique turns out to be closely related to the Lehmann representation of the self-energy. While the Lehmann representation is obtained from an effective medium with diagonal virtual sector, an equivalent continued fraction representation of the self-energy can be derived from a block-tridiagonal form. Therewith, we have for the first time generalized the Mori-Zwanzig approach to far-from-equilibrium states in fermionic lattice models. Let us emphasize here that the standard derivation of this important technique (e.g., Ref. 88) is invalid beyond the linear response regime. Concerning the matrix elements of the block-tridiagonal effective medium we have derived an analytical relation to higher-ordered correlation functions using a Lanczos-like algorithm. Assuming they can be evaluated, preferably in a self-consistent manner, we are in the position to study correlated systems on large timescales by numerical means as an inversion of Dyson's equation on the Keldysh contour can be avoided.

As a first application, we have developed a two-pole approximation for the time-dependent Hubbard model. Slightly improving upon the results obtained by Roth [81, 82], we derived a symmetrized decoupling scheme that preserves important symmetries of the corresponding correlation functions. Furthermore, we did not assume translational invariance such that our results apply also for inhomogeneous setups. Regarding time-dependent problems, we discussed the issue of missing energy and particle-number conservation. We showed that, by specializing the theory from a two-time Green's-function-based view to a time-local density-matrix variant, local constraints implying energy and particle-number conservation can be enforced. As a remaining challenge, we found an ambiguity regarding the question on how to obtain the initial state in the time-local specialization.

With the theoretical foundations completely laid out, our results call for a numerical implementation of the method and we expect no severe complications in the process of this. Furthermore, the availability of a non-trivial test case, i.e., dynamics in a two-site cluster with a zero-temperature non-degenerate initial state, will serve well in verifying the implementation for correctness. Then, already for a pure equilibrium study it will be interesting to see how our averaged decoupling scheme performs versus Roth's original procedure. Regarding time-dependent problems, a comparison of the two-time and time-local self-consistency schemes would be very interesting: How striking is the violation of conservation laws if using the time-non-local scheme? Will there be a *qualitative* difference in the dynamics between the two schemes? Can we see prethermalization or steady states in the long-time limit?

A particular appealing application of our method are two-dimensional systems. Here, exact numerical studies underline the importance of nonlocal contributions to the self-energy [63, 148]. In our nonequilibrium two-pole approach, these terms are approximated by means of a Roth-like decoupling scheme, i.e., short-range spatial correlations are taken into account. Since we have furthermore refrained from assuming translational invariance, we are in the position to pick up on a scenario commonly realized in experiments with ultracold atoms (e.g., Ref. 17): The dynamics of interacting fermions in the presence of a confining lattice potential. Another fascinating field that has drawn a lot of attention recently is many-body localization [149]. Here, the potential of a conceptionally simple two-pole approach was pointed out in a recent work [139]. Rather intuitively, Hubbard-I can be shown to be become exact in the limit of strong correlations where the eigenstates become localized. Then, first order corrections can be shown to be nonlocal and might thus be well approximated by our Roth-like decoupling scheme.

Furthermore, the time-dependence of magnetic systems seems an area worthwhile to focus on. In fact, the very first application of the steady state generalization of the spectral density approach (SDA) was targeted at such systems [83, 143, 144]. This comes to no surprise considering the many successful studies of magnetism using the SDA [138, 150–152] in the past. Let us note in this context that, by construction, our nonequilibrium two-pole approach is consistent up to the fourth-order in the spectral moments. Interestingly, a consistent treatment of the fourth-order moment has often been emphasized to be crucial in describing magnetic effects [152] since it provides for a spin-dependent shift of the centers of gravity of the two Hubbard bands. Far-from-equilibrium, we therefore similarly expect an important influence on the dynamics and it will be fascinating to see what kind of time-dependent phenomena future numerical studies will bring to light.

Lastly, with the groundwork being done, the door is opened for a generalization of other successful n-pole approaches. Interesting candidates include the modeling of quasiparticle damping [85] or an extension of the Roth decoupling to Kondo systems [153]. As both approaches are formulated in frequency space, the first step would to be to carefully check if a time-local effective-medium-based generalization to nonequilibrium is possible. If not, a time-nonlocal generalization in spirit of the continued fraction representation might be applicable. In any case, the future might see a variety of nonequilibrium n-pole approaches specifically crafted for the description of distinct phenomena.

7. Conclusions and Perspectives

In this thesis, we have developed two new approximate methods for the description of out-of-equilibrium dynamics of fermions on a lattice in the presence of short range spatial correlations: The *conserving cluster perturbation theory* and the *nonequilibrium two-pole approach*. Central for the derivation of these approaches is a general insight, which we have rigorously established as part of this thesis: It is possible to exactly map any time-dependent fermionic lattice model from the original Hamiltonian with a quartic interaction term to a quadratic one-particle Hamiltonian. We refer to this free model as the *effective medium*. It consists out of the following terms: The original hopping matrix, renormalized by the Hartree-Fock corrections; an exponentially large number of additional one-particle degrees of freedom, which we call *virtual* sites in distinction of the original *physical* sites; a hybridization term which couples the physical and virtual sites. Ultimately leading us to the mentioned new methods, we have explored two different directions to explicitly construct the effective medium:

1. From the time-evolved eigenstates of the initial (original, interacting) Hamiltonian, the effective medium can be constructed such that the there is no coupling between the virtual sites, i.e., the virtual sites are only coupled to the physical sites but not among each other. Interestingly, by integrating out the virtual sites we could proof a fundamental property of *the nonequilibrium self-energy: It can be expressed in form a Lehmann representation, i.e., as a superposition of noninteracting, isolated modes.* In fact, up to its time-local Hartree-Fock term, the self-energy is nothing else but the hybridization function obtained from integrating out the virtual sites. Let us emphasize that, while the existence of a Lehmann representation of the nonequilibrium self-energy was first conjectured and numerically verified in the context of nonequilibrium DMFT [50], a rigorous analytical construction has been lacking up to now.

2. We have also constructed a block-tridiagonal form of the effective medium. Its matrix elements are then related to higher order correlation functions which can be stated explicitly. Interestingly, this construction can be understood as a *generalization of the Mori-Zwanzig projection technique (MZPT) [86–88] to Keldysh-Matsubara Green's functions.* Therefore, our result enables for the first time the usage of this well-established technique in far-from-equilibrium setups. To clarify this statement let us underline that, despite often been mentioned in the context of nonequilibrium statistical mechanics, the standard formulation of the Mori-Zwanzig projection technique is only valid if perturbations are small, i.e., in the linear response regime. Our generalized construction is independent of this assumption.

Cluster perturbation theory

The first result is especially useful in the context of cluster-based methods, where an approximate self-energy is obtained from a small reference system. The standard way to obtain the desired lattice Green's function is to invert Dyson's equation on the Keldysh-Matsubara contour—a computationally expensive operation. However, by interpreting the self-energy as a hybridization function, an equivalent effective medium can be stated [50]. In the effective-medium description, the time propagation is Markovian, i.e., there is no memory kernel. To explicitly construct the effective medium, we have developed and implemented a numerical algorithm which is most efficient if applied to small cluster systems. In contrast to Ref. 50, where the nonequilibrium self-energy must first be determined explicitly (an operation that typically scales cubic in the maximal propagation time t_{max}) and is then decomposed using a Cholesky decomposition, our algorithm derives the effective medium directly from the time-evolved eigenstates of the initial Hamiltonian and therefore scales linear in t_{max} and exponential in the cluster size.

The simplest application of our algorithm is possible within the cluster perturbation theory (CPT). Here, as a proof of concept, we have considered the time evolution of local magnetic moments in the fermionic Hubbard model after an interaction quench from the noninteracting initial state. Indeed, in comparison to prior studies that have been limited to maximal propagation times $t_{\mathrm{max}} = 10$–20 inverse hoppings [110, 112], we were able to propagate the one-particle density matrix up to a much longer time, $t_{\mathrm{max}} = 10^4$ inverse hoppings, for an *inhomogeneous* setup.

While the CPT is of course a simple theory that lacks a selfconsistent coupling between reference system and the desired lattice Green's function, we have nevertheless found some interesting results for quenches to weak U_{fin}. In this regime, the CPT simulations showed a separation of the dynamics into two time scales, in agreement with general perturbative considerations [124, 125, 127–129]: For short times, the noninteracting fix point, $U_{\mathrm{fin}} = 0$, constraints the dynamics such that the time-evolution of the magnetic moments qualitatively follows the noninteracting case. For large times, however, the constraints are broken up due to the interaction and the system shows signs of relaxation. While one might be tempted to link this to a possible thermalization of the system [154], our data clearly shows a persistence of memory effects in the density matrix up to the largest simulated times. We therefore conclude that a simple, non-selfconsistent CPT approach is insufficient to capture this important many-body effect.

Conserving cluster perturbation theory

More severe than the lack of thermalization in the long time limit is the violation of fundamental conservation laws by the CPT. Our numerical results showed that neither energy nor magnetization are conserved during the time-evolution. This is due to the missing feedback between the lattice Green's function and the approximate self-energy from the reference system. To address this problem, while at the same time avoiding the significant additional complexity of more systematic theories such as the nonequilibrium DMFT [30] or the nonequilibrium self-energy functional theory [76], we explored a rather pragmatic idea: The macroscopic conservation laws can be formulated in terms of local constraints

for the spin-dependent particle and doublon density [76]. These constraints are violated within standard CPT but can be enforced if viewing the CPT as an all-order perturbation theory [110] in the inter-cluster hopping around a system of decoupled clusters. From this viewpoint, the one-particle part of the decoupled clusters is not predetermined and can be renormalized such that the local constraints are fulfilled.

We have formulated this *conserving* CPT using the effective-medium-based approach. Therefore, the method profits from our previous results, i.e., it is not bottlenecked by an inversion of Dyson's equation on the Keldysh-Matsubara contour. To minimize the computational overhead of obtaining the correct renormalization, we have exploited the inherently causal structure of the CPT: By carefully analyzing the order (in the sense of a Taylor series) at which the renormalization at the last time slice enters the local constraints, we have developed a time-stepping algorithm which updates the renormalization only at this very last slice. Furthermore, our algorithm allows to also determine the time-derivatives of the renormalization (up to arbitrary order) such that the propagation error per time step can be systematically controlled. The macroscopic conservation laws are then respected up to machine precision.

Our first numerical simulation have indeed shown that enforcing the local constraints for spin-dependent particle and doublon density has profound impact on the dynamics. We have considered weak interaction quenches in the half-filled two-dimensional Hubbard model on a square lattice. While spin- and particle-number conservation hold trivially in this case due to particle-hole symmetry, we additionally enforced energy conservation by renormalizing the intra-cluster hopping of a 2×1 reference cluster. In a plain CPT calculation, this rather small cluster size leads to heavy artificial oszillations. In the conserving CPT, however, these unphysical oszillations are almost completely suppressed and the doublon density shows an ultrafast, monotonous relaxation against a stationary state. Such a (prethermal) plateau is compatible with previous exact calculations for one- and infinite-dimensional lattices [58, 79]

As a complicating but nevertheless highly interesting aspect, we found singular points of non-intertibility of the conditional equations, i.e., points where the inversion for the optimal renormalization parameter becomes ill-defined. From a technical viewpoint, the emergence of these singularities currently restricts the accessible timescale. However, it is well conceivable that a propagation beyond those singular points is possible in principle if a proper regularization scheme is used.

Nonequilibrium two-pole approximation

As a different direction, the construction of the effective-medium in a block-tridiagonal form has lead us to discover a generalization of the Mori-Zwanzig projection technique [86–88] to Keldysh-Matsubara Green's functions. In particular, by integrating out the virtual sites, we have found a generalized continued fraction representation of the one-particle Green's function in analogy to Mori's famous result [88]. Yet it should be noted that, while this representation can efficiently be worked with in frequency space, it is less practical in nonequilibrium studies where each fraction requires the inversion of a Dyson-like equation on the Keldysh-Matsubara contour. The much simpler approach is to refrain from integrating out the virtual lattice sites and work directly with the effec-

tive medium which is of a sparse, block-tridiagonal form with the matrix elements being given as higher order correlation functions.

The standard way to construct an approximation in the Mori-Zwanzig formalism is to truncate the continued fraction after the n-th order yielding a so called n-pole approximation [88]. From the effective-medium viewpoint, this is equivalent to truncate the block-tridiagonal one-particle Hamilton matrix after the n-th block (equivalent to the $n-1$-th virtual sector). If all its matrix elements can be expressed in terms of matrix elements of the corresponding one-particle Green's function (which comprises the physical as well as $n-1$ virtual sectors), one can formulate a fully self-consistent approximation that can efficiently be propagated to arbitrary long times.

As the simplest approximation that goes beyond Hartree-Fock we have explicitly constructed a nonequilibrium two-pole approximation. To selfconsistently express the two particle correlation functions appearing in the effective medium, we have derived a slightly improved variant of the decoupling scheme first stated by Roth [81, 82] which preserves the correct symmetries of the correlation functions. A remaining issue troubling the decoupling process is the to be expected violation of conservation laws in time-dependent setups. Yet, if one is interested in time-local matrix elements of the Green's function only (i.e., the one-particle density matrix of the physical as well as the single virtual sector), time-local constraints equivalent to particle number and energy conservation can easily be implemented. The resulting theory is conserving. A last remaining challenge appears if the initial state cannot be obtained exactly, i.e., if the system is initially *not* in the noninteracting or the atomic limit. Then, determining the initial state turns out to be ambiguous in the time-local specialization.

Perspectives

The cluster perturbation theory lies at the heart of self-energy functional theory (SFT) [75] and its recently developed generalization to nonequilibrium [76]. In a typical nonequilibrium SFT calculation [155], the reference cluster is of a small, constant size and can thus efficiently be treated using the effective-medium-based algorithm developed in this thesis. Therefore, the development of a fully time-local formulation of this important technique suggests itself. Similar to the steps taken in developing the conserving CPT approach, the main task would be to express the defining equations for the optimal parameters using the effective medium. To this end, a proper starting point seems to be given by the Euler-Lagrange equations developed in Ref. 76. In developing a time-stepping algorithm, it would again be necessary to carefully trace the order in which the optimal parameters at the last time-step enter the self-consistency equation.[1] From here, a worthwhile endeavor would surely be the integration of the conserving CPT into the more versatile framework of the nonequilibrium SFT. Concerning the latter, the local constraint for the spin-dependent density is known to be fulfilled by construction [76]. The local constraint for the doublon density, however, is violated such that there is no energy conservation.

---

[1] This applies also to the time-nonlocal formulation of the SFT. Indeed, in Ref. 155, a different scaling in the optimal parameter at the last time step of two otherwise equivalent formulations of the nonequilibrium SFT was proven numerically. As a result, only one of the two formulations turned out to be numerically stable.

Yet, due to its variationally controlled character, the constraint for the doublon density can straightforwardly be integrated into the formalism. The resulting theory would thus be conserving, variationally controlled and formulated by means of the effective medium, i.e., free from being bottlenecked by an inversion of Dyson's equation on the Keldysh-Matsubara contour.

To successfully employ such a theory numerically, however, substantial progress is needed concerning the treatment of singular points which appear during the time-evolution of both, the conserving CPT as well as the nonequilibrium SFT (private communication with Felix Hofmann; cf. also the thesis summary in [155]). While concerning the conserving CPT one might be tempted to attribute this complication to the somewhat ad hoc construction, the construction of the nonequilibrium SFT from a variational principle is highly systematic and suggests that there could be a hidden, deeper mechanism at work. In Ref. 155 it was for example speculated, that non-analytic behavior expected for observables at a dynamical phase transition might translate to divergent behavior of the mean-field in an approximate cluster approach. Considering the still on-going evolution of theory aimed at describing dynamic phase transitions [36], this is certainly a highly interesting topic and important insights are to expected in the future.

Assuming a suitable solution to the singular-points problem can be found, our study of the 2D Hubbard model using the conserving CPT should be revisited. Considering, for example, that the nonequilibrium SFT proved the study of the dynamical Mott-transition to be possible using a simple two-site cluster [78], it seems well conceivable that signs of this transition can also be found in the conserving CPT approach if quenching to larger U_{fin}. Furthermore, it should be clarified if a stationary state in the long-time limit can be expected in the whole parameter range. Finally, the dependence of our results on the cluster size and shape should be studied. To this end, it is important to note that depending on the reference cluster this implies the necessity to optimize more than a single parameter. Corresponding to the four local constraints (two for the spin-dependent density, two for the doublon density), up to $4L_{\mathrm{c}}$ parameters must be optimized for an arbitrary cluster of size L_{c}. In case of an insufficient number of free parameters, a possible workaround is to couple additional uncorrelated "bath" sites to the reference cluster—much in the spirit of dynamical mean-field theory.

Shifting our attention to the nonequilibrium two-pole approximation, the next step is certainly a numerical implementation of the method. With the fully developed theory at hand, we expect no severe complications in the process of this. Furthermore, verifying the implementation for correctness should efficiently be possible since there exists a non-trivial test case where the theory becomes exact—dynamics in a two-site cluster with the initial state being at zero temperature and non-degenerate. Having the implementation up and running, already the influence of the symmetry-restoring averaging in our Roth-like decoupling scheme compared to previous studies [81, 82, 84] will be interesting. Concerning nonequilibrium dynamics, the comparison of the time-local conserving versus the time-non-local non-conserving variant raises interesting questions: How strong is the violation of energy and particle-number conservation in the latter? Are there qualitative differences between the two approaches? Finally, as a first benchmark calculation, the study of interaction quenches in the homogeneous Hubbard model suggests themselves due to the considerable amount of available data, e.g., Refs. 73, 78, 79 and 116.

7. Conclusions and Perspectives

With a well-tested numerical apparatus in place, the door is opened up to aim at a variety of intriguing, physical questions. As our Roth-like decoupling scheme includes the effect of short-range correlations, one particular interesting route is the study of two-dimensional systems where nonlocal terms of the self-energy are known to be of particular importance [63, 148]. Since furthermore inhomogeneous setups seem very well tractable, one could, for example, explore the dynamics of interacting fermions on a 2D-lattice under the influence of a confining potential—a scenario often realized in experiments with ultracold atoms on optical lattices (e.g., Ref. 17). Another fascinating field is the study of the interplay of strong correlations and disorder. In a recent work it was argued that in the limit of large disorder correlations are so short-ranged that even Hubbard-I becomes a reasonable approximation [139]. Furthermore, the leading corrections to the self-energy were shown to be non-local and might therefore be well approximated by our Roth-like decoupling. As two-dimensional disordered interacting systems are hard to access, our approach might be able to provide valuable insights especially regarding the dynamics of such systems.

Inspired by the successes of the spectral density approach [83, 138, 143, 144, 150–152], also the study of time-dependent magnetic effects seems an attractive endeavor. Until now, the spectral density approach (SDA) has only been generalized for the study of nonequilibrium steady states where it has successfully been applied to investigate the induced switching of the magnetization by employing of a current [143, 144]. The nonequilibrium two-pole approach developed in this thesis can be seen as a further generalization which also captures transient dynamics. From the viewpoint of the SDA, it is selfconsistent up to the fourth spectral moment. The importance of this fourth spectral moment for magnetic properties has often been emphasized [152], as it introduces a spin-dependent shift of the centers of gravity of the two Hubbard bands. Of course, also far from equilibrium the description of magnetic systems can be expected to profit from correctly capturing this spin-dependent feedback during the time evolution. Fascinating insights into such system are to be revealed by future numerical investigations.

Lastly, our generalization of the two-pole approach to nonequilibrium lays the groundwork to revisit and possibly generalize other n-pole approximations as well. Two interesting examples are the modeling of quasi-particle damping [85] or the description of Kondo-like singlets [153]. Depending on the details of a specific approach, a formulation might again be possible within a effective-medium-based description. Otherwise, the numerically more involved continued fraction representation of the nonequilibrium Green's function must be used. Nevertheless, the use of n-pole approaches for the description of far-from-equilibrium dynamics has just begun and interesting new developments can be expected in the future.

A. Enforcing conservation laws in nonequilibrium CPT

A.1. Local constraint on the doublon density

Within this subsection we will use the shorthand notation $G^{(2l)} \equiv G^{(2l)}_{T,U}$ and $G^{(2r)} \equiv G^{(2r)}_{T,U}$. To prove the local constraint on the doublon density, we consider

$$-i\partial_t d_i(t) = \langle [\hat{H}_{T,U}(t), \hat{n}_{i\uparrow}(t)\hat{n}_{i\downarrow}(t)] \rangle_{H_{T,U}}$$

$$= \sum_\sigma \langle \left[\sum_{jk} T_{jk\sigma}(t)\hat{c}^\dagger_{j\sigma}(t)\hat{c}_{k\sigma}(t), \hat{n}_{i\sigma}(t) \right] \hat{n}_{i\bar\sigma}(t) \rangle_{H_{T,U}},$$

where we used that the double occupation operator commutes with the interaction term of the Hamiltonian $H_{T,U}$. Using further that

$$\sum_{jk} T_{jk\sigma}(t) \left[\hat{c}^\dagger_{j\sigma}(t)\hat{c}_{k\sigma}(t), \hat{n}_{i\sigma}(t) \right] = \sum_{jk} T_{jk\sigma}(t) \left(\delta_{ki}\hat{c}^\dagger_{j\sigma}(t)\hat{c}_{i\sigma}(t) - \delta_{ji}\hat{c}^\dagger_{i\sigma}(t)\hat{c}_{k\sigma}(t) \right),$$

(A.1)

we find the final form by comparing with Eqs. (4.3) and (4.5) and using the relation $d_i(t) = -G^{(2l)}_{ii\sigma}(t,t^+) = -G^{(2r)}_{ii\sigma'}(t,t^+)$. This implies

$$-2i\partial_t d_i(t) = i\partial_t \left[G^{(2l)}_{ii\sigma}(t,t^+) + G^{(2r)}_{ii\sigma}(t,t^+) \right]$$

(A.2)

$$= 2 \sum_{j\sigma} \left[T_{ij\sigma}(t)G^{(2r)}_{ji\sigma}(t,t^+) - G^{(2l)}_{ij\sigma}(t,t^+)T_{ji\sigma}(t) \right],$$

which completes our derivation of Eq. (5.2).

To prove that Eq. (A.2) indeed ensures energy conservation, let us consider a time-independent Hamiltonian with $T_{ij\sigma}(t) = T_{ij\sigma}$ and $U(t) = U$. We consider the time-derivative of the kinetic energy first. Since the kinetic part of the Hamiltonian trivially commutes with itself, one obtains

$$i\partial_t E_{\text{kin}}(t) = \langle \sum_{ij\sigma} T_{ij\sigma}\hat{c}^\dagger_{i\sigma}\hat{c}_{j\sigma}, U \sum_l n_{l\uparrow}n_{l\downarrow} \rangle_{H_{T,U}}$$

(A.3)

$$= U \sum_{ij\sigma} \left[T_{ij\sigma}G^{(2r)}_{ji\sigma}(t,t^+) - G^{(2l)}_{ij\sigma}(t,t^+)T_{ji\sigma} \right],$$

This term cancels with $i\partial_t E_{\text{int}}(t) = U \sum_i i\partial_t d_i(t)$ assuming Eq. (A.2) holds thus proving energy conservation for a time-independent Hamiltonian.

A.2. Calculating the time-local variation of η

Let $h' = h_{T'-\lambda,U}$ denote the matrix elements of the effective Hamiltonian of the reference system $H^{\text{eff}}_{T'-\lambda,U}$, cf. Eq. (4.7). Through Eq. (4.11), or equivalently Eq. (4.8), a corresponding matrix $\eta' \equiv \eta_{T'-\lambda,U}$ is defined. We are interested in how it transforms under time-local variations. Since η' is an integrated quantity in λ, we first calculate its derivative with respect to time. Eq. (4.8) implies

$$i\partial_t \eta'_{ix\sigma}(t) = -\sum_y \eta'_{iy\sigma}(t) h'_{yx\sigma}(t) + \sum_{mn} \left[i\partial_t R'_{i\sigma(m,n)}(t) \right] [O']^\dagger_{(m,n)x\sigma}(t), \tag{A.4}$$

where $R' \equiv R_{T'-\lambda,U}$ and $O' \equiv O_{T'-\lambda,U}$. With $H' = H_{T'-\lambda,U}$, the time-local variation of $i\partial_t R'_{i\sigma(m,n)}(t)$ is given by

$$\delta_{\text{loc}} \left[i\partial_t R'_{i\sigma(m,n)}(t) \right] = z^{(m,n)} \langle m| \delta_{\text{loc}} \left[\hat{n}_{i\bar\sigma}(t)\hat{c}_{i\sigma}(t), \hat{H}'(t) \right] |n\rangle \tag{A.5}$$

$$= -z^{(m,n)} \sum_j \langle m| \delta\lambda_{ij\sigma}(t) \hat{n}_{i\bar\sigma}(t)\hat{c}_{j\sigma}(t)$$

$$+ \delta\lambda_{ij\bar\sigma}(t) \left[\hat{c}^\dagger_{i\bar\sigma}(t)\hat{c}_{j\bar\sigma}(t) - \hat{c}^\dagger_{j\bar\sigma}(t)\hat{c}_{i\bar\sigma}(t) \right] \hat{c}_{i\sigma}(t)|n\rangle,$$

where we further introduced $z^{(m,n)} = \sqrt{(e^{-\beta E_m} + e^{-\beta E_n})/Z}$ and exploited $\delta\lambda_{ij\sigma} = \delta\lambda_{ji\sigma}$. The time-local variation of $O'(t)$, on the other hand, vanishes since it is an integrated quantity in λ. We define

$$\gamma^{l\sigma}_{ix\sigma}(t) = \sum_{mn} z^{(m,n)} \langle m| \hat{n}_{i\bar\sigma}(t)\hat{c}_{l\sigma}(t)|n\rangle [O']^*_{x\sigma(m,n)}(t), \tag{A.6}$$

$$\gamma^{l\bar\sigma}_{ix\sigma}(t) = \sum_{mn} z^{(m,n)} \langle m| \left[\hat{c}^\dagger_{i\bar\sigma}(t)\hat{c}_{l\bar\sigma}(t) - \hat{c}^\dagger_{l\bar\sigma}(t)\hat{c}_{i\bar\sigma}(t) \right] \hat{c}_{i\sigma}(t)|n\rangle [O']^*_{x\sigma(m,n)}(t),$$

and therewith obtain Eq. (5.13).

B. Nonequilibrium two-pole approximation

B.1. Derivation of the matrix elements in the first virtual sector

Within this subsection we suppress every explicit time-dependence to allow for a leaner notation, i.e., $T_{ij\sigma} \equiv T_{ij\sigma}(t), U \equiv U(t), \hat{A} \equiv \hat{A}(t), h_{ik\sigma}^{(1,1)} \equiv h_{ik\sigma}^{(1,1)}(t), \ldots$, and also use the shorthand notation $\langle \cdot \rangle \equiv \langle \cdot \rangle_H$. To obtain $h_{ik\sigma}^{(1,1)} = \langle \{ i\partial_t \hat{\gamma}_{i\sigma}, \hat{\gamma}_{k\sigma}^\dagger \} \rangle$, we first of all note that the derivative of the norm alone can be written as

$$\langle \{ [\hat{n}_{i\bar{\sigma}} - \langle \hat{n}_{i\bar{\sigma}} \rangle] \hat{c}_{i\sigma}, \hat{\gamma}_{k\sigma}^\dagger \} \rangle i\partial_t \frac{1}{\sqrt{\langle \hat{n}_{i\sigma} \rangle - \langle \hat{n}_{i\sigma} \rangle^2}} = -\frac{1}{2} \delta_{ik} i\partial_t \left[\ln(C_{i\sigma}) \right], \qquad \text{(B.1)}$$

$$C_{i\sigma} \equiv \langle \hat{n}_{i\sigma} \rangle - \langle \hat{n}_{i\sigma} \rangle^2.$$

We consider

$$\begin{aligned}
h_{ik\sigma}^{(1,1)} &= -\delta_{ik} \frac{i\partial_t}{2} \ln(C_{i\sigma}) + \frac{\langle \{ [i\partial_t \hat{n}_{i\bar{\sigma}}] \hat{c}_{i\sigma} + \hat{n}_{i\bar{\sigma}} [i\partial_t \hat{c}_{i\sigma}] - \langle \hat{n}_{i\bar{\sigma}} \rangle [i\partial_t \hat{c}_{i\sigma}], \hat{\gamma}_{k\sigma}^\dagger \} \rangle}{\sqrt{\langle \hat{n}_{i\sigma} \rangle - \langle \hat{n}_{i\sigma} \rangle^2}} \\
&= -\delta_{ik} \frac{i\partial_t}{2} \ln(C_{i\sigma}) - \delta_{ik} U \langle \hat{n}_{i\bar{\sigma}} \rangle + \frac{\langle \{ [i\partial_t \hat{n}_{i\bar{\sigma}} \hat{c}_{i\sigma}], \hat{\gamma}_{k\sigma}^\dagger \} \rangle}{\sqrt{\langle \hat{n}_{i\sigma} \rangle - \langle \hat{n}_{i\sigma} \rangle^2}} \\
&= \delta_{ik} \left[-\frac{i\partial_t}{2} \ln(C_{i\sigma}) + h_{i\sigma}^{\text{at}} \right] + \frac{\langle \{ [\hat{n}_{i\bar{\sigma}} \hat{c}_{i\sigma}, \hat{H}_T], \hat{\gamma}_{k\sigma}^\dagger \} \rangle}{\sqrt{\langle \hat{n}_{i\sigma} \rangle - \langle \hat{n}_{i\sigma} \rangle^2}},
\end{aligned} \qquad \text{(B.2)}$$

where we defined $H_T \equiv \sum_{i \neq j} T_{ij\sigma} \hat{c}_{i\sigma}^\dagger \hat{c}_{i\sigma}$ as well as $h_{i\sigma}^{\text{at}} \equiv T_{ii\sigma} - \mu + U(1 - \langle \hat{n}_{i\bar{\sigma}} \rangle)$ which includes all terms that arise in the atomic limit, i.e., when $T_{ij\sigma} = 0$ for $i \neq j$. Note that in this case $C_{i\sigma} = \text{const.}$ such that $h_{ii\sigma}^{(1,1)}$ is real. To evaluate the remaining term, we consider

B. Nonequilibrium two-pole approximation

separately

$$\langle\{[\hat{n}_{i\bar{\sigma}}, \hat{H}_T]\hat{c}_{i\sigma}, \hat{n}_{k\bar{\sigma}}\hat{c}^\dagger_{k\sigma}\}\rangle = \langle[\hat{n}_{i\bar{\sigma}}, \hat{H}_T]\hat{c}_{i\sigma}\hat{n}_{k\bar{\sigma}}\hat{c}^\dagger_{k\sigma} + \hat{n}_{k\bar{\sigma}}\hat{c}^\dagger_{k\sigma}[\hat{n}_{i\bar{\sigma}}, \hat{H}_T]\hat{c}_{i\sigma}\rangle \tag{B.3}$$

$$= \frac{1}{2}\langle\{[\hat{n}_{i\bar{\sigma}}, \hat{H}_T], \hat{n}_{k\bar{\sigma}}\}\hat{c}_{i\sigma}\hat{c}^\dagger_{k\sigma} + [[\hat{n}_{i\bar{\sigma}}, \hat{H}_T], \hat{n}_{k\bar{\sigma}}]\hat{c}_{i\sigma}\hat{c}^\dagger_{k\sigma}\rangle$$

$$+ \frac{1}{2}\langle\{[\hat{n}_{i\bar{\sigma}}, \hat{H}_T], \hat{n}_{k\bar{\sigma}}\}\hat{c}^\dagger_{k\sigma}\hat{c}_{i\sigma} + [\hat{n}_{k\bar{\sigma}}, [\hat{n}_{i\bar{\sigma}}, \hat{H}_T]]\hat{c}^\dagger_{k\sigma}\hat{c}_{i\sigma}\rangle$$

$$= \delta_{ik}\frac{1}{2}\langle\{[\hat{n}_{i\bar{\sigma}}, \hat{H}_T], \hat{n}_{k\bar{\sigma}}\}\rangle + \frac{1}{2}\langle[[\hat{n}_{i\bar{\sigma}}, \hat{H}_T], \hat{n}_{k\bar{\sigma}}][\hat{c}_{i\sigma}, \hat{c}^\dagger_{k\sigma}]\rangle$$

$$= \delta_{ik}\frac{1}{2}\langle[\hat{n}_{i\bar{\sigma}}, \hat{H}_T] + [[\hat{n}_{i\bar{\sigma}}, \hat{H}_T], \hat{n}_{i\bar{\sigma}}](1 - 2\,\hat{n}_{i\sigma})\rangle - \delta_{i\neq k}\langle[[\hat{n}_{i\bar{\sigma}}, \hat{H}_T], \hat{n}_{k\bar{\sigma}}]\hat{c}^\dagger_{k\sigma}\hat{c}_{i\sigma}\rangle.$$

Furthermore

$$\langle\{[\hat{n}_{i\bar{\sigma}}, \hat{H}_T]\hat{c}_{i\sigma}, \hat{c}^\dagger_{k\sigma}\}\rangle = \langle[\hat{n}_{i\bar{\sigma}}, \hat{H}_T]\{\hat{c}_{i\sigma}, \hat{c}^\dagger_{k\sigma}\}\rangle = \delta_{ik}\langle[\hat{n}_{i\bar{\sigma}}, \hat{H}_T]\rangle \tag{B.4}$$

$$\langle\{\hat{n}_{i\bar{\sigma}}[\hat{c}_{i\sigma}, \hat{H}_T], \hat{n}_{k\bar{\sigma}}\hat{c}^\dagger_{k\sigma}\}\rangle = \langle\hat{n}_{i\bar{\sigma}}\hat{n}_{k\bar{\sigma}}\{[\hat{c}_{i\sigma}, \hat{H}_T], \hat{c}^\dagger_{k\sigma}\}\rangle = \sum_{l\neq i}T_{il\sigma}\langle\hat{n}_{i\bar{\sigma}}\hat{n}_{k\bar{\sigma}}\{\hat{c}_{l\sigma}, \hat{c}^\dagger_{k\sigma}\}\rangle$$

$$= \delta_{i\neq k}T_{ik\sigma}\langle\hat{n}_{i\bar{\sigma}}\hat{n}_{k\bar{\sigma}}\rangle,$$

$$\langle\{\hat{n}_{i\bar{\sigma}}[\hat{c}_{i\sigma}, \hat{H}_T], \hat{c}^\dagger_{k\sigma}\}\rangle = \langle\hat{n}_{i\bar{\sigma}}\{[\hat{c}_{i\sigma}, \hat{H}_T], \hat{c}^\dagger_{k\sigma}\}\rangle = \delta_{i\neq k}T_{ik\sigma}\langle\hat{n}_{i\bar{\sigma}}\rangle.$$

We therefore find that

$$\frac{i\partial_t}{2}\ln(C_{i\sigma}) = \frac{\frac{1}{2}\langle[\hat{n}_{i\bar{\sigma}}, \hat{H}_T]\rangle - \langle\hat{n}_{i\bar{\sigma}}\rangle\langle[\hat{n}_{i\bar{\sigma}}, \hat{H}_T]\rangle}{\langle\hat{n}_{i\bar{\sigma}}\rangle - \langle\hat{n}_{i\bar{\sigma}}\rangle^2} \tag{B.5}$$

cancels. Assuringly, the remaining terms are clearly hermitian. We find

$$h^{(1,1)}_{ii\sigma} = h^{\text{at}}_{i\sigma} + \frac{1}{2}\frac{\langle[[\hat{n}_{i\bar{\sigma}}, \hat{H}_T], \hat{n}_{i\bar{\sigma}}](1 - 2\hat{n}_{i\sigma})\rangle}{\langle\hat{n}_{i\bar{\sigma}}\rangle - \langle\hat{n}_{i\bar{\sigma}}\rangle^2} \tag{B.6}$$

$$= h^{\text{at}}_{i\sigma} - \frac{1}{2}\frac{\langle\sum_{j\neq i}\left(T_{ij\bar{\sigma}}\hat{c}^\dagger_{i\bar{\sigma}}\hat{c}_{j\bar{\sigma}} + T_{ji\bar{\sigma}}\hat{c}^\dagger_{j\bar{\sigma}}\hat{c}_{i\bar{\sigma}}\right)(1 - 2\hat{n}_{i\sigma})\rangle}{\langle\hat{n}_{i\bar{\sigma}}\rangle - \langle\hat{n}_{i\bar{\sigma}}\rangle^2}$$

$$= h^{\text{at}}_{i\sigma} - \left(\frac{1}{2} - \langle\hat{n}_{i\sigma}\rangle\right)\sum_{j\neq i}\frac{\langle T_{ij\bar{\sigma}}\hat{c}^\dagger_{i\bar{\sigma}}\hat{c}_{j\bar{\sigma}} + \text{cc.}\rangle}{\langle\hat{n}_{i\bar{\sigma}}\rangle - \langle\hat{n}_{i\bar{\sigma}}\rangle^2} + \sum_{j\neq i}\frac{\langle\left(T_{ij\bar{\sigma}}\hat{c}^\dagger_{i\bar{\sigma}}\hat{c}_{j\bar{\sigma}} + \text{cc.}\right)(\hat{n}_{i\sigma} - \langle\hat{n}_{i\sigma}\rangle)\rangle}{\langle\hat{n}_{i\bar{\sigma}}\rangle - \langle\hat{n}_{i\bar{\sigma}}\rangle^2}$$

$$= h^{\text{at}}_{i\sigma} - \left(\frac{1}{2} - \langle\hat{n}_{i\sigma}\rangle\right)\sum_{j\neq i}\frac{\langle T_{ij\bar{\sigma}}\hat{c}^\dagger_{i\bar{\sigma}}\hat{c}_{j\bar{\sigma}} + \text{cc.}\rangle}{\langle\hat{n}_{i\bar{\sigma}}\rangle - \langle\hat{n}_{i\bar{\sigma}}\rangle^2} + \frac{\sqrt{\langle\hat{n}_{i\sigma}\rangle - \langle\hat{n}_{i\sigma}\rangle^2}}{\sqrt{\langle\hat{n}_{i\bar{\sigma}}\rangle - \langle\hat{n}_{i\bar{\sigma}}\rangle^2}}\sum_{j\neq i}\frac{\langle T_{ij\bar{\sigma}}\hat{\gamma}^\dagger_{i\bar{\sigma}}\hat{c}_{j\bar{\sigma}} + \text{cc.}\rangle}{\sqrt{\langle\hat{n}_{i\bar{\sigma}}\rangle - \langle\hat{n}_{i\bar{\sigma}}\rangle^2}}.$$

We consider the commutator separately

$$[[\hat{n}_{i\bar{\sigma}}, \hat{H}_T], \hat{n}_{k\bar{\sigma}}] = \left[\left(\sum_j -T_{ji\bar{\sigma}}\hat{c}^\dagger_{j\bar{\sigma}}\hat{c}_{i\bar{\sigma}} + T_{ij\bar{\sigma}}\hat{c}^\dagger_{i\bar{\sigma}}\hat{c}_{j\bar{\sigma}}\right), \hat{n}_{k\bar{\sigma}}\right] \tag{B.7}$$

$$= -\delta_{ki}\sum_{j\neq i}\left(T_{ij\bar{\sigma}}\hat{c}^\dagger_{i\bar{\sigma}}\hat{c}_{j\bar{\sigma}} + T_{ji\bar{\sigma}}\hat{c}^\dagger_{j\bar{\sigma}}\hat{c}_{i\bar{\sigma}}\right) + \sum_{j\neq i}\delta_{kj}\left(T_{ij\bar{\sigma}}\hat{c}^\dagger_{i\bar{\sigma}}\hat{c}_{j\bar{\sigma}} + T_{ji\bar{\sigma}}\hat{c}^\dagger_{j\bar{\sigma}}\hat{c}_{i\bar{\sigma}}\right)$$

$$= -\delta_{ki}\sum_{j\neq i}\left(T_{ij\bar{\sigma}}\hat{c}^\dagger_{i\bar{\sigma}}\hat{c}_{j\bar{\sigma}} + T_{ji\bar{\sigma}}\hat{c}^\dagger_{j\bar{\sigma}}\hat{c}_{i\bar{\sigma}}\right) + \delta_{k\neq i}\left(T_{ik\bar{\sigma}}\hat{c}^\dagger_{i\bar{\sigma}}\hat{c}_{k\bar{\sigma}} + T_{ki\bar{\sigma}}\hat{c}^\dagger_{k\bar{\sigma}}\hat{c}_{i\bar{\sigma}}\right),$$

such that we find for the off-diagonal elements ($i \neq k$):

$$h_{ik\sigma}^{(1,1)} = \frac{T_{ik\sigma}\left[\langle\hat{n}_{i\bar{\sigma}}\hat{n}_{k\bar{\sigma}}\rangle - \langle\hat{n}_{i\bar{\sigma}}\rangle\langle\hat{n}_{k\bar{\sigma}}\rangle\right] - \langle\left[[\hat{n}_{i\bar{\sigma}}, \hat{H}_T], \hat{n}_{k\bar{\sigma}}\right]\hat{c}_{k\sigma}^{\dagger}\hat{c}_{i\sigma}\rangle}{\sqrt{\langle\hat{n}_{i\bar{\sigma}}\rangle - \langle\hat{n}_{i\bar{\sigma}}\rangle^2}\sqrt{\langle\hat{n}_{k\bar{\sigma}}\rangle - \langle\hat{n}_{k\bar{\sigma}}\rangle^2}}$$ (B.8)

$$= \frac{T_{ik\sigma}\left[\langle\hat{n}_{i\bar{\sigma}}\hat{n}_{k\bar{\sigma}}\rangle - \langle\hat{n}_{i\bar{\sigma}}\rangle\langle\hat{n}_{k\bar{\sigma}}\rangle\right] - \langle\left(T_{ik\bar{\sigma}}\hat{c}_{i\bar{\sigma}}^{\dagger}\hat{c}_{k\bar{\sigma}} + T_{ki\bar{\sigma}}\hat{c}_{k\bar{\sigma}}^{\dagger}\hat{c}_{i\bar{\sigma}}\right)\hat{c}_{k\sigma}^{\dagger}\hat{c}_{i\sigma}\rangle}{\sqrt{\langle\hat{n}_{i\bar{\sigma}}\rangle - \langle\hat{n}_{i\bar{\sigma}}\rangle^2}\sqrt{\langle\hat{n}_{k\bar{\sigma}}\rangle - \langle\hat{n}_{k\bar{\sigma}}\rangle^2}}.$$

B.2. Solution of Eq. (6.55) for the desired correlation functions

Throughout this section, we use the shorthand notation $\hat{A} \equiv \hat{A}(t)$ for operators in the Heisenberg picture, as well as $\langle\cdot\rangle \equiv \langle\cdot\rangle_H$. Furthermore, we assume $i \neq k$ throughout the entire section.

B.2.1. Solving for $\langle\hat{n}_{i\bar{\sigma}}\hat{n}_{k\bar{\sigma}}\rangle$

We start with density-density correlations. As it will turn out that solving for $\langle\hat{n}_{i\bar{\sigma}}\hat{n}_{k\bar{\sigma}}\rangle$ requires to obtain an expression for $\langle\hat{n}_{i\bar{\sigma}}\hat{n}_{k\sigma}\rangle$ as well, our starting point is the following symmetrized expression which we obtained from Eq. (6.55):

$$\langle\hat{n}_{i\bar{\sigma}}\hat{n}_{k\bar{\sigma}}\rangle = \frac{1}{4}\left(\langle\hat{c}_{k\bar{\sigma}}^{\dagger}\hat{\Gamma}_{ik\bar{\sigma}}^{(1)}\rangle + \langle\hat{c}_{i\bar{\sigma}}^{\dagger}\hat{\Gamma}_{ki\bar{\sigma}}^{(1)}\rangle + \text{cc.}\right),$$ (B.9)

$$\langle\hat{n}_{i\bar{\sigma}}\hat{n}_{k\sigma}\rangle = \frac{1}{4}\left(\langle\hat{c}_{k\sigma}^{\dagger}\hat{\Gamma}_{ik\bar{\sigma}}^{(2)}\rangle + \langle\hat{c}_{i\bar{\sigma}}^{\dagger}\hat{\Gamma}_{ki\sigma}^{(2)}\rangle + \text{cc.}\right).$$

Here, we defined the following operators

$$\hat{\Gamma}_{ik\bar{\sigma}}^{(1)} \equiv \hat{n}_{i\bar{\sigma}}\hat{c}_{k\bar{\sigma}}, \quad \hat{\Gamma}_{ik\bar{\sigma}}^{(2)} \equiv \hat{n}_{i\bar{\sigma}}\hat{c}_{k\sigma}.$$ (B.10)

We proceed by determining parts which lie within the active subspace. Starting with $\Gamma^{(1)}$ yields

$$\langle\left\{\hat{\Gamma}_{ik\bar{\sigma}}^{(1)}, \hat{c}_{j\bar{\sigma}}^{\dagger}\right\}\rangle = \langle\left\{\hat{c}_{j\bar{\sigma}}^{\dagger}, \hat{c}_{k\bar{\sigma}}\right\}\hat{n}_{i\bar{\sigma}} - \hat{c}_{k\bar{\sigma}}\left[\hat{c}_{j\bar{\sigma}}^{\dagger}, \hat{n}_{i\bar{\sigma}}\right]\rangle$$ (B.11)

$$= \delta_{jk}\langle\hat{n}_{i\bar{\sigma}}\rangle - \delta_{ji}\langle\hat{c}_{i\bar{\sigma}}^{\dagger}\hat{c}_{k\bar{\sigma}}\rangle,$$

$$\langle\left\{\hat{\Gamma}_{ik\bar{\sigma}}^{(1)}, \hat{\gamma}_{j\bar{\sigma}}^{\dagger}\right\}\rangle = \langle\delta_{kj}\left\{\hat{\gamma}_{k\bar{\sigma}}^{\dagger}, \hat{c}_{k\bar{\sigma}}\right\}\hat{n}_{i\bar{\sigma}} - \delta_{ji}\hat{c}_{k\bar{\sigma}}\left[\hat{\gamma}_{i\bar{\sigma}}^{\dagger}, \hat{n}_{i\bar{\sigma}}\right]\rangle$$

$$= \delta_{kj}\frac{\langle\hat{n}_{k\sigma}\hat{n}_{i\bar{\sigma}}\rangle - \langle\hat{n}_{k\sigma}\rangle\langle\hat{n}_{i\bar{\sigma}}\rangle}{\sqrt{\langle\hat{n}_{k\sigma}\rangle - \langle\hat{n}_{k\sigma}\rangle^2}} - \delta_{ji}\langle\hat{\gamma}_{i\bar{\sigma}}^{\dagger}\hat{c}_{k\bar{\sigma}}\rangle,$$

where we have made use of the relations

$$\left\{\hat{\gamma}_{j\bar{\sigma}}^{\dagger}, \hat{c}_{k\bar{\sigma}}\right\} = \delta_{kj}\left\{\frac{\hat{n}_{k\sigma} - \langle\hat{n}_{k\sigma}\rangle}{\sqrt{\langle\hat{n}_{k\sigma}\rangle - \langle\hat{n}_{k\sigma}\rangle^2}}\hat{c}_{k\bar{\sigma}}^{\dagger}, \hat{c}_{k\bar{\sigma}}\right\} = \delta_{kj}\frac{\hat{n}_{k\sigma} - \langle\hat{n}_{k\sigma}\rangle}{\sqrt{\langle\hat{n}_{k\sigma}\rangle - \langle\hat{n}_{k\sigma}\rangle^2}},$$ (B.12)

$$\left[\hat{\gamma}_{i\bar{\sigma}}^{\dagger}, \hat{n}_{i\bar{\sigma}}\right] = \left[\frac{\hat{n}_{i\sigma} - \langle\hat{n}_{i\sigma}\rangle}{\sqrt{\langle\hat{n}_{i\sigma}\rangle - \langle\hat{n}_{i\sigma}\rangle^2}}\hat{c}_{i\bar{\sigma}}^{\dagger}, \hat{n}_{i\bar{\sigma}}\right] = -\frac{\hat{n}_{i\sigma} - \langle\hat{n}_{i\sigma}\rangle}{\sqrt{\langle\hat{n}_{i\sigma}\rangle - \langle\hat{n}_{i\sigma}\rangle^2}}\hat{c}_{i\bar{\sigma}}^{\dagger} = -\hat{\gamma}_{i\bar{\sigma}}^{\dagger}.$$

B. Nonequilibrium two-pole approximation

In the same fashion, we find for $\Gamma^{(2)}$:

$$\left\langle \left\{ \hat{\Gamma}^{(2)}_{ik\bar{\sigma}}, \hat{c}^{\dagger}_{j\sigma} \right\} \right\rangle = \delta_{kj} \langle \hat{n}_{i\bar{\sigma}} \rangle, \tag{B.13}$$

$$\left\langle \left\{ \hat{\Gamma}^{(2)}_{ik\bar{\sigma}}, \hat{\gamma}^{\dagger}_{j\sigma} \right\} \right\rangle = \left\langle \left\{ \hat{\gamma}^{\dagger}_{j\sigma}, \hat{c}_{k\sigma} \right\} \hat{n}_{i\bar{\sigma}} \right\rangle = \delta_{kj} \frac{\langle \hat{n}_{k\bar{\sigma}} \hat{n}_{i\bar{\sigma}} \rangle - \langle \hat{n}_{k\bar{\sigma}} \rangle \langle \hat{n}_{i\bar{\sigma}} \rangle}{\sqrt{\langle \hat{n}_{k\bar{\sigma}} \rangle - \langle \hat{n}_{k\bar{\sigma}} \rangle^2}}.$$

Eqs. (B.11) and (B.13) enable us to define operators $\hat{a}^{(1)}_{ik\bar{\sigma}}$ and $\hat{a}^{(2)}_{ik\bar{\sigma}}$ which are orthogonal to the active subspace $\mathcal{A}$, i.e., $\hat{a}^{(1)}_{ik\bar{\sigma}}, \hat{a}^{(2)}_{ik\bar{\sigma}} \in \mathcal{A}^{\perp}$:

$$\hat{a}^{(1)}_{ik\bar{\sigma}} \equiv \hat{\Gamma}^{(1)}_{ik\bar{\sigma}} - \langle \hat{n}_{i\bar{\sigma}} \rangle \hat{c}_{k\bar{\sigma}} + \langle \hat{c}^{\dagger}_{i\bar{\sigma}} \hat{c}_{k\bar{\sigma}} \rangle \hat{c}_{i\bar{\sigma}} - \frac{\langle \hat{n}_{k\sigma} \hat{n}_{i\bar{\sigma}} \rangle - \langle \hat{n}_{k\sigma} \rangle \langle \hat{n}_{i\bar{\sigma}} \rangle}{\sqrt{\langle \hat{n}_{k\sigma} \rangle - \langle \hat{n}_{k\sigma} \rangle^2}} \hat{\gamma}_{k\bar{\sigma}} + \langle \hat{\gamma}^{\dagger}_{i\bar{\sigma}} \hat{c}_{k\bar{\sigma}} \rangle \hat{\gamma}_{i\bar{\sigma}}, \tag{B.14}$$

$$\hat{a}^{(2)}_{ik\bar{\sigma}} \equiv \hat{\Gamma}^{(2)}_{ik\bar{\sigma}} - \langle \hat{n}_{i\bar{\sigma}} \rangle \hat{c}_{k\sigma} - \frac{\langle \hat{n}_{k\bar{\sigma}} \hat{n}_{i\bar{\sigma}} \rangle - \langle \hat{n}_{k\bar{\sigma}} \rangle \langle \hat{n}_{i\bar{\sigma}} \rangle}{\sqrt{\langle \hat{n}_{k\bar{\sigma}} \rangle - \langle \hat{n}_{k\bar{\sigma}} \rangle^2}} \hat{\gamma}_{k\sigma}.$$

Therefore, any expectation value $\langle \hat{c}^{\dagger}_{x} \hat{a}^{(n)}_{ik\bar{\sigma}} \rangle$, $\hat{c}_x \in \mathcal{A}$, $n \in \{1, 2\}$, must vanish since the effective medium does not connect operators from the active subspace and its orthogonal complement, cf. Sec. 6.1.5. Insertion into Eq. (B.9) yields

$$\langle \hat{n}_{k\bar{\sigma}} \hat{n}_{i\bar{\sigma}} \rangle = \langle \hat{n}_{k\sigma} \hat{n}_{i\bar{\sigma}} \rangle \times \frac{1}{2} \xi_{k\bar{\sigma}}(t) + \langle \hat{n}_{i\sigma} \hat{n}_{k\bar{\sigma}} \rangle \times \frac{1}{2} \xi_{i\bar{\sigma}}(t) + \frac{1}{2} \left[w^{(1)}_{ik\bar{\sigma}} + w^{(1)}_{ki\bar{\sigma}} \right], \tag{B.15}$$

$$\langle \hat{n}_{k\sigma} \hat{n}_{i\bar{\sigma}} \rangle = \langle \hat{n}_{k\bar{\sigma}} \hat{n}_{i\bar{\sigma}} \rangle \times \frac{1}{2} \xi_{k\sigma}(t) + \langle \hat{n}_{k\sigma} \hat{n}_{i\sigma} \rangle \times \frac{1}{2} \xi_{i\bar{\sigma}}(t) + \frac{1}{2} \left[w^{(2)}_{ik\bar{\sigma}} + w^{(2)}_{ki\bar{\sigma}} \right],$$

where we defined

$$w^{(1)}_{ik\bar{\sigma}} \equiv -\langle \hat{n}_{k\sigma} \rangle \langle \hat{n}_{i\bar{\sigma}} \rangle \xi_{k\bar{\sigma}} + \langle \hat{n}_{i\bar{\sigma}} \rangle \langle \hat{n}_{k\bar{\sigma}} \rangle - \left| \langle \hat{c}^{\dagger}_{i\bar{\sigma}} \hat{c}_{k\bar{\sigma}} \rangle \right|^2 - \left| \langle \hat{\gamma}^{\dagger}_{i\bar{\sigma}} \hat{c}_{k\bar{\sigma}} \rangle \right|^2, \tag{B.16}$$

$$w^{(2)}_{ik\bar{\sigma}} \equiv -\langle \hat{n}_{k\bar{\sigma}} \rangle \langle \hat{n}_{i\bar{\sigma}} \rangle \xi_{k\sigma} + \langle \hat{n}_{i\bar{\sigma}} \rangle \langle \hat{n}_{k\sigma} \rangle,$$

$$\xi_{k\sigma} \equiv \frac{1}{2} \frac{\langle \hat{c}^{\dagger}_{k\sigma} \hat{\gamma}_{k\sigma} \rangle + \langle \hat{\gamma}^{\dagger}_{k\sigma} \hat{c}_{k\sigma} \rangle}{\sqrt{\langle \hat{n}_{k\bar{\sigma}} \rangle - \langle \hat{n}_{k\bar{\sigma}} \rangle^2}}.$$

Casting Eq. (B.15) into a matrix-vector multiplication and solving by matrix-inversion yields the final result, Eq. (6.56), in the main text.

B.2.2. Solving for $\langle \hat{c}^{\dagger}_{k\sigma} \hat{c}_{k\bar{\sigma}} \hat{c}^{\dagger}_{i\bar{\sigma}} \hat{c}_{i\sigma} \rangle$

For the spin-flip correlation function we proceed analogously. Via Eq. (6.55) it is given as

$$\langle \hat{c}^{\dagger}_{k\sigma} \hat{c}_{k\bar{\sigma}} \hat{c}^{\dagger}_{i\bar{\sigma}} \hat{c}_{i\sigma} \rangle = \frac{1}{4} \left(\langle \hat{c}^{\dagger}_{k\sigma} \hat{\Gamma}^{(3)}_{ik\bar{\sigma}} \rangle + \langle \hat{c}^{\dagger}_{i\bar{\sigma}} \hat{\Gamma}^{(3)}_{ki\sigma} \rangle + \langle [\hat{\Gamma}^{(3)}_{ki\bar{\sigma}}]^{\dagger} \hat{c}_{i\sigma} \rangle + \langle [\hat{\Gamma}^{(3)}_{ik\sigma}]^{\dagger} \hat{c}_{k\bar{\sigma}} \rangle \right), \tag{B.17}$$

where we have defined

$$\hat{\Gamma}^{(3)}_{ik\bar{\sigma}} \equiv \hat{c}^{\dagger}_{i\bar{\sigma}} \hat{c}_{i\sigma} \hat{c}_{k\bar{\sigma}}. \tag{B.18}$$

94

Determination of parts which are non-orthogonal to the active subspace yields:

$$\langle\{\hat{\Gamma}^{(3)}_{ik\bar{\sigma}},\hat{c}^{\dagger}_{j\sigma}\}\rangle = -\delta_{ji}\langle\hat{c}^{\dagger}_{i\bar{\sigma}}\hat{c}_{k\bar{\sigma}}\rangle, \tag{B.19}$$

$$\langle\{\hat{\Gamma}^{(3)}_{ik\bar{\sigma}},\hat{\gamma}^{\dagger}_{j\sigma}\}\rangle = -\langle\{\hat{\gamma}^{\dagger}_{j\sigma},\hat{c}_{k\bar{\sigma}}\}\hat{c}_{i\sigma}\hat{c}^{\dagger}_{i\bar{\sigma}} - \hat{c}_{k\bar{\sigma}}\left[\hat{\gamma}^{\dagger}_{j\sigma},\hat{c}_{i\sigma}\hat{c}^{\dagger}_{i\bar{\sigma}}\right]\rangle$$

$$= -\delta_{kj}\frac{\langle\hat{c}^{\dagger}_{k\sigma}\hat{c}_{k\bar{\sigma}}\hat{c}^{\dagger}_{i\bar{\sigma}}\hat{c}_{i\sigma}\rangle}{\sqrt{\langle\hat{n}_{k\bar{\sigma}}\rangle - \langle\hat{n}_{k\bar{\sigma}}\rangle^2}}$$

$$- \delta_{ij}\left[\frac{\sqrt{\langle\hat{n}_{i\sigma}\rangle - \langle\hat{n}_{i\sigma}\rangle^2}}{\sqrt{\langle\hat{n}_{i\bar{\sigma}}\rangle - \langle\hat{n}_{i\bar{\sigma}}\rangle^2}}\langle\hat{\gamma}^{\dagger}_{i\sigma}\hat{c}_{k\bar{\sigma}}\rangle - \frac{\langle\hat{n}_{i\bar{\sigma}}\rangle - \langle\hat{n}_{i\sigma}\rangle}{\sqrt{\langle\hat{n}_{i\bar{\sigma}}\rangle - \langle\hat{n}_{i\bar{\sigma}}\rangle^2}}\langle\hat{c}^{\dagger}_{i\bar{\sigma}}\hat{c}_{k\bar{\sigma}}\rangle\right],$$

where we exploited the relation

$$\left[\hat{\gamma}^{\dagger}_{j\sigma},\hat{c}_{i\sigma}\hat{c}^{\dagger}_{i\bar{\sigma}}\right] = \delta_{ij}\left(\{\hat{\gamma}^{\dagger}_{i\sigma},\hat{c}_{i\sigma}\}\hat{c}^{\dagger}_{i\bar{\sigma}} - \hat{c}_{i\sigma}\{\hat{\gamma}^{\dagger}_{i\sigma},\hat{c}^{\dagger}_{i\bar{\sigma}}\}\right)$$

$$= \delta_{ij}\left(\frac{\hat{n}_{i\bar{\sigma}} - \langle\hat{n}_{i\bar{\sigma}}\rangle}{\sqrt{\langle\hat{n}_{i\bar{\sigma}}\rangle - \langle\hat{n}_{i\bar{\sigma}}\rangle^2}}\hat{c}^{\dagger}_{i\bar{\sigma}} - \frac{\hat{c}_{i\sigma}\hat{c}^{\dagger}_{i\sigma}}{\sqrt{\langle\hat{n}_{i\bar{\sigma}}\rangle - \langle\hat{n}_{i\bar{\sigma}}\rangle^2}}\hat{c}^{\dagger}_{i\bar{\sigma}}\right)$$

$$= \delta_{ij}\left[\frac{\sqrt{\langle\hat{n}_{i\sigma}\rangle - \langle\hat{n}_{i\sigma}\rangle^2}}{\sqrt{\langle\hat{n}_{i\bar{\sigma}}\rangle - \langle\hat{n}_{i\bar{\sigma}}\rangle^2}}\hat{\gamma}^{\dagger}_{i\bar{\sigma}} - \left(\frac{\langle\hat{n}_{i\bar{\sigma}}\rangle - \langle\hat{n}_{i\sigma}\rangle}{\sqrt{\langle\hat{n}_{i\bar{\sigma}}\rangle - \langle\hat{n}_{i\bar{\sigma}}\rangle^2}}\hat{c}^{\dagger}_{i\bar{\sigma}}\right)\right]. \tag{B.20}$$

Components orthogonal to the active subspace are defined as the operator $\hat{a}^{(3)}_{ik\bar{\sigma}} \in \mathcal{A}^{\perp}$:

$$\hat{a}^{(3)}_{ik\bar{\sigma}} \equiv \hat{\Gamma}^{(3)}_{ik\bar{\sigma}} + \langle\hat{c}^{\dagger}_{i\bar{\sigma}}(t)\hat{c}_{k\bar{\sigma}}(t)\rangle\hat{c}_{i\sigma} + \frac{\langle\hat{c}^{\dagger}_{k\sigma}\hat{c}_{k\bar{\sigma}}\hat{c}^{\dagger}_{i\bar{\sigma}}\hat{c}_{i\sigma}\rangle}{\sqrt{\langle\hat{n}_{k\bar{\sigma}}\rangle - \langle\hat{n}_{k\bar{\sigma}}\rangle^2}}\hat{\gamma}_{k\sigma} \tag{B.21}$$

$$+ \left[\frac{\sqrt{\langle\hat{n}_{i\sigma}\rangle - \langle\hat{n}_{i\sigma}\rangle^2}}{\sqrt{\langle\hat{n}_{i\bar{\sigma}}\rangle - \langle\hat{n}_{i\bar{\sigma}}\rangle^2}}\langle\hat{\gamma}^{\dagger}_{i\sigma}(t)\hat{c}_{k\bar{\sigma}}(t)\rangle - \frac{\langle\hat{n}_{i\bar{\sigma}}\rangle - \langle\hat{n}_{i\sigma}\rangle}{\sqrt{\langle\hat{n}_{i\bar{\sigma}}\rangle - \langle\hat{n}_{i\bar{\sigma}}\rangle^2}}\langle\hat{c}^{\dagger}_{i\bar{\sigma}}\hat{c}_{k\bar{\sigma}}\rangle\right]\hat{\gamma}_{i\sigma}.$$

Therefore, expectation values of the form $\langle\hat{c}^{\dagger}_{x}\hat{a}^{(3)}_{ik\bar{\sigma}}\rangle$, $\hat{c}_x \in \mathcal{A}$, must vanish since the effective medium does not connect operators from the active subspace and its orthogonal complement, cf. Sec. 6.1.5. Insertion into Eq. (B.17) yields

$$\langle\hat{c}^{\dagger}_{k\sigma}\hat{c}_{k\bar{\sigma}}\hat{c}^{\dagger}_{i\bar{\sigma}}\hat{c}_{i\sigma}\rangle = -\langle\hat{c}^{\dagger}_{k\sigma}\hat{c}_{k\bar{\sigma}}\hat{c}^{\dagger}_{i\bar{\sigma}}\hat{c}_{i\sigma}\rangle \times \frac{1}{4}\left(\zeta_{k\sigma} + \zeta^{*}_{k\bar{\sigma}} + \zeta_{i\bar{\sigma}} + \zeta^{*}_{i\sigma}\right)$$

$$- \frac{1}{4}\left[w^{(3)}_{ik\bar{\sigma}} + w^{(3)}_{ki\sigma} + [w^{(3)}_{ik\sigma}]^* + [w^{(3)}_{ki\bar{\sigma}}]^*\right] \tag{B.22}$$

follows with the definitions

$$w^{(3)}_{ik\bar{\sigma}} \equiv \langle\hat{c}^{\dagger}_{i\bar{\sigma}}\hat{c}_{k\bar{\sigma}}\rangle\langle\hat{c}^{\dagger}_{k\sigma}\hat{c}_{i\sigma}\rangle + \left[\frac{\sqrt{\langle\hat{n}_{i\sigma}\rangle - \langle\hat{n}_{i\sigma}\rangle^2}}{\sqrt{\langle\hat{n}_{i\bar{\sigma}}\rangle - \langle\hat{n}_{i\bar{\sigma}}\rangle^2}}\langle\hat{\gamma}^{\dagger}_{i\bar{\sigma}}\hat{c}_{k\bar{\sigma}}\rangle - \frac{\langle\hat{n}_{i\bar{\sigma}}\rangle - \langle\hat{n}_{i\sigma}\rangle}{\sqrt{\langle\hat{n}_{i\bar{\sigma}}\rangle - \langle\hat{n}_{i\bar{\sigma}}\rangle^2}}\langle\hat{c}^{\dagger}_{i\bar{\sigma}}\hat{c}_{k\bar{\sigma}}\rangle\right]\langle\hat{c}^{\dagger}_{k\sigma}\hat{\gamma}_{i\sigma}\rangle,$$

$$\zeta_{k\sigma} = \frac{\langle\hat{c}^{\dagger}_{k\sigma}\hat{\gamma}_{k\sigma}\rangle}{\sqrt{\langle\hat{n}_{k\bar{\sigma}}\rangle - \langle\hat{n}_{k\bar{\sigma}}\rangle^2}}. \tag{B.23}$$

Solving Eq. (B.22) for the spin-flip correlation function yields the final result, Eq. (6.58), in the main text.

B. Nonequilibrium two-pole approximation

B.2.3. Solving for $\langle \hat{c}_{k\sigma}^\dagger \hat{c}_{k\bar{\sigma}}^\dagger \hat{c}_{i\bar{\sigma}} \hat{c}_{i\sigma} \rangle$

The motion of doublons on the lattice is described by

$$\langle \hat{c}_{k\sigma}^\dagger \hat{c}_{k\bar{\sigma}}^\dagger \hat{c}_{i\bar{\sigma}} \hat{c}_{i\sigma} \rangle = \frac{1}{4} \left(\langle \hat{c}_{k\sigma}^\dagger \hat{\Gamma}_{ik\bar{\sigma}}^{(4)} \rangle + \langle \hat{c}_{k\bar{\sigma}}^\dagger \hat{\Gamma}_{ik\sigma}^{(4)} \rangle + \langle [\hat{\Gamma}_{ki\bar{\sigma}}^{(4)}]^\dagger \hat{c}_{i\sigma} \rangle + \langle [\hat{\Gamma}_{ki\sigma}^{(4)}]^\dagger \hat{c}_{i\bar{\sigma}} \rangle \right), \qquad \text{(B.24)}$$

where we have defined

$$\hat{\Gamma}_{ik\bar{\sigma}}^{(4)} \equiv \hat{c}_{k\bar{\sigma}}^\dagger \hat{c}_{i\bar{\sigma}} \hat{c}_{i\sigma}. \qquad \text{(B.25)}$$

Determination of parts which are non-orthogonal to the active subspace yields:

$$\langle \left\{ \hat{\Gamma}_{ik\bar{\sigma}}^{(4)}, \hat{c}_{j\sigma}^\dagger \right\} \rangle = \delta_{ji} \langle \hat{c}_{k\bar{\sigma}}^\dagger \hat{c}_{i\bar{\sigma}} \rangle \qquad \text{(B.26)}$$

$$\langle \left\{ \hat{\Gamma}_{ik\bar{\sigma}}^{(4)}, \hat{\gamma}_{j\sigma}^\dagger \right\} \rangle = -\langle \left\{ \hat{\gamma}_{j\sigma}^\dagger, \hat{c}_{i\sigma} \right\} \hat{c}_{i\bar{\sigma}} \hat{c}_{k\bar{\sigma}}^\dagger - \hat{c}_{i\sigma} \left[\hat{\gamma}_{j\sigma}^\dagger, \hat{c}_{i\bar{\sigma}} \hat{c}_{k\bar{\sigma}}^\dagger \right] \rangle$$

$$= -\delta_{ij} \frac{\langle \hat{n}_{i\bar{\sigma}} \rangle \langle \hat{c}_{k\bar{\sigma}}^\dagger \hat{c}_{i\bar{\sigma}} \rangle}{\sqrt{\langle \hat{n}_{i\bar{\sigma}} \rangle - \langle \hat{n}_{i\bar{\sigma}} \rangle^2}} - \frac{\delta_{ij} \langle (\hat{n}_{i\sigma} - 1) \hat{c}_{k\bar{\sigma}}^\dagger \hat{c}_{i\bar{\sigma}} \rangle}{\sqrt{\langle \hat{n}_{i\bar{\sigma}} \rangle - \langle \hat{n}_{i\bar{\sigma}} \rangle^2}} + \frac{\delta_{kj} \langle \hat{c}_{k\sigma}^\dagger \hat{c}_{k\bar{\sigma}}^\dagger \hat{c}_{i\bar{\sigma}} \hat{c}_{i\sigma} \rangle}{\sqrt{\langle \hat{n}_{k\bar{\sigma}} \rangle - \langle \hat{n}_{k\bar{\sigma}} \rangle^2}}$$

$$= \delta_{ij} \frac{(1 - \langle \hat{n}_{i\bar{\sigma}} \rangle - \langle \hat{n}_{i\sigma} \rangle) \langle \hat{c}_{k\bar{\sigma}}^\dagger \hat{c}_{i\bar{\sigma}} \rangle}{\sqrt{\langle \hat{n}_{i\bar{\sigma}} \rangle - \langle \hat{n}_{i\bar{\sigma}} \rangle^2}} - \delta_{ij} \frac{\sqrt{\langle \hat{n}_{i\sigma} \rangle - \langle \hat{n}_{i\sigma} \rangle^2}}{\sqrt{\langle \hat{n}_{i\bar{\sigma}} \rangle - \langle \hat{n}_{i\bar{\sigma}} \rangle^2}} \langle \hat{c}_{k\bar{\sigma}}^\dagger \hat{\gamma}_{i\bar{\sigma}} \rangle$$

$$- \frac{\delta_{kj} \langle \hat{c}_{k\sigma}^\dagger \hat{c}_{k\bar{\sigma}}^\dagger \hat{c}_{i\bar{\sigma}} \hat{c}_{i\sigma} \rangle}{\sqrt{\langle \hat{n}_{k\bar{\sigma}} \rangle - \langle \hat{n}_{k\bar{\sigma}} \rangle^2}}.$$

where we used

$$\hat{c}_{i\sigma} \left[\hat{\gamma}_{j\sigma}^\dagger, \hat{c}_{i\bar{\sigma}} \hat{c}_{k\bar{\sigma}}^\dagger \right] = \hat{c}_{i\sigma} \left\{ \hat{\gamma}_{j\sigma}^\dagger, \hat{c}_{i\bar{\sigma}} \right\} \hat{c}_{k\bar{\sigma}}^\dagger - \hat{c}_{i\sigma} \hat{c}_{i\bar{\sigma}} \left\{ \hat{\gamma}_{j\sigma}^\dagger, \hat{c}_{k\bar{\sigma}}^\dagger \right\} \qquad \text{(B.27)}$$

$$= \frac{\hat{c}_{i\sigma}}{\sqrt{\langle \hat{n}_{j\bar{\sigma}} \rangle - \langle \hat{n}_{j\bar{\sigma}} \rangle^2}} \left(\left\{ \hat{n}_{j\bar{\sigma}} \hat{c}_{j\sigma}^\dagger, \hat{c}_{i\bar{\sigma}} \right\} \hat{c}_{k\bar{\sigma}}^\dagger - \hat{c}_{i\bar{\sigma}} \left\{ \hat{n}_{j\bar{\sigma}} \hat{c}_{j\sigma}^\dagger, \hat{c}_{k\bar{\sigma}}^\dagger \right\} \right)$$

$$= \frac{\hat{c}_{i\sigma}}{\sqrt{\langle \hat{n}_{j\bar{\sigma}} \rangle - \langle \hat{n}_{j\bar{\sigma}} \rangle^2}} \left(-\hat{c}_{j\sigma}^\dagger \left[\hat{c}_{i\bar{\sigma}}, \hat{n}_{j\bar{\sigma}} \right] \hat{c}_{k\bar{\sigma}}^\dagger + \hat{c}_{i\bar{\sigma}} \left[\hat{c}_{k\bar{\sigma}}^\dagger, \hat{n}_{j\bar{\sigma}} \right] \hat{c}_{j\sigma}^\dagger \right)$$

$$= \frac{\hat{c}_{i\sigma}}{\sqrt{\langle \hat{n}_{j\bar{\sigma}} \rangle - \langle \hat{n}_{j\bar{\sigma}} \rangle^2}} \left(-\delta_{ij} \hat{c}_{i\sigma}^\dagger \hat{c}_{i\bar{\sigma}} \hat{c}_{k\bar{\sigma}}^\dagger - \delta_{kj} \hat{c}_{i\bar{\sigma}} \hat{c}_{k\bar{\sigma}}^\dagger \hat{c}_{k\sigma}^\dagger \right)$$

$$= \frac{\delta_{ij} (1 - \hat{n}_{i\sigma}) \hat{c}_{k\bar{\sigma}}^\dagger \hat{c}_{i\bar{\sigma}}}{\sqrt{\langle \hat{n}_{j\bar{\sigma}} \rangle - \langle \hat{n}_{j\bar{\sigma}} \rangle^2}} - \frac{\delta_{kj} \hat{c}_{k\sigma}^\dagger \hat{c}_{k\bar{\sigma}}^\dagger \hat{c}_{i\bar{\sigma}} \hat{c}_{i\sigma}}{\sqrt{\langle \hat{n}_{k\bar{\sigma}} \rangle - \langle \hat{n}_{k\bar{\sigma}} \rangle^2}}.$$

Components orthogonal to the active subspace are defined as the operator $\hat{a}_{ik\bar{\sigma}}^{(4)} \in \mathcal{A}^\perp$:

$$\hat{a}_{ik\bar{\sigma}}^{(4)} \equiv \hat{\Gamma}_{ik\bar{\sigma}}^{(4)} - \langle \hat{c}_{k\bar{\sigma}}^\dagger \hat{c}_{i\bar{\sigma}} \rangle \hat{c}_{i\sigma} - \frac{(1 - \langle \hat{n}_{i\bar{\sigma}} \rangle - \langle \hat{n}_{i\sigma} \rangle) \langle \hat{c}_{k\bar{\sigma}}^\dagger \hat{c}_{i\bar{\sigma}} \rangle}{\sqrt{\langle \hat{n}_{i\bar{\sigma}} \rangle - \langle \hat{n}_{i\bar{\sigma}} \rangle^2}} \hat{\gamma}_{i\sigma} \qquad \text{(B.28)}$$

$$+ \frac{\sqrt{\langle \hat{n}_{i\sigma} \rangle - \langle \hat{n}_{i\sigma} \rangle^2}}{\sqrt{\langle \hat{n}_{i\bar{\sigma}} \rangle - \langle \hat{n}_{i\bar{\sigma}} \rangle^2}} \langle \hat{c}_{k\bar{\sigma}}^\dagger \hat{\gamma}_{i\bar{\sigma}} \rangle \hat{\gamma}_{i\sigma} + \frac{\langle \hat{c}_{k\sigma}^\dagger \hat{c}_{k\bar{\sigma}}^\dagger \hat{c}_{i\bar{\sigma}} \hat{c}_{i\sigma} \rangle}{\sqrt{\langle \hat{n}_{k\bar{\sigma}} \rangle - \langle \hat{n}_{k\bar{\sigma}} \rangle^2}} \hat{\gamma}_{k\sigma}$$

Therefore, expectation values of the form $\langle \hat{c}_x^\dagger \hat{a}_{ik\bar{\sigma}}^{(4)} \rangle$, $\hat{c}_x \in \mathcal{A}$, must vanish since the effective medium does not connect operators from the active subspace and its orthogonal complement, cf. Sec. 6.1.5. Insertion into Eq. (B.24) yields

$$\langle \hat{c}_{k\sigma}^\dagger \hat{c}_{k\bar{\sigma}}^\dagger \hat{c}_{i\bar{\sigma}} \hat{c}_{i\sigma} \rangle \equiv -\langle \hat{c}_{k\sigma}^\dagger \hat{c}_{k\bar{\sigma}}^\dagger \hat{c}_{i\bar{\sigma}} \hat{c}_{i\sigma} \rangle \times \frac{1}{4} \sum_{\sigma'} [\zeta_{k\sigma'} + \zeta_{i\sigma'}^*] + \frac{1}{4} \left[w_{ik\bar{\sigma}}^{(4)} + w_{ik\sigma}^{(4)} + [w_{ki\sigma}^{(4)}]^* + [w_{ki\bar{\sigma}}^{(4)}]^* \right]$$

(B.29)

where we defined

$$w_{ik\bar{\sigma}}^{(4)} \equiv \langle \hat{c}_{k\bar{\sigma}}^\dagger \hat{c}_{i\bar{\sigma}} \rangle \langle \hat{c}_{k\sigma}^\dagger \hat{c}_{i\sigma} \rangle$$

(B.30)

$$+ \left[\frac{(1 - \langle \hat{n}_{i\bar{\sigma}} \rangle - \langle \hat{n}_{i\sigma} \rangle) \langle \hat{c}_{k\bar{\sigma}}^\dagger \hat{c}_{i\bar{\sigma}} \rangle}{\sqrt{\langle \hat{n}_{i\bar{\sigma}} \rangle - \langle \hat{n}_{i\bar{\sigma}} \rangle^2}} - \frac{\sqrt{\langle \hat{n}_{i\sigma} \rangle - \langle \hat{n}_{i\sigma} \rangle^2}}{\sqrt{\langle \hat{n}_{i\bar{\sigma}} \rangle - \langle \hat{n}_{i\bar{\sigma}} \rangle^2}} \langle \hat{c}_{k\bar{\sigma}}^\dagger \hat{\gamma}_{i\bar{\sigma}} \rangle \right] \langle \hat{c}_{k\sigma}^\dagger \hat{\gamma}_{i\sigma} \rangle.$$

Solving Eq. (B.29) for the spin-flip correlation function yields the final result, Eq. (6.60), in the main text.

Bibliography

[1] J. W. von Goethe, *Faust: A Tragedy, Parts One and Two, Fully Revised* (Yale University Press, 2014) (cited on page 1).

[2] J. W. von Goethe, *Faust I: Der Tragödie erster Teil* (Reclam Verlag, 1986) (cited on page 1).

[3] R. Kubo, "The fluctuation-dissipation theorem", Reports on Progress in Physics **29**, 255 (1966) (cited on page 1).

[4] A. Einstein, "Über die von der molekularkinetischen Theorie der Wärme geforderte Bewegung von in ruhenden Flüssigkeiten suspendierten Teilchen", Annalen der Physik **322**, 549–560 (1905) (cited on page 1).

[5] H. Nyquist, "Thermal Agitation of Electric Charge in Conductors", Phys. Rev. **32**, 110–113 (1928) (cited on page 1).

[6] L. Onsager, "Reciprocal Relations in Irreversible Processes. I.", Phys. Rev. **37**, 405–426 (1931) (cited on page 1).

[7] M. Imada, A. Fujimori, and Y. Tokura, "Metal-insulator transitions", Rev. Mod. Phys. **70**, 1039–1263 (1998) (cited on page 1).

[8] T. Ogasawara, M. Ashida, N. Motoyama, H. Eisaki, S. Uchida, Y. Tokura, H. Ghosh, A. Shukla, S. Mazumdar, and M. Kuwata-Gonokami, "Ultrafast Optical Nonlinearity in the Quasi-One-Dimensional Mott Insulator Sr_2CuO_3", Phys. Rev. Lett. **85**, 2204–2207 (2000) (cited on pages 1, 2).

[9] L. Perfetti, P. A. Loukakos, M. Lisowski, U. Bovensiepen, H. Berger, S. Biermann, P. S. Cornaglia, A. Georges, and M. Wolf, "Time Evolution of the Electronic Structure of $1T$-TaS_2 through the Insulator-Metal Transition", Phys. Rev. Lett. **97**, 067402 (2006) (cited on pages 1, 2).

[10] C. Kübler, H. Ehrke, R. Huber, R. Lopez, A. Halabica, R. F. Haglund, and A. Leitenstorfer, "Coherent Structural Dynamics and Electronic Correlations during an Ultrafast Insulator-to-Metal Phase Transition in VO_2", Phys. Rev. Lett. **99**, 116401 (2007) (cited on pages 1, 2).

[11] D. Wegkamp, M. Herzog, L. Xian, M. Gatti, P. Cudazzo, C. L. McGahan, R. E. Marvel, R. F. Haglund, A. Rubio, M. Wolf, and J. Stähler, "Instantaneous Band Gap Collapse in Photoexcited Monoclinic VO_2 due to Photocarrier Doping", Phys. Rev. Lett. **113**, 216401 (2014) (cited on pages 1, 2).

[12] V. R. Morrison, R. P. Chatelain, K. L. Tiwari, A. Hendaoui, A. Bruhács, M. Chaker, and B. J. Siwick, "A photoinduced metal-like phase of monoclinic VO2 revealed by ultrafast electron diffraction", Science **346**, 445–448 (2014) (cited on pages 1, 2).

[13]   I. Bloch, J. Dalibard, and W. Zwerger, "Many-body physics with ultracold gases", Rev. Mod. Phys. **80**, 885–964 (2008) (cited on pages 1, 4).

[14]   D. C. McKay and B. DeMarco, "Cooling in strongly correlated optical lattices: prospects and challenges", Reports on Progress in Physics **74**, 054401 (2011) (cited on pages 1, 4, 5).

[15]   U. Schneider, L. Hackermüller, S. Will, T. Best, I. Bloch, T. A. Costi, R. W. Helmes, D. Rasch, and A. Rosch, "Metallic and Insulating Phases of Repulsively Interacting Fermions in a 3D Optical Lattice", Science **322**, 1520 (2008) (cited on pages 1, 4).

[16]   R. Jördens, N. Strohmaier, K. Günter, H. Moritz, and T. Esslinger, "A Mott insulator of fermionic atoms in an optical lattice", Nature **455**, 204 (2008) (cited on pages 1, 4).

[17]   U. Schneider, L. Hackermüller, J. P. Ronzheimer, S. Will, S. Braun, T. Best, I. Bloch, E. Demler, S. Mandt, D. Rasch, and A. Rosch, "Fermionic transport and out-of-equilibrium dynamics in a homogeneous Hubbard model with ultracold atoms", Nature Physics **8**, 213 (2012) (cited on pages 1, 4, 33, 81, 88).

[18]   L. W. Cheuk, M. A. Nichols, K. R. Lawrence, M. Okan, H. Zhang, E. Khatami, N. Trivedi, T. Paiva, M. Rigol, and M. W. Zwierlein, "Observation of spatial charge and spin correlations in the 2D Fermi-Hubbard model", Science **353**, 1260–1264 (2016) (cited on pages 1, 4).

[19]   M. Boll, T. A. Hilker, G. Salomon, A. Omran, J. Nespolo, L. Pollet, I. Bloch, and C. Gross, "Spin- and density-resolved microscopy of antiferromagnetic correlations in Fermi-Hubbard chains", Science **353**, 1257–1260 (2016) (cited on pages 1, 4).

[20]   A. A. Kordyuk, "ARPES experiment in fermiology of quasi-2D metals (Review Article)", Low Temperature Physics **40**, 286–296 (2014) (cited on page 2).

[21]   Z. Yang, C. Ko, and S. Ramanathan, "Oxide electronics utilizing ultrafast metal-insulator transitions", Annual Review of Materials Research **41**, 337–367 (2011) (cited on page 2).

[22]   N. F. Mott, "The Basis of the Electron Theory of Metals, with Special Reference to the Transition Metals", Proceedings of the Physical Society. Section A **62**, 416 (1949) (cited on page 2).

[23]   F. Gebhard, *The Mott Metal-Insulator Transition* (Springer, 1997) (cited on pages 2, 59).

[24]   N. W. Ashcroft and N. D. Mermin, *Solid State Physics* (Cengage Learning Emea, 1976) (cited on pages 2, 4).

[25]   B. Keimer, S. A. Kivelson, M. R. Norman, S. Uchida, and J. Zaanen, "From quantum matter to high-temperature superconductivity in copper oxides", Nature **518**, Review, 179–186 (2015) (cited on page 2).

[26]   D. J. Scalapino, "The 2D Hubbard Model and the High T_c Cuprate Problem", Journal of Superconductivity and Novel Magnetism **19**, 195–200 (2006) (cited on page 2).

[27] J. Hubbard, "Electron correlations in narrow energy bands", Proceedings of the Royal Society of London A: Mathematical, Physical and Engineering Sciences **276**, 238–257 (1963) (cited on pages 2, 6, 59, 60).

[28] J. Kanamori, "Electron Correlation and Ferromagnetism of Transition Metals", Progress of Theoretical Physics **30**, 275–289 (1963) (cited on page 2).

[29] M. C. Gutzwiller, "Effect of Correlation on the Ferromagnetism of Transition Metals", Phys. Rev. Lett. **10**, 159–162 (1963) (cited on pages 2, 5).

[30] H. Aoki, N. Tsuji, M. Eckstein, M. Kollar, T. Oka, and P. Werner, "Nonequilibrium dynamical mean-field theory and its applications", Rev. Mod. Phys. **86**, 779–837 (2014) (cited on pages 3, 4, 84).

[31] C. Gramsch, K. Balzer, M. Eckstein, and M. Kollar, "Hamiltonian-based impurity solver for nonequilibrium dynamical mean-field theory", Phys. Rev. B **88**, 235106 (2013) (cited on pages 3, 4, 12, 13, 16, 19, 20, 111).

[32] R. van Leeuwen and G. Stefanucci, *Nonequilibrium Many-Body Theory of Quantum Systems* (Cambridge University Press, 2013) (cited on pages 3, 7, 9, 11).

[33] M. Heyl, A. Polkovnikov, and S. Kehrein, "Dynamical Quantum Phase Transitions in the Transverse-Field Ising Model", Phys. Rev. Lett. **110**, 135704 (2013) (cited on page 3).

[34] E. Canovi, P. Werner, and M. Eckstein, "First-Order Dynamical Phase Transitions", Phys. Rev. Lett. **113**, 265702 (2014) (cited on page 3).

[35] M. Heyl, "Scaling and Universality at Dynamical Quantum Phase Transitions", Phys. Rev. Lett. **115**, 140602 (2015) (cited on page 3).

[36] A. A. Zvyagin, "Dynamical quantum phase transitions (Review Article)", Low Temperature Physics **42**, 971–994 (2016) (cited on pages 3, 87).

[37] J. M. Zhang and H.-T. Yang, "Cusps in the quench dynamics of a Bloch state", EPL (Europhysics Letters) **114**, 60001 (2016) (cited on page 3).

[38] W. Magnus, "On the exponential solution of differential equations for a linear operator", Communications on Pure and Applied Mathematics **7**, 649–673 (1954) (cited on page 3).

[39] W. Metzner and D. Vollhardt, "Correlated Lattice Fermions in $d = \infty$ Dimensions", Phys. Rev. Lett. **62**, 324–327 (1989) (cited on pages 3, 16, 59).

[40] A. Georges and G. Kotliar, "Hubbard model in infinite dimensions", Phys. Rev. B **45**, 6479–6483 (1992) (cited on pages 3, 16).

[41] *DMFT at 25: Infinite Dimensions* (Verlag des Forschungszentrum Jülich, 2014) (cited on page 3).

[42] P. Schmidt and H. Monien, "Nonequilibrium dynamical mean-field theory of a strongly correlated system", arXiv:cond-mat/0202046 (2002) (cited on pages 4, 16).

[43] L. V. Keldysh, "Diagram Technique for Nonequilibrium Processes", J. Exptl. Theoret. Phys. **47**, 1515 (1964) (cited on pages 4, 7).

[44] J. K. Freericks, V. M. Turkowski, and V. Zlatić, "Nonequilibrium Dynamical Mean-Field Theory", Phys. Rev. Lett. **97**, 266408 (2006) (cited on pages 4, 16).

[45] G. Cohen, E. Gull, D. R. Reichman, and A. J. Millis, "Taming the Dynamical Sign Problem in Real-Time Evolution of Quantum Many-Body Problems", Phys. Rev. Lett. **115**, 266802 (2015) (cited on page 4).

[46] Q. Dong, I. Krivenko, J. Kleinhenz, A. E. Antipov, G. Cohen, and E. Gull, "Quantum Monte Carlo solution of the dynamical mean field equations in real time", Phys. Rev. B **96**, 155126 (2017) (cited on page 4).

[47] F. A. Wolf, I. P. McCulloch, and U. Schollwöck, "Solving nonequilibrium dynamical mean-field theory using matrix product states", Phys. Rev. B **90**, 235131 (2014) (cited on pages 4, 13).

[48] K. Balzer, Z. Li, O. Vendrell, and M. Eckstein, "Multiconfiguration time-dependent Hartree impurity solver for nonequilibrium dynamical mean-field theory", Phys. Rev. B **91**, 045136 (2015) (cited on pages 4, 13).

[49] Z. He and A. J. Millis, "Entanglement entropy and computational complexity of the Anderson impurity model out of equilibrium: Quench dynamics", Phys. Rev. B **96**, 085107 (2017) (cited on page 4).

[50] K. Balzer and M. Eckstein, "Auxiliary Hamiltonian representation of the nonequilibrium Dyson equation", Phys. Rev. B **89**, 035148 (2014) (cited on pages 4, 6, 15, 16, 19, 83, 84).

[51] U. Schollwöck, "The density-matrix renormalization group", Rev. Mod. Phys. **77**, 259–315 (2005) (cited on page 4).

[52] S. R. White, "Density matrix formulation for quantum renormalization groups", Phys. Rev. Lett. **69**, 2863–2866 (1992) (cited on page 4).

[53] S. R. White and A. E. Feiguin, "Real-Time Evolution Using the Density Matrix Renormalization Group", Phys. Rev. Lett. **93**, 076401 (2004) (cited on page 4).

[54] A. J. Daley, C. Kollath, U. Schollwöck, and G. Vidal, "Time-dependent density-matrix renormalization-group using adaptive effective Hilbert spaces", Journal of Statistical Mechanics: Theory and Experiment **2004**, P04005 (2004) (cited on page 4).

[55] G. Vidal, "Efficient Simulation of One-Dimensional Quantum Many-Body Systems", Phys. Rev. Lett. **93**, 040502 (2004) (cited on page 4).

[56] C. Kollath, U. Schollwöck, and W. Zwerger, "Spin-Charge Separation in Cold Fermi Gases: A Real Time Analysis", Phys. Rev. Lett. **95**, 176401 (2005) (cited on page 4).

[57] C. J. Bolech, F. Heidrich-Meisner, S. Langer, I. P. McCulloch, G. Orso, and M. Rigol, "Long-Time Behavior of the Momentum Distribution During the Sudden Expansion of a Spin-Imbalanced Fermi Gas in One Dimension", Phys. Rev. Lett. **109**, 110602 (2012) (cited on page 4).

[58] R. Rausch and M. Potthoff, "Filling-dependent doublon dynamics in the one-dimensional Hubbard model", Phys. Rev. B **95**, 045152 (2017) (cited on pages 4, 56, 85).

[59] E. H. Lieb and F. Y. Wu, "Absence of Mott Transition in an Exact Solution of the Short-Range, One-Band Model in One Dimension", Phys. Rev. Lett. **20**, 1445–1448 (1968) (cited on pages 4, 59).

[60] E. H. Lieb and F. Wu, "The one-dimensional Hubbard model: a reminiscence", Physica A **321**, 1 (2003) (cited on page 4).

[61] T. Oka and H. Aoki, "Dielectric breakdown in a Mott insulator: Many-body Schwinger-Landau-Zener mechanism studied with a generalized Bethe ansatz", Phys. Rev. B **81**, 033103 (2010) (cited on page 4).

[62] T. Prosen, "Exact Nonequilibrium Steady State of an Open Hubbard Chain", Phys. Rev. Lett. **112**, 030603 (2014) (cited on page 4).

[63] J. E. Hirsch, "Two-dimensional Hubbard model: Numerical simulation study", Phys. Rev. B **31**, 4403–4419 (1985) (cited on pages 4, 81, 88).

[64] C. N. Varney, C.-R. Lee, Z. J. Bai, S. Chiesa, M. Jarrell, and R. T. Scalettar, "Quantum Monte Carlo study of the two-dimensional fermion Hubbard model", Phys. Rev. B **80**, 075116 (2009) (cited on page 4).

[65] F. Goth and F. F. Assaad, "Time and spatially resolved quench of the fermionic Hubbard model showing restricted equilibration", Phys. Rev. B **85**, 085129 (2012) (cited on page 4).

[66] R. P. Feynman, "Simulating physics with computers", International Journal of Theoretical Physics **21**, 467–488 (1982) (cited on page 4).

[67] R. Onofrio, "All-optical cooling of Fermi gases via Pauli inhibition of spontaneous emission", Phys. Rev. A **93**, 033414 (2016) (cited on page 4).

[68] H. F. Hess, "Evaporative cooling of magnetically trapped and compressed spin-polarized hydrogen", Phys. Rev. B **34**, 3476–3479 (1986) (cited on page 5).

[69] N. Tsuji, P. Barmettler, H. Aoki, and P. Werner, "Nonequilibrium dynamical cluster theory", Phys. Rev. B **90**, 075117 (2014) (cited on page 5).

[70] C. Jung, A. Lieder, S. Brener, H. Hafermann, B. Baxevanis, A. Chudnovskiy, A. Rubtsov, M. Katsnelson, and A. Lichtenstein, "Dual-fermion approach to non-equilibrium strongly correlated problems", Ann. Phys. **524**, 49–61 (2011) (cited on page 5).

[71] C. V. Kraus, N. Schuch, F. Verstraete, and J. I. Cirac, "Fermionic projected entangled pair states", Phys. Rev. A **81**, 052338 (2010) (cited on page 5).

[72] M. Schiró and M. Fabrizio, "Time-Dependent Mean Field Theory for Quench Dynamics in Correlated Electron Systems", Phys. Rev. Lett. **105**, 076401 (2010) (cited on page 5).

[73] M. Schiró and M. Fabrizio, "Quantum quenches in the Hubbard model: Time-dependent mean-field theory and the role of quantum fluctuations", Phys. Rev. B **83**, 165105 (2011) (cited on pages 5, 87).

[74] M. C. Gutzwiller, "Correlation of Electrons in a Narrow s Band", Phys. Rev. **137**, A1726–A1735 (1965) (cited on page 5).

[75] M. Potthoff, "Self-energy-functional approach to systems of correlated electrons", Eur. Phys. J. B **32**, 429–436 (2003) (cited on pages 5, 16, 57, 86).

[76] F. Hofmann, M. Eckstein, E. Arrigoni, and M. Potthoff, "Nonequilibrium self-energy functional theory", Phys. Rev. B **88**, 165124 (2013) (cited on pages 5, 16, 32, 38, 41, 57, 84–86).

[77] J. Frenkel, *Wave Mechanics* (Dover Publications, 1950) (cited on page 5).

[78] F. Hofmann, M. Eckstein, and M. Potthoff, "Nonequilibrium self-energy functional approach to the dynamical Mott transition", Phys. Rev. B **93**, 235104 (2016) (cited on pages 5, 32, 87).

[79] M. Eckstein, M. Kollar, and P. Werner, "Thermalization after an Interaction Quench in the Hubbard Model", Phys. Rev. Lett. **103**, 056403 (2009) (cited on pages 5, 33, 56, 85, 87).

[80] M. Sandri, M. Schiró, and M. Fabrizio, "Linear ramps of interaction in the fermionic Hubbard model", Phys. Rev. B **86**, 075122 (2012) (cited on page 5).

[81] L. M. Roth, "New Method for Linearizing Many-Body Equations of Motion in Statistical Mechanics", Phys. Rev. Lett. **20**, 1431–1434 (1968) (cited on pages 6, 60, 61, 80, 86, 87).

[82] L. M. Roth, "Electron Correlation in Narrow Energy Bands I. The Two-Pole Approximation in a Narrow S Band", Phys. Rev. **184**, 451–459 (1969) (cited on pages 6, 60, 61, 66, 75, 80, 86, 87).

[83] W. Nolting, "Methode der Spektralmomente für das Hubbard-Modell eines schmalen S-Bandes", Zeitschrift für Physik A Hadrons and nuclei **255**, 25–39 (1972) (cited on pages 6, 60, 81, 88).

[84] B. Mehlig, H. Eskes, R. Hayn, and M. B. J. Meinders, "Single-particle spectral density of the Hubbard model", Phys. Rev. B **52**, 2463–2470 (1995) (cited on pages 6, 60, 87).

[85] R. Hayn, P. Lombardo, and K. Matho, "Spectral density of the Hubbard model by the continued fraction method", Phys. Rev. B **74**, 205124 (2006) (cited on pages 6, 60, 81, 88).

[86] R. Zwanzig, "Ensemble Method in the Theory of Irreversibility", The Journal of Chemical Physics **33**, 1338–1341 (1960) (cited on pages 6, 65, 69, 80, 83, 85).

[87] H. Mori, "Transport, Collective Motion, and Brownian Motion", Progress of Theoretical Physics **33**, 423–455 (1965) (cited on pages 6, 65, 69, 80, 83, 85).

[88] H. Mori, "A Continued-Fraction Representation of the Time-Correlation Functions", Progress of Theoretical Physics **34**, 399–416 (1965) (cited on pages 6, 60, 65, 69, 70, 72, 80, 83, 85, 86).

[89] A. L. Fetter and J. D. Walecka, *Quantum Theory of Many-Particle Systems* (Dover Publications, 2003) (cited on pages 7, 11).

[90] F. J. Dyson, "The Radiation Theories of Tomonaga, Schwinger, and Feynman", Phys. Rev. **75**, 486–502 (1949) (cited on page 7).

[91]   R. P. Feynman, "Space-Time Approach to Quantum Electrodynamics", Phys. Rev. **76**, 769–789 (1949) (cited on page 7).

[92]   M. Gell-Mann and F. Low, "Bound States in Quantum Field Theory", Phys. Rev. **84**, 350–354 (1951) (cited on page 7).

[93]   T. Matsubara, "A New Approach to Quantum-Statistical Mechanics", Progress of Theoretical Physics **14**, 351–378 (1955) (cited on page 7).

[94]   G. C. Wick, "The Evaluation of the Collision Matrix", Phys. Rev. **80**, 268–272 (1950) (cited on page 7).

[95]   P. Danielewicz, "Quantum theory of nonequilibrium processes, I", Annals of Physics **152**, 239–304 (1984) (cited on page 7).

[96]   M. Wagner, "Expansions of nonequilibrium Green's functions", Phys. Rev. B **44**, 6104–6117 (1991) (cited on page 7).

[97]   P. C. Martin and J. Schwinger, "Theory of Many-Particle Systems. I", Phys. Rev. **115**, 1342–1373 (1959) (cited on pages 7, 10).

[98]   G. Baym and L. P. Kadanoff, *Quantum Statistical Mechanics* (W.A. Benjamin, 1962) (cited on page 7).

[99]   G. Baym, "Conservation laws and the quantum theory of transport: The early days", Progress in Nonequilibrium Green's Functions World Scientific (1999) (cited on page 7).

[100] P. C. Martin, "Quantum kinetic equations", Progress in Nonequilibrium Green's Functions World Scientific (1999) (cited on page 7).

[101] L. V. Keldysh, "Real-time nonequilibrium Green's functions", Progress in Nonequilibrium Green's Functions II World Scientific (2002) (cited on page 7).

[102] A. V. Joura, J. K. Freericks, and A. I. Lichtenstein, "Long-lived nonequilibrium states in the Hubbard model with an electric field", Phys. Rev. B **91**, 245153 (2015) (cited on page 11).

[103] M. G. Zacher, R. Eder, E. Arrigoni, and W. Hanke, "Evolution of the stripe phase as a function of doping from a theoretical analysis of angle-resolved photoemission data", Phys. Rev. B **65**, 045109 (2002) (cited on page 12).

[104] M. Aichhorn, E. Arrigoni, M. Potthoff, and W. Hanke, "Variational cluster approach to the Hubbard model: Phase-separation tendency and finite-size effects", Phys. Rev. B **74**, 235117 (2006) (cited on page 12).

[105] C. Gramsch and M. Potthoff, "Lehmann representation of the nonequilibrium self-energy", Phys. Rev. B **92**, 235135 (2015) (cited on pages 15, 27, 30, 32, 46, 53, 111).

[106] G. Stefanucci, Y. Pavlyukh, A.-M. Uimonen, and R. van Leeuwen, "Diagrammatic expansion for positive spectral functions beyond GW: Application to vertex corrections in the electron gas", Phys. Rev. B **90**, 115134 (2014) (cited on page 15).

[107] C. Gros and R. Valentí, "Cluster expansion for the self-energy: A simple many-body method for interpreting the photoemission spectra of correlated Fermi systems", Phys. Rev. B **48**, 418–425 (1993) (cited on pages 16, 27, 30).

[108] D. Sénéchal, D. Perez, and M. Pioro-Ladrière, "Spectral Weight of the Hubbard Model through Cluster Perturbation Theory", Phys. Rev. Lett. **84**, 522–525 (2000) (cited on pages 16, 27, 30).

[109] D. Sénéchal, D. Perez, and D. Plouffe, "Cluster perturbation theory for Hubbard models", Phys. Rev. B **66**, 075129 (2002) (cited on page 16).

[110] M. Balzer and M. Potthoff, "Nonequilibrium cluster perturbation theory", Phys. Rev. B **83**, 195132 (2011) (cited on pages 16, 30, 33, 40, 43, 84, 85).

[111] M. Knap, W. von der Linden, and E. Arrigoni, "Nonequilibrium steady state for strongly correlated many-body systems: Variational cluster approach", Phys. Rev. B **84**, 115145 (2011) (cited on page 16).

[112] P. Jurgenowski and M. Potthoff, "Dynamical symmetry between spin and charge excitations studied by a plaquette mean-field approach in two dimensions", Phys. Rev. B **87**, 205118 (2013) (cited on pages 16, 30, 33, 40, 53, 84).

[113] F. Hofmann, M. Eckstein, and M. Potthoff, "Nonequilibrium variational-cluster approach to real-time dynamics in the Fermi-Hubbard model", Journal of Physics: Conference Series **696**, 012002 (2016) (cited on pages 16, 32).

[114] S. Blanes, F. Casas, J. Oteo, and J. Ros, "The Magnus expansion and some of its applications", Physics Reports **470**, 151–238 (2009) (cited on page 23).

[115] A. Alvermann and H. Fehske, "High-order commutator-free exponential time-propagation of driven quantum systems", Journal of Computational Physics **230**, 5930–5956 (2011) (cited on page 23).

[116] C. Gramsch and M. Potthoff, "Enforcing conservation laws in nonequilibrium cluster perturbation theory", Phys. Rev. B **95**, 205130 (2017) (cited on pages 27, 43, 87, 111).

[117] N. Schuch and F. Verstraete, "Computational complexity of interacting electrons and fundamental limitations of density functional theory", Nature Physics **5**, 732–735 (2009) (cited on page 27).

[118] S. Aaronson, "P $\overset{?}{=}$ NP", Open Problems in Mathematics, Springer (2016) (cited on page 27).

[119] S. Yamada, T. Imamura, T. Kano, Y. Ohashi, H. Matsumoto, and M. Machida, "Ultra Large-scale Exact-diagonalization for Confined Fermion-Hubbard Model on the Earth Simulator: Exploration of Superfluidity in Confined Strongly-Correlated Systems", Journal of the Earth Simulator **7**, 23–35 (2007) (cited on page 27).

[120] F. Hofmann and M. Potthoff, "Time-dependent Mott transition in the periodic Anderson model with nonlocal hybridization", The European Physical Journal B **89**, 178 (2016) (cited on page 32).

[121] C. Kollath, A. M. Läuchli, and E. Altman, "Quench Dynamics and Nonequilibrium Phase Diagram of the Bose-Hubbard Model", Phys. Rev. Lett. **98**, 180601 (2007) (cited on page 33).

[122] S. Trotzky, Y.-A. Chen, A. Flesch, I. P. McCulloch, U. Schollwöck, J. Eisert, and I. Bloch, "Probing the relaxation towards equilibrium in an isolated strongly correlated one-dimensional Bose gas", Nat. Phys. **8**, 325–330 (2012) (cited on page 33).

[123] M. Eckstein, M. Kollar, and P. Werner, "Interaction quench in the Hubbard model: Relaxation of the spectral function and the optical conductivity", Phys. Rev. B **81**, 115131 (2010) (cited on page 33).

[124] M. Moeckel and S. Kehrein, "Interaction Quench in the Hubbard Model", Phys. Rev. Lett. **100**, 175702 (2008) (cited on pages 33, 34, 40, 56, 84).

[125] M. Stark and M. Kollar, "Kinetic description of thermalization dynamics in weakly interacting quantum systems", arXiv:1308.1610 (2013) (cited on pages 33, 34, 40, 84).

[126] M. Rigol, V. Dunjko, and M. Olshanii, "Thermalization and its mechanism for generic isolated quantum systems", Nature **452**, 854 (2008) (cited on page 34).

[127] M. Moeckel and S. Kehrein, "Real-time evolution for weak interaction quenches in quantum systems", Annals of Physics **324**, 2146–2178 (2009) (cited on pages 34, 40, 84).

[128] M. Moeckel and S. Kehrein, "Crossover from adiabatic to sudden interaction quenches in the Hubbard model: prethermalization and non-equilibrium dynamics", New Journal of Physics **12**, 055016 (2010) (cited on pages 34, 40, 84).

[129] M. Kollar, F. A. Wolf, and M. Eckstein, "Generalized Gibbs ensemble prediction of prethermalization plateaus and their relation to nonthermal steady states in integrable systems", Phys. Rev. B **84**, 054304 (2011) (cited on pages 34, 40, 84).

[130] G. Baym and L. P. Kadanoff, "Conservation Laws and Correlation Functions", Phys. Rev. **124**, 287–299 (1961) (cited on pages 44, 45).

[131] G. Baym, "Self-Consistent Approximations in Many-Body Systems", Phys. Rev. **127**, 1391–1401 (1962) (cited on pages 44, 45).

[132] D. M. Kennes, J. C. Pommerening, J. Diekmann, C. Karrasch, and V. Meden, "Small quenches and thermalization", Phys. Rev. B **95**, 035147 (2017) (cited on page 56).

[133] R. Bulla, "Zero Temperature Metal-Insulator Transition in the Infinite-Dimensional Hubbard Model", Phys. Rev. Lett. **83**, 136–139 (1999) (cited on page 60).

[134] F. Mancini and A. Avella, "The Hubbard model within the equations of motion approach", Advances in Physics **53**, 537–768 (2004) (cited on page 60).

[135] J. Beenen and D. M. Edwards, "Superconductivity in the two-dimensional Hubbard model", Phys. Rev. B **52**, 13636–13651 (1995) (cited on page 60).

[136] A. I. Lichtenstein and M. I. Katsnelson, "*Ab initio* calculations of quasiparticle band structure in correlated systems: LDA++ approach", Phys. Rev. B **57**, 6884–6895 (1998) (cited on page 60).

[137] G. Geipel and W. Nolting, "Ferromagnetism in the strongly correlated Hubbard model", Phys. Rev. B **38**, 2608–2621 (1988) (cited on page 60).

[138]   W. Nolting and W. Borgiel, "Band magnetism in the Hubbard model", Phys. Rev. B **39**, 6962–6978 (1989) (cited on pages 60, 81, 88).

[139]   Y. Song, S. Bulut, R. Wortis, and W. Atkinson, "Effects of strong correlations on the disorder-induced zero-bias anomaly in the extended Anderson–Hubbard model", Journal of Physics: Condensed Matter **21**, 385601 (2009) (cited on pages 60, 81, 88).

[140]   J. Hubbard, "Electron correlations in narrow energy bands III. An improved solution", Proceedings of the Royal Society of London A: Mathematical, Physical and Engineering Sciences **281**, 401–419 (1964) (cited on page 60).

[141]   P. R. Grzybowski and R. W. Chhajlany, "Hubbard-I approach to the Mott transition", physica status solidi (b) **249**, 2231–2238 (2012) (cited on page 60).

[142]   L. S. Campana, A. C. D'Auria, M. D'Ambrosio, U. Esposito, L. De Cesare, and G. Kamieniarz, "Spectral-density method for classical systems: Heisenberg ferromagnet", Phys. Rev. B **30**, 2769–2775 (1984) (cited on page 60).

[143]   N. Sandschneider and W. Nolting, "Microscopic model for current-induced switching of magnetization for half-metallic leads", Phys. Rev. B **79**, 184423 (2009) (cited on pages 60, 81, 88).

[144]   N. Sandschneider, "Strominduziertes Schalten der Magnetisierung", PhD thesis (Humboldt-Universität zu Berlin, Mathematisch-Naturwissenschaftliche Fakultät I, 2009) (cited on pages 60, 81, 88).

[145]   K. Lanczos, "An iteration method for the solution of the eigenvalue problem of linear differential and integral operators", J. Res. Natl. Bur. Stand. **45**, 225 (1950) (cited on pages 60, 67, 69).

[146]   A. N. Krylov, "On the numerical solution of the equation by which, in technical questions, frequencies of small oscillations of material systems are determined [title translated from Russian]", Izvestija AN SSSR, Otdel. mat. i estest. nauk, VII, No. 4, 491–539 (1931) (cited on page 69).

[147]   A. Avella and F. Mancini, "The Composite Operator Method (COM)", in *Strongly Correlated Systems: Theoretical Methods*, edited by A. Avella and F. Mancini (Springer Berlin Heidelberg, Berlin, Heidelberg, 2012), pp. 103–141 (cited on page 78).

[148]   S. R. White, D. J. Scalapino, R. L. Sugar, E. Y. Loh, J. E. Gubernatis, and R. T. Scalettar, "Numerical study of the two-dimensional Hubbard model", Phys. Rev. B **40**, 506–516 (1989) (cited on pages 81, 88).

[149]   D. A. Abanin and Z. Papić, "Recent progress in many-body localization", Annalen der Physik **529**, 1700169, 1700169–n/a (2017) (cited on page 81).

[150]   T. Herrmann and W. Nolting, "Ferromagnetism in the Hubbard model: Influence of the lattice structure", Solid State Communications **103**, 351–356 (1997) (cited on pages 81, 88).

[151]   T. Herrmann and W. Nolting, "Magnetism in the single-band Hubbard model", Journal of Magnetism and Magnetic Materials **170**, 253–276 (1997) (cited on pages 81, 88).

[152] M. Potthoff, T. Herrmann, T. Wegner, and W. Nolting, "The Moment Sum Rule and Its Consequences for Ferromagnetism in the Hubbard Model", physica status solidi (b) **210**, 199–228 (1998) (cited on pages 81, 88).

[153] D. Villani, E. Lange, A. Avella, and G. Kotliar, "Two-Scale Analysis of the SU(N) Kondo Model", Phys. Rev. Lett. **85**, 804–807 (2000) (cited on pages 81, 88).

[154] A. Polkovnikov, K. Sengupta, A. Silva, and M. Vengalattore, "*Colloquium* : Nonequilibrium dynamics of closed interacting quantum systems", Rev. Mod. Phys. **83**, 863–883 (2011) (cited on page 84).

[155] F. Hofmann, "Nonequilibrium self-energy functional theory : Accessing the real-time dynamics of strongly correlated fermionic lattice systems", PhD thesis (Universität Hamburg, 2016) (cited on pages 86, 87).

[156] C. Gramsch and M. Rigol, "Quenches in a quasidisordered integrable lattice system: Dynamics and statistical description of observables after relaxation", Phys. Rev. A **86**, 053615 (2012) (cited on page 111).

List of publications

Major parts of this thesis have previously been published as refereed journal articles. To allow for a streamlined presentation, structural changes have been made including the removal of overlapping contents as well as the adaption of the notations.

Reproduced with the permission of the American Physical Society:

- C. Gramsch and M. Potthoff, "Enforcing conservation laws in nonequilibrium cluster perturbation theory", Phys. Rev. B **95**, 205130 (2017).

- C. Gramsch and M. Potthoff, "Lehmann representation of the nonequilibrium self-energy", Phys. Rev. B **92**, 235135 (2015).

Other publications:

- C. Gramsch, K. Balzer, M. Eckstein, and M. Kollar, "Hamiltonian-based impurity solver for nonequilibrium dynamical mean-field theory", Phys. Rev. B **88**, 235106 (2013).

- C. Gramsch and M. Rigol, "Quenches in a quasidisordered integrable lattice system: Dynamics and statistical description of observables after relaxation", Phys. Rev. A **86**, 053615 (2012).

Eidesstattliche Erklärung

Declaration on oath

Hiermit erkläre ich an Eides statt, dass ich die vorliegende Dissertationsschrift selbst verfasst und keine anderen als die angegebenen Quellen und Hilfsmittel benutzt habe.

I hereby declare, on oath, that I have written the present dissertation by my own and have not used other than the acknowledged resources and aids.

Hamburg, den 30. November 2017
Christian Gramsch